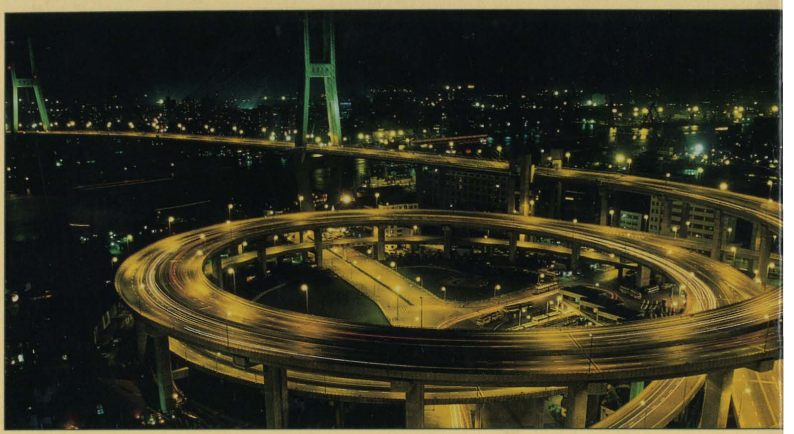
MTP
MACMILLAN TECHNICAL PUBLISHING U·S·A



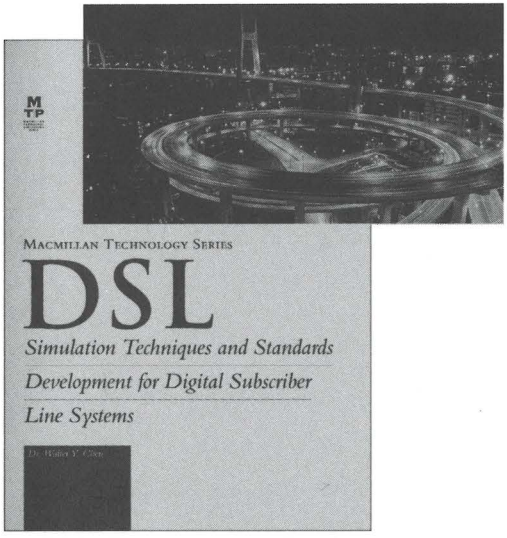
MACMILLAN TECHNOLOGY SERIES

DSL

Simulation Techniques and Standards Development for Digital Subscriber Line Systems

Dr. Walter Y. Chen

ENTROPIC EXHIBIT 2009
DISH v. Entropic
IPR2024-00373



Copyright© 1998

YAT NIN CHAN

The Image Bank

The 8,346-metre-long **Nanpu Bridge** in Shanghai, China, has a clearance of 46 metres, allowing ships with a tonnage of 55,000 to pass under it. As a cable suspension bridge, the Nanpu's main bridge is 846 metres long and 30.35 metres wide, divided into six lanes. The approaches to the bridge have a combined length of 7,500 metres, and the West Shanghai spiral approach is 3,754 metres long. The Nanpu Bridge cost a total of 820 million yuan and was completed and opened to traffic on December 1, 1991. The bridge spans the Huangpu River like a flying dragon and has realized the dreams of the locals of having a bridge across the Huangpu River.

DSL

Simulation Techniques and Standards Development for Digital Subscriber Line Systems

Dr. Walter Y. Chen

MACMILLAN TECHNICAL PUBLISHING U·S·A

Macmillan Technical Publishing, Indianapolis, Indiana

DSL: Simulation Techniques and Standards Development for Digital Subscriber Line Systems

By Dr. Walter Y. Chen

Published by:
Macmillan Technical Publishing
201 West 103rd Street
Indianapolis, IN 46290 USA

All rights reserved. No part of this book may be reproduced or transmitted in any form or by any means, electronic or mechanical, including photocopying, recording, or by any information storage and retrieval system, without written permission from the publisher, except for the inclusion of brief quotations in a review.

Copyright © 1998 by Macmillan Technical Publishing

Printed in the United States of America 1 2 3 4 5 6 7 8 9 0

Library of Congress Cataloging-in-Publication Data

Library of Congress Catalog No.: 96-80469

ISBN: 1-57870-017-5

Warning and Disclaimer

This book is designed to provide information about **Digital Subscriber Line technology**. Every effort has been made to make this book as complete and as accurate as possible, but no warranty or fitness is implied.

The information is provided on an "as is" basis. The author and Macmillan Technical Publishing shall have neither liability nor responsibility to any person or entity with respect to any loss or damages arising from the information contained in this book or from the use of the disks or programs that may accompany it.

Publisher *Jim LeValley*
Executive Editor *David Gibson*
Managing Editor *Caroline Roop*

Acquisitions Editor
Tracy Hughes
Development Editor
Christopher Cleveland
Project Editor
Brian Sweany
Copyeditor
Thomas Cirtin
Technical Editor
Jacky Chow
Market Reviewers
Brian Armstrong
Dr. J.J. Werner
Team Coordinator
Amy Lewis
Manufacturing Coordinator
Brook Farling
Book Designer
Ann Jones
Cover Designer
Sandra Schroeder
Cover Production
Aren Howell
Director of Production
Larry Klein
Production Team Supervisor
Andrew Stone
Graphics Image Specialists
Steve Adams
Debi Bolhuis
Kevin Cliburn
Sadie Crawford
Wil Cruz
Tammy Graham
Oliver Jackson
Production Analysts
Dan Harris
Erich J. Richter
Production Team
Chris Barrick
Jeanne Clark
Christy M. Lemasters
Julie Searls
Sossity Smith
Heather Stephenson
Indexer
Kevin Fulcher

Trademark Acknowledgments

All terms mentioned in this book that are known to be trademarks or service marks have been appropriately capitalized. Macmillan Technical Publishing cannot attest to the accuracy of this information. The use of a term in this book should not be regarded as affecting the validity of any trademark or service mark.

About the Author

Dr. Walter Y. Chen was born in Shanghai, China, on September 8, 1956. He received a B.S. (summa cum laude) degree in electrical engineering from the Polytechnic Institute of New York, Brooklyn, in 1982, an M.S. degree in electrical engineering from California Institute of Technology, Pasadena, in 1983, and a Ph.D. in electrical engineering from Polytechnic University of New York in 1989.

From 1982 to 1987, he was a Member of Technical Staff at AT&T Bell Laboratories, where he worked on PBX systems engineering and voice band modem VLSI ship design. From 1987 to 1989, he was a Member of Technical Staff at NYNEX Science and Technology, where he conducted computer network traffic and adaptive signal processing simulation studies. From 1989 to 1995, he was a research scientist at Bellcore, where he was involved with HDSL, ADSL, and HFC modem simulation studies and standards development. From 1995 to 1997, he was a research branch manager at the DSPS R&D Center of Texas Instruments, Inc., for the development of DSL technologies and High-throughput Digital Home Networks.

Dr. Chen is currently with the Information Systems Group of Motorola working on next-generation DSL and Digital Home Network technologies. Since 1989, he has made more than 40 technical contributions at T1E1.4, ADSL Forum, and IEEE 802.14 standards committees. His main research interest is the application of circuit and system theories to the area of advanced digital communication. He holds four U.S. patents and has several others pending.

Dedication

To Aaron and Brian, and to Nancy and our parents.

Acknowledgments

First, I would like to thank all the folks at Macmillan Technical Publishing for making this book a reality. Especially, I would like to thank Jim LeValley for getting me started with his inquiring email message. I also would like to thank Amy Lewis and Tracy Hughes for their assistance, guidance, and patience during the course of this project.

I would like to express my deep gratitude to my development editor, Chris Cleveland, for his tireless efforts at improving my writing and coordinating other related issues. I also would like to express my appreciation to my review editors, Brian Armstrong, Jacky Chow, and J. J. Werner, for their valuable comments, suggestions, and corrections in a very timely fashion.

I would like to thank my project editor, Brian Sweany, and all those who sent me a Christmas card. It was nice to receive that card when I was working like crazy and cutting off from TI.

I am so happy to see my idol Joe Lechleider willing to take time off from his busy schedule to read this manuscript and to come up with an insightful foreword for this book. Without Uncle Joe's early speculation on ADSL, we would probably be working on some other projects right now.

I would like to acknowledge that my work experience at Bellcore had inspired and prepared me for this book. I have enjoyed and benefited very much from working with my Bellcore colleagues. Especially, I would like to mention Barry Blake, Ken Kerpez, Ron McConell, Rich McDonald, Kamran Sistanizadeh, and Craig Valenti. Their contributions have provided key input to the formation of many DSL systems.

I feel very privileged to have had the opportunity to work with many research pioneers and industry leaders on DSL system issues at T1E1.4 working group meetings and other related standards activities. Their contributions have been reflected by many references addressed throughout this book. I would like to thank Richard Goodson, Mike Rude, and Hiroshi Takatori for keeping me informed on the most recent developments of HDSL2.

I would like to thank Don Shaver and Bob Hewes of Texas Instruments, Inc., for allowing me to prepare this manuscript on company computers during my spare time. I really appreciate Vedat Eyuboglu and Mike Taylor of Motorola for giving me support during the final editing period of this book.

I probably never would have been able to make any contributions to the data communications industry without many supportive managers during the last 17 years of my career at many research organizations. I would like to thank Don Stewart for his encouragement and patience during my early career at Bell Labs preparing memos for PBX system engineering. I would like to express my gratitude to J.J. Werner for helping my selection of a Ph.D. thesis topic. I would also like to express my appreciation to Jeff Waldhuter for supporting my part-time Ph.D. study during the period of completing my thesis. I would like to thank Dave

Waring for bringing me to the Bellcore DSL group and for his leadership on HDSL and ADSL projects. I would like to express my gratitude to Russell Hsing for encouraging me to go forward with technical publication. I would like to express my appreciation to Don Shaver for giving me a second chance to work on ADSL and the opportunity of trying out the role of a research manager.

I have very much enjoyed working with my colleagues at Texas Instruments, Inc., DSPS R&D Center. I have also enjoyed working with Peng Zhang and Alan Wetzel for the advancement of a high-speed digital home network especially for the idea of a long distance 1394.

I would like to express my deep gratitude to my wife for her support, especially for her giving up a high-paying consulting job to accept more responsibilities at home. This allowed me to spend most of my time during the last 60 weekends concentrating on this book. I also appreciate my son's early offer to help me proofread and create technical drawings. My wife and son have provided me with a lot of enlightenment during many of those long working days.

I would like to take another opportunity to thank my uncle and his family for bringing our family to this promised land. I would like to express my appreciation to my parents and my sister for their beliefs in my talent and ability. Finally, I hope this book makes my late grandmother in heaven really proud.

Contents at a Glance

Part I: Fundamentals: Transmission Environment and Signal Processing

1 Introduction 3
2 Telephone Subscriber Loop Environment 15
3 Twisted-Pair Channel Modeling 35
4 Transceiver Front-End Noise Models 59
5 Channel Capacity 75
6 Hybrid Circuits 91
7 Analog Front-End Precision 115
8 Channel Equalization 149
9 Echo Cancellation 215
10 Error Correction and Trellis Coding 237

Part II: DSL Systems: System and Transceiver Architectures

11 DSL (Digital Subscriber Lines) 293
12 HDSL (High-Bit-Rate Digital Subscriber Lines) 347
13 ADSL (Asymmetrical Digital Subscriber Lines) 427
14 SHDSL (Single-Pair High-Bit-Rate Digital Subscriber Lines).. 517
15 VDSL (Very-High-Bit-Rate Digital Subscriber Lines) 565
Glossary 601
Index 613

Table of Contents

Part I: Fundamentals: Transmission Environment and Signal Processing

1 INTRODUCTION 3

1.1 Digital Access Methods Through POTS Loops 4
1.1.1 Digital Access Through Analog Voice Channels 4
1.1.2 Digital Access Through Digital Switches 5
1.1.3 Digital Access Through POTS Splitters 6
1.1.4 Next-Generation Digital Switches 6
1.2 DSL System Engineering 7
1.3 The General DSL Transceiver Architecture 8
1.4 DSL Systems and Standards 9
1.4.1 Early DSL System Standards 10
1.4.2 HDSL System Standards 10
1.4.3 ADSL System Standards 11
1.4.4 HDSL2 System Standards 11
1.4.5 VDSL System Standards 12
1.5 Chapter-by-Chapter Overview 12
End Notes 14

2 TELEPHONE SUBSCRIBER LOOP ENVIRONMENT 15

2.1 Central Offices and Customer Premises 16
2.2 Subscriber Loop Structure and Twisted-Pair Cables 19
2.2.1 Bridged Taps 20
2.2.2 Loaded Loops 21
2.2.3 Twisted-Pair Loop Composition 22
2.3 Loop Plant Design Rules 23
2.3.1 Resistance Design Rule 23
2.3.2 DLC Systems and CSA Guidelines 25
2.3.3 T1 Line Configurations 27
2.4 Voice Channel Characteristics 28
2.4.1 Companding Methods 29
2.4.2 Voice Channel Attenuation and Phase Delay 30
2.4.3 Voice Channel Signaling Tones 31
End Notes 33

3 Twisted-Pair Channel Modeling 35

3.1 Primary and Secondary Parameters of Twisted-Pair Cables 36
3.2 Two-Port Networks and ABCD Parameters 41
3.2.1 Two-Port Networks in Series 45
3.2.2 Two-Port Networks in Parallel 45
3.3 Channel Transfer Function and Impulse Response 48
3.4 Extended Twisted-Pair Primary Constants 53
End Notes 58

4 Transceiver Front-End Noise Models 59

4.1 Crosstalk Noise 60
4.1.1 NEXT Coupling Configurations 61
4.1.2 FEXT Coupling Configurations 62
4.1.3 Distribution of Crosstalk Coupling Losses 62
4.1.4 The Unger NEXT and Simplified NEXT/FEXT Models 64
4.2 Impulse Noise 67
4.3 Background and Receiver Front-End Thermal Noise 71
End Notes 72

5 Channel Capacity 75

5.1 Signal-to-Noise Ratio 77
5.1.1 NEXT Signal-to-Noise Ratios 78
5.1.2 FEXT Signal-to-Noise Ratios 79
5.2 Channel Capacity Calculations 80
5.2.1 Basic Concepts of Channel Capacity 81
5.2.2 Channel Capacity for Frequency-Dependent SNR 83
5.2.3 Channel Capacity with Implementation Constraints 88
End Notes 90

6 Hybrid Circuits 91

6.1 Single-Ended Hybrid Circuits 93
6.2 Differential Hybrid Circuits 96
6.3 Transformer Equivalent Circuits 100
6.3.1 ISDN Transformer Equivalent Circuit Parameters 101
6.3.2 HDSL Transformer Equivalent Circuit Parameters 102
6.3.3 ADSL Transformer Equivalent Circuit Parameters 102
6.4 Echo Path Model 103
End Notes 114

7 ANALOG FRONT-END PRECISION 115

7.1 Transmit Signal Peak-to-Average Voltage Ratio 117
7.1.1 PAR of Passband Single Carrier Line Codes 119
7.1.2 PAR of DMT Line Codes 123
7.2 Transmit Filter, Channel, and Echo Path Effects 126
7.2.1 Baseband Square Root Nyquist Shaping Filters 128
7.2.2 Passband Square Root Nyquist Shaping Filters 128
7.2.3 Baseband Channel Impulse Response 129
7.2.4 Passband Channel Impulse Response 129
7.2.5 Baseband Echo Path 130
7.3 ADC and DAC Characteristics 130
7.3.1 Calculation of Quantization Noise 131
7.3.2 ADC and DAC Nonlinearity 133
7.4 DAC and ADC Dynamic Range Requirements 136
7.4.1 DAC Resolution Requirements for Baseband Transmitters 136
7.4.2 DAC Resolution Requirements for Passband Transmitters 138
7.4.3 DAC Resolution Requirements for DMT Transmitters 140
7.4.4 The Effect of ADC Quantization Noise 141
7.4.5 ADC Precision Requirements Considering Channel Loss 142
7.4.6 ADC Precision Requirements Considering Echo Path 145
End Notes 147

8 CHANNEL EQUALIZATION 149

8.1 Adaptive Linear Channel Equalization 150
8.1.1 Compensating for Channel Distortion 151
8.1.2 Obtaining Optimal Equalizer Coefficients 155
8.1.3 Baud Rate Equalizer Performance 161
8.1.4 Fractionally Spaced Equalizer Performance 162
8.1.5 Noise Power After Equalization 167
8.2 Decision Feedback Channel Equalization 169
8.2.1 Determining DFE Coefficients 169
8.2.2 DFE MMSE Levels 174
8.2.3 DFE Error Propagation and Precoding 176
8.3 Passband Equalization and Carrierless AM/PM 180
8.3.1 QAM Baseband and Passband Implementation 180
8.3.2 Calculation of QAM Linear Equalizer 184
8.3.3 Calculation of QAM DFE 190

8.3.4 From QAM to CAP 193
8.3.5 Calculation of CAP Linear Equalizer 195
8.3.6 Calculation of CAP DFE 204
8.4 Equalizers for Discrete Multitone Systems 207
End Notes 213

9 ECHO CANCELLATION 215

9.1 Echo Cancellation Requirements 216
9.1.1 Echo Path Transfer Function and Impulse Response 217
9.1.2 The Effect of Transformer and Bandpass Filtering 219
9.1.3 Required Echo Cancellation Level and Length of Echo Canceller 221
9.2 Echo Canceller Requirements 222
9.2.1 Adaptation Step Size 222
9.2.2 Echo Canceller Precision Requirements 225
9.3 Asymmetrical Echo Cancellation 226
9.3.1 High Bandwidth Echo Cancellation 228
9.3.2 Low Bandwidth Echo Cancellation 229
9.4 Crosstalk Cancellation 230
9.4.1 Derivation of the Crosstalk Impulse Response 231
9.4.2 NEXT Cancellation Architecture 235
End Notes 236

10 ERROR CORRECTION AND TRELLIS CODING 237

10.1 Parity Check Codes 238
10.1.1 Achieving Error Correction 240
10.1.2 Cyclic Codes 245
10.1.3 Galois Field Arithmetic 246
10.1.4 Extended Galois Field Arithmetic 247
10.2 Reed-Solomon Codes 249
10.2.1 Generating Reed-Solomon Code Words 250
10.2.2 Reed-Solomon Encoder Implementation 252
10.2.3 Decoding of Reed-Solomon Code 252
10.2.4 DSL Applications of Reed-Solomon Codes 256
10.3 Convolution Codes 257
10.3.1 Convolution Encoder State 261
10.3.2 Viterbi Decoding 265
10.4 Trellis Code Modulation 267
10.4.1 Achieving Significant Trellis Coding Gain 269
10.4.2 Feedback/Feedforward Implementations 274
10.4.3 An Analytical Trellis Encoder Description 277

10.4.4 Phase Invariant Trellis Encoders 281
10.4.5 Multidimensional Trellis Codes 287
End Notes 287

Part II: DSL Systems: System and Transceiver Architectures

11 DSL (Digital Subscriber Lines) 293

11.1 DSL Technology Development 294
11.1.1 FDM Transmission for DSL 295
11.1.2 TCM Transmission for DSL 296
11.1.3 EC-Based Transmission for DSL 296
11.1.4 Candidate DSL Line Code Characteristics 298
11.1.5 Candidate DSL Line Code Transmission Performance 299
11.2 DSL Transceiver Structure and Line Code 302
11.2.1 DSL 2B1Q Line Code Parameters 303
11.2.2 DSL Equalizer Requirements 304
11.2.3 DSL Echo Canceller Requirements 305
11.2.4 DSL Timing Recovery Circuits 308
11.3 DSL Semiconductor Technologies 310
11.3.1 A COM DSL Analog Front-End Chip from Siemens 310
11.3.2 A DSL Analog and Digital Chip Set from AT&T 313
11.3.3 A Single-Chip DSL Solution from Mitel Semiconductor 313
11.3.4 A Single-Chip DSL Solution from National Semiconductor 317
11.4 DSL Performance Objectives 320
11.5 DSL Network Interfaces 327
11.5.1 DSL T Interfaces 331
11.6 DSL Standards 333
11.6.1 Bit-to-Symbol Encoders 334
11.6.2 DSL Pulse Mask 334
11.6.3 DSL Transmit Power Mask 334
11.6.4 Nonlinearity Measurements 336
11.6.5 DSL Transmission Performance Measurement 336
11.6.6 The DSL Frame Structure 338
11.6.7 The DSL Super Frame Structure 338
11.6.8 DSL Scrambler/Descrambler 340
11.6.9 The DSL Startup Sequence 341
End Notes 341

12 HDSL (High-Bit-Rate Digital Subscriber Lines) 347

12.1 HDSL Technology Development 348
12.1.1 The Initial Definition of HDSL 348
12.1.2 Studies on Baseband 2B1Q Line Code 349
12.1.3 Studies on Passband QAM Line Code with Coding ... 350
12.1.4 Studies Toward an HDSL Technical Report 350
12.1.5 Performance Measurements of HDSL Prototypes 351
12.2 HDSL Transceiver Structures and Line Codes 353
12.2.1 HDSL Transceiver Parameters 355
12.2.2 HDSL Channel Equalizer Requirements 356
12.2.3 HDSL Echo Canceller Requirements 358
12.2.4 HDSL Timing Recovery Circuits 361
12.2.5 HDSL DFE/EC Semiconductor Technologies 366
12.3 Performance Objectives 372
12.3.1 General HDSL Performance Objectives 373
12.3.2 The Effect of Termination Resistance Value 378
12.3.3 Measures to Handle the Slight Data Rate Difference in Opposite Directions 381
12.4 HDSL Network Interfaces 396
12.4.1 The DS1 Infrastructure 397
12.5 HDSL Technical Report 402
12.5.1 2B1Q Bit-to-Symbol Encoding 402
12.5.2 Transmit Signal Pulse Mask 403
12.5.3 Transmit Signal Power Mask 404
12.5.4 HDSL Test Loops 404
12.5.5 HDSL Performance Test Configuration 405
12.5.6 Measurement Calibration Procedures 407
12.5.7 Scambler and Descrambler 408
12.5.8 HDSL Initialization Procedure 410
12.5.9 Key Features of the Optional CAP HDSL 413
End Notes 419

13 ADSL (Asymmetrical Digital Subscriber Lines) 427

13.1 Development of ADSL Technology 429
13.1.1 Convergence of Initial Ideas on ADSL 432
13.1.2 Concerns for POTS Interference 435
13.1.3 The Convergence of ADSL Standards 436
13.2 Transceiver Structures and Line Codes 436
13.2.1 DMT Line Code 436
13.2.2 CAP Line Code 461

13.3 Performance Objectives for Mid-CSA Test Loops 474
13.3.1 ADSL Noise Environments 475
13.3.2 DMT ADSL Transmission Throughput Estimation 477
13.3.3 Estimating CAP ADSL Performance 480
13.4 Network and Premises Interfaces 481
13.4.1 Central Office Service Capabilities 484
13.4.2 POTS Splitters 485
13.4.3 Application of POTS Splitter 489
13.5 ADSL Standards (T1.413) 491
13.5.1 Frame Structure 491
13.5.2 Interleaving 497
13.5.3 Reed-Solomon Coding 498
13.5.4 Bit Encoding 498
13.5.5 Scramblers 501
13.5.6 Initialization 502
End Notes 507

14 SHDSL (Single-Pair High-Bit-Rate Digital Subscriber Lines) 517

14.1 The Desired Performance Improvements 518
14.1.1 EC/FDM-Based CAP SHDSL Systems 519
14.1.2 DMT Line Code for SHDSL Systems 520
14.1.3 Comparison of PAM and CAP/QAM Line Codes 520
14.1.4 Channel Capacity for SHDSL Systems 523
14.1.5 Modifying the NEXT Model to Improve Performance 527
14.1.6 Spectrum Compatibility 528
14.2 Searching for the Required Coding Gain 529
14.2.1 Trellis Codes 529
14.2.2 Viterbi Decoding 532
14.2.3 Sequential Decoding 533
14.2.4 Coding Gain and Latency 540
14.3 Minimizing Self and Foreign NEXT with Spectrum Shaping 542
14.3.1 POET-PAM Systems 542
14.3.2 TCSFDM Systems 545
14.3.3 OverCAPped Systems 546
14.3.4 SST Systems 550
14.4 Status of the HDSL2 Standard 551
14.4.1 The Rationale for a 5 dB Performance Margin 551
14.4.2 The Programmable Encoder and 512-State Trellis Codes 552

14.4.3 The OPTIS Transmit Spectra 554
14.4.4 Analyzing SHDSL Transceiver Complexity 557
End Notes 560

15 VDSL (Very-High-Bit-Rate Digital Subscriber Lines) 565

15.1 Transmission Environment for VDSL 566
15.1.1 VDSL Channel Model 567
15.1.2 VDSL Crosstalk Model 568
15.1.3 Radio Frequency Interference 569
15.2 General System Architecture 576
15.3 VDSL System Line Code Proposals 583
15.3.1 CAP/QAM Proposal 583
15.3.2 DMT Proposal 589
15.4 Twisted-Pair Primary Constants for VDSL 593
End Notes 599

Glossary 601

Index 613

Foreword

The second half of the twentieth century has been a remarkable period for technological innovation, and particularly so for telecommunications. In 1950, telecommunications was almost entirely in the analog mode. Digital transmission of pulse code modulated voice in the telephone exchange carrier plant, and low-speed data communications were the first ventures into digital transmission in the wire-pair telephone loop plant. Both of these radical departures required engineering design of transmission circuits. The invention of the transistor and the subsequent explosion of integrated circuit technology quickly led to a revolution in consumer electronics and in communications in general. It was not until the eighties, however, that the idea of an adaptive digital subscriber line that permitted turnkey installation without prescription engineering or plant conditioning began to emerge.

There were several key innovations that made this possibility into a reality. Certainly, decision-directed echo cancellation made feasible the use of the switched telephone network for the conveyance of data between modems. Decision feedback equalization reduced the problem of transmission distortion to an economic one in contrast to a technical unfeasibility. These new technologies coupled with the invention and progress in forward error correcting codes made the future look promising for telephone transmission over plant that was designed for analog voice frequency signals. Indeed, it was possible to transmit at speeds as high as 1200 bps over telephone loop plant without conditioning. Also, conditioned loops could be used as a medium for 56 Kbps data at a limited range.

Notwithstanding this great advance, the possibility of inline signal processing at high speeds seemed remote. But integrated circuit technology continued its inexorable march. ISDN transmission at 80 Kbps second over unconditioned and unselected loops seemed like a brash idea at first, but 160 Kbps duplex transmission proved feasible before ISDN standards for basic access were set. Key to this advance was the emergence of compression techniques with far greater dynamic range than was earlier thought feasible.

The new technologies led to reconsideration of the way that ISDN Primary access—access to the switched network at low megabit speeds—was provided. Before the emergence of the technology used for Basic Access, Primary Access was provided by using two simplex loops operating at the DS-1 (E-1 in Europe) rate; near-end crosstalk was suppressed by shortening regenerator spacing in the plant or by separating the two directions of transmission into separate cable binder groups. The new Basic Access technology suggested that most of the loops in the telephone plant could be used to provide Primary access by using two duplex loops operating at half the bit rate. Furthermore, no plant conditioning or special engineering was required. Thus, the High-rate Digital Subscriber Line (HDSL) was born. The

magic of the HDSL compared to the simplex version of Primary access is that the HDSL uses the full transmission capacity of each cable pair in *both* directions and not only in one direction.

More magic was to follow. The success of the HDSL idea and the apparent emergence of video compression techniques that would allow entertainment video coding at DS-1 rates (MPEG-1) suggested that there might be an application for a system that transmitted to the customer at a higher rate than in the upstream direction. The idea of a network of backend computers serving individual customers also suggested a need for such an asymmetric service. This apparently emerging market, coupled with the fact that the most significant impairment to loop transmission—near-end crosstalk—would be considerably suppressed with an asymmetric channel, ultimately led to the conception of the Asymmetrical Digital Subscriber Line (ADSL).

At about this time, Trellis coding and Viterbi receivers emerged as economically feasible approaches to reliable transmission on copper pairs. Fortunately, signal processing speeds and the complexity of processor chips develops at a pace concomitant with the needs of the emerging processing and transmission technologies. The impact of this advance on modem technology is now well appreciated. Its impact on Digital Subscriber Line technology is still evolving. There are, at present, several laboratories that are researching new DSLs employing the new coding techniques with capabilities unimagined just a short time ago.

This rapid evolution of technology required conviction, on the part of equipment vendors, that the proposed new technologies would performance satisfactorily in the extant telephone loop plant before any serious commitment to development could be made. This required knowledge of the transmission and noise characteristics of telephone loop plant. Loop survey information was used to help predict performance through simulation of the proposed new systems. These simulation activities are continuing today, as the technology of DSLs continues to evolve. The requisite simulations are needed to assure that proposed technology is adequate to satisfactory performance on the overwhelming majority of loops selected at random from a large population. Thus, numerous simulations are necessary at each step in the evolution of a new technology. The simulations are also necessary for parameter setting in new technologies. For example, simulations determined the sensitivity required of analog to digital converters (ADCs) used prior to processing received signals in DSL transceivers. To attempt to conduct the studies that are the modern province of simulation would be prohibitively expense in a physical laboratory.

The remarkable pace of innovation in DSL technology did not take place in a vacuum. Standards bodies the world over considered, in considerable detail, the suitability of numerous proposals for the embodiment of DSLs. The deliberations of these groups were not merely

the coming together of different vendors to guarantee the compatibility of different equipment and the feasibility of compliance to an agreed upon specification. The efforts of these bodies were, and continue to be, a collaborative effort in creating a new technology. The best engineers from some of the greatest communications laboratories in the world shared and modified ideas and data in order to produce a good, and workable product. The meetings of these bodies rank with the most sophisticated engineering and scientific symposia in their contribution to the fund of the world's technical knowledge and wisdom. They continue to guide the evolution of an extremely dynamic technology.

The book by Dr. Walter Chen thus arrives at a most opportune time. The amount of capital and human resources that are involved in DSL technology and its evolution is large, indeed. Dr. Chen's book is, I believe, the only book of its kind that is available to those that need to understand and predict the performance of DSLs. It is a welcome and sorely needed addition to the libraries of communications engineers.

Dr. Joseph W. Lechleider

February 13, 1998

PART I

Fundamentals: Transmission Environment and Signal Processing

1 *Introduction* 3

2 *Telephone Subscriber Loop Environment* 15

3 *Twisted-Pair Channel Modeling* 35

4 *Transceiver Front-End Noise Models* 59

5 *Channel Capacity* 75

6 *Hybrid Circuits* 91

7 *Analog Front-End Precision* 115

8 *Channel Equalization* 149

9 *Echo Cancellation* 215

10 *Error Correction and Trellis Coding* 237

CHAPTER 1

Introduction

When telecommunication was first invented as a telegraph, letters were coded in binary form: a combination of dots and dashes, as specified by the Morse code. In some sense, early telegraph was a digital system. The later invention of the telephone made the most popular telecommunication means into the analog format. Today, most telephone subscriber loops are still in analog format for the sole purpose of carrying analog telephone services.

Nonetheless, the *Public Switched Telephone Network* (PSTN) is dominated by digital technologies. High-speed digital transmission links between different telephone Central Offices (COs) are capable of multiplexing and concentrating local traffic according to the digital hierarchy with a minimum number of physical cable connections. A flexible digital network also is efficient at carrying new feature services, delivering information other than voice signals.

With the advanced development of computer and consumer electronics, traditional telephone subscribers are ready for new services based on digital technologies. There is a lot of useful information, such as news, weather, and stock prices, on the Internet. As a result of this new information channel, there will be a stronger need by consumers to access the Internet for telecommunication, shopping, and "infotainment." There are some digital information appliances, such as PCs, satellite receivers, and digital audio/video recorders, in the home already. When the digital television technology becomes a reality, the average household will be more digitally oriented.

Along with the digitization of public and private information and of consumer electronics, the amount of information associated with their applications has been drastically increased. First-generation PCs had a RAM size of 256KB and a hard disk drive of 20MB. Now, a consumer-grade PC has 16MB of RAM and a hard disk drive of 1GB. During the last 15

years, the PC memory and storage size increase factors have been about 62.5 and 50, respectively; however, the increase of transmission throughput for a voice band modem, which has become a popular PC communication device, is only about a factor of 14–33.4 kbps vs. 2.4 kbps.

With a much more powerful PC processing lots of information, the capability of a voice band modem, which is limited by the 3.3 kHz voice channel, becomes a limiting factor in integrating consumers to the evolving high-speed digital communication network. The drawback of a voice band modem can be overcome with the *Digital Subscriber Line* (DSL) technology. By bypassing the *Plain Old Telephone Set* (POTS) interface at a local CO, a DSL system can utilize the full potential of a copper telephone subscriber loop to deliver a transmission throughput of up to a few hundred times that of a voice band modem.

1.1 Digital Access Methods Through POTS Loops

Currently, there are three ways to provide digital access through a telephone subscriber loop:

- Analog voice channel
- Digital switches
- POTS splitters

1.1.1 Digital Access Through Analog Voice Channels

Figure 1.1 shows the first approach of providing digital transmission through the existing POTS switch and PSTN network.

Figure 1.1 Digital Access Through an Analog Voice Channel

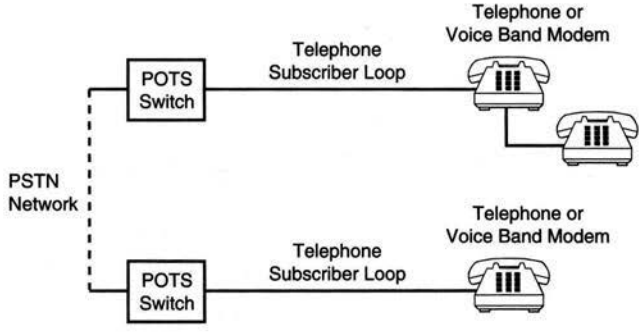


Figure 1.1 shows the configuration for today's voice band modem. There is no switch and network infrastructure change involved for this approach. A subscriber can connect to another subscriber or to an *Information service provider* (ISP) with compatible voice band modems via an existing voice band telephone protocol. The transmission throughput is limited, however, by the bandwidth of the analog voice channel.

At the subscriber end, multiple telephone sets and voice band modems can be connected to the same subscriber loop through in-house telephone wiring, although only one voice band modem can be active at a given time.

1.1.2 Digital Access Through Digital Switches

Figure 1.2 shows the second approach of digital access through special digital switch line cards.

Figure 1.2 Digital Access Through a Special Digital Switch

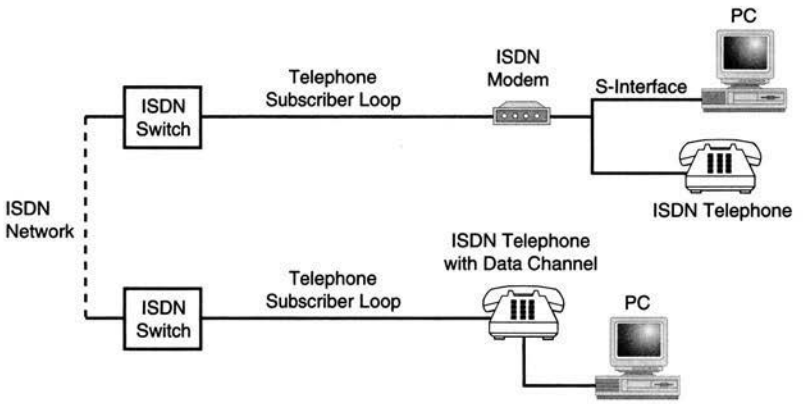


Figure 1.2 shows the configuration for the *Basic Rate Access Integrated Services Digital Network* (ISDN) service. An ISDN-capable digital switch is required for this second approach. A subscriber can connect to another subscriber or to an ISP equipped with an ISDN modem or telephone set via a digital switching protocol. A fixed transmission throughput can be defined for the worst-case condition telephone subscriber loop if the digital access service is to be available for all telephone subscribers.

At the subscriber end, only one ISDN modem or one ISDN telephone set with a U-interface is connected to the telephone subscriber loop. Multiple telephone sets and PCs can share the same digital access service through the S-interface, which can be implemented with the installation of a new in-house twisted-pair wiring. Basic Rate Access ISDN is the first DSL system.

1.1.3 Digital Access Through POTS Splitters

Figure 1.3 shows the third approach of digital access through the addition of POTS splitters.

Figure 1.3 Digital Access Through a POTS Splitter

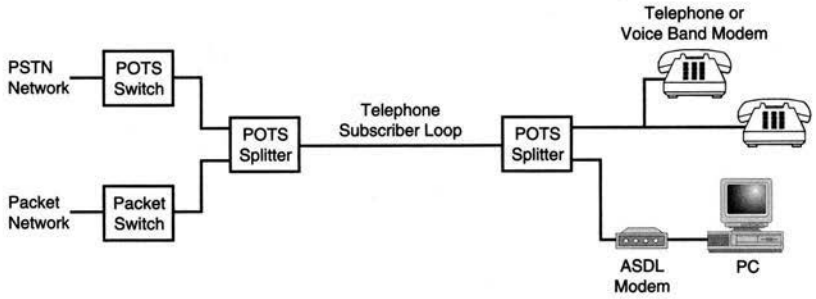


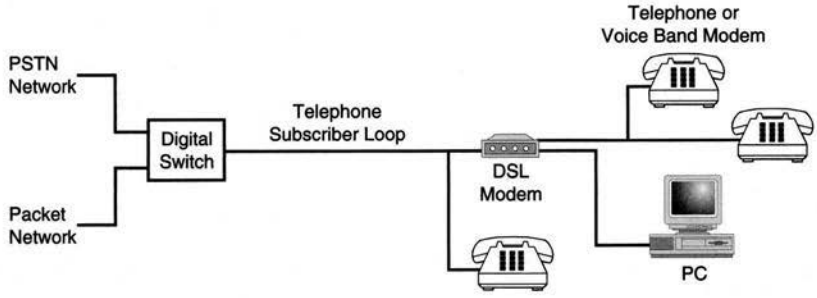
Figure 1.3 shows the configuration for *Asymmetrical Digital Subscriber Lines* (ADSL). A POTS splitter separates the voice channel from that of DSL through highpass and lowpass filters to provide co-existing services. At a CO, POTS splitters are used to merge a POTS switch and a packet switch.

At the subscriber end, a POTS splitter can be installed between the telephone subscriber loop and the existing in-house telephone wiring to avoid extensive reflection. New in-house wiring is required to connect a DSL modem to the POTS splitter. Through proper design, the interference between voice and DSL services can be kept at a minimum level.

1.1.4 Next-Generation Digital Switches

Figure 1.4 shows the possibility of providing digital transmission through a next-generation digital switch.

Figure 1.4 Digital Access Through a Digital Switch



The digital switch can recognize a particular subscriber device—a POTS telephone set, a voice band modem, or a DSL modem—and will adjust its hardware parameters and software "modem" accordingly to establish an analog or digital connection. Proper network connection also will be selected. POTS service can be provided directly through the digital switch or indirectly through the subscriber-end DSL modem. With careful design and engineering, the simultaneous operation of multiple analog and digital devices also is feasible.

1.2 DSL System Engineering

The twisted-pair telephone loop between a CO and a subscriber premises can have a length of from a few kilofeet (kft) to a few tens of kilofeet. A twisted-pair telephone loop usually consists of many cable sections of sizes from 19 gauge to 26 gauge. Due to the installation practice, there are bridged taps associated with telephone subscriber loops. To compensate for the effect of magnitude and phase distortion for the broad DSL signaling band and reflections caused by bridged taps and terminal impedance mismatch, some inter-symbol interference counter measures, such as adaptive channel equalization and multi-carrier modulation, become necessary.

For every section, there are many twisted pairs sharing the same electrical sheath and plastic covering within a single twisted-pair cable. Crosstalks exist between adjacent twisted pairs. Because twisted-pair telephone cables are originally engineered for the voice band, the crosstalk noise level could become quite severe for DSL applications. Besides the telephone loop plant background noise, the crosstalk noise is a limiting factor for the performance of a DSL system. There are Near End Crosstalk (NEXT) noise and Far End Crosstalk (FEXT) noise. The effect of NEXT is usually worse than that of FEXT.

Extensive digital signal processing techniques, such as adaptive channel equalizers and adaptive echo cancellers, have been adapted for DSL transceivers. The implementation of these signal processing techniques is made possible by the advancement of *Very-Large-Scale Integrated Circuit* (VLSI). VLSI can be a combination of *Application Specific Integrated Circuit* (ASIC) and a general-purpose *Digital Signal Processor* (DSP). The advancement of VLSI also made the application of extensive *Trellis Coded Modulation* (TCM) and forward error correction coding, such as *Reed-Solomon coding,* possible for low-cost DSL transceivers.

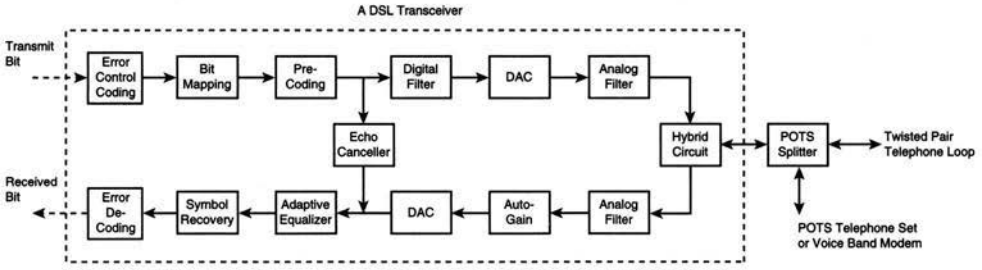
It has been a common practice, to combine the current and upcoming expected capabilities of VLSI with the desired performance of a DSL system under development. This combination has resulted in both a challenge and a rewarding experience for participating DSL system developers. For example, high-resolution, low sampling rate and low-resolution, high sampling rate Analog to Digital Converters (ADCs) have been developed for voice and video applications, respectively. The development of *High-Bit-Rate Digital Subscriber Line*

(HDSL) technology resulted in a market need of a high-resolution high sampling rate, 12 bits and 800 kHz, ADC. Furthermore, there are many other unique requirements within a DSL transceiver.

1.3 The General DSL Transceiver Architecture

Figure 1.5 shows the general structure of a DSL transceiver. As far as the semiconductor is concerned, there is an analog part and a digital part of a DSL transceiver chip set. The analog part covers analog transmit and receiver filters, the Digital to Analog Converter (DAC), the automatic gain device, and the ADC. The digital part of a DSL chip set has three major functions: modulation/demodulation, coding/decoding, and bit packing/unpacking.

Figure 1.5 A Typical DSL Transceiver Block Diagram



Specifically, the modulation/demodulation function, which involves lots of digital signal processing, includes the following:

- *Fast Fourier Transform* (FFT) and *Inverse Fast Fourier Transform* (IFFT) for the case of *Discrete MultiTone* (DMT) line code
- Constellation mapping
- Precoding for the case of using Tomlison precoding
- Digital shaping filter for the cases of *Carrierless AM/PM* (CAP) or *Quadrature Amplitude Modulation* (QAM) line codes
- Adaptive echo canceller
- Adaptive channel equalizer
- Symbol/bit conversion
- Timing recovery

A DSL can have either or both Trellis code and Reed-Solomon code, such as ADSL. Earlier DSL systems—such as the Digital Subscriber Lines (DSL), which have been adapted as the physical layer of the Basic Rate Access ISDN channel—and HDSL have no coding required. New DSL systems—such as HDSL2, which is intended to deliver twice the transmission throughput of HDSL under the similar loop condition—have considered coding as a critical part of a DSL transceiver. A coding gain of 5 to 6 dB can bring the performance of a DSL system very close to the theoretical channel capacity.

The *Transmission Convergence* (TC) layer, which belongs to the general bit-packing/unpacking function, has received a lot of attention in recent development of DSL systems. A DSL system with a properly designed TC layer will not only make a simplified network interface, but also reduce the complexity of a DSL chip set. The proper design of a bit-packing/unpacking function also is a requirement for integrated DSL systems, such as a DSL PC plug-in card or a DSL CO switch line card for which specific frame rates and frame sizes are necessary to be compatible with their host systems.

Besides the DSL chip set covering analog and digital function, some discrete components—such as the hybrid circuit, which converts a four-wire, dual half-duplex interface to a two-wire, full-duplex one, and the POTS splitter, which separates voice channel from the DSL spectrum—also are important parts of a DSL system. The improved performance of these discrete components can sometimes ease up the demand for a DSL chip set. For example, a better hybrid circuit can reduce the requirement for an echo canceller. Special techniques implemented with discrete components can be tailored for different DSL systems.

1.4 DSL Systems and Standards

There are many different signal-processing algorithms capable of achieving a particular transmission performance objective. For a particular algorithm, system and hardware parameters can vary depending on preferences. For network and service providers, an interchangeable DSL transceiver from different vendors is a key to drive hardware cost down. A common agreement is necessary to insure DSL transceivers from different developers can interoperate with each other.

A process for establishing standards is necessary—not only to define transceiver line and network interfaces, but also to identify the proper combination of signal processing algorithms and VLSI semiconductor technologies. DSL standards have been defined earlier by ANSI T1D1.3 and recently by ANSI T1E1.4 working groups.

1.4.1 *Early DSL System Standards*

The first DSL system is the DSL developed for the Basic Rate Access ISDN application during 1982 and 1988. DSL is designed to operate on all non-load telephone subscriber loops confirming the resistance design rule. ANSI documents "Integrated Service Digital Network (ISDN): Basic Access Interface for Use on Metallic Loops for Application on the Network Side of the NT-Layer 1 Specification"[1] and "Integrated Services Digital Network (ISDN): Basic Access Interface for S and T Reference Points (Layer 1 Specification)"[2] describe the *U-interface* of the DSL and the *S-interface* of the DSL, respectively.

The U-interface defines transmission specifications over the telephone subscriber loop, while the S-interface defines transmission specifications over a local distribution medium, such as a residential wiring or a PBX extension wiring. The DSL, as defined by the ANSI standard, uses a baseband four-level line code, also called 2B1Q for *2 Bits per Quaternary* symbol, over the telephone subscriber loop. The transmission throughput of the DSL is 160 kbps with a baud rate of 80 kHz.

The DSL is capable of supplying two B channels of 64 kbps and one D channel of 16 kbps. The remaining transmission throughput is consumed by *Operational, Administrative, Maintenance, and Provisioning* (OAM) channels. A DSL transceiver relies on a baud rate adaptive channel equalizer to achieve full-duplex transmission, and on a baud rate adaptive channel equalizer to overcome the effect of channel inter-symbol interference.

1.4.2 *HDSL System Standards*

The HDSL system can be considered as a technology extension of the DSL. HDSL was mainly developed as a dual-duplex repeaterless T1 technology from 1988 to 1991. HDSL is designed to serve non-load telephone subscriber loops confirming the *Carrier Serving Area* (CSA) guideline. ANSI Technical report, "A Technical Report on High-Bit-Rate Digital Subscriber Lines (HDSL),"[3] defines transmission specifications over the telephone subscriber loop, as well as associate T1 network interface.

The HDSL also uses the 2B1Q baseband four-level line code. However, both the transmission throughput of 900 kbps and the baud rate of 400 kHz are five times those of the DSL. A pair of HDSL transceivers can be used as a T1 carrier to carry 24 B channels plus associated OAM channels. Higher operation rate adaptive echo canceller and adaptive channel equalizer of an HDSL transceiver demand more digital signal processing power compared with those of a DSL transceiver.

1.4.3 ADSL System Standards

The ADSL system was developed for video-on-demand services from 1991 to 1995 with a high transmission throughput from a CO to telephone subscribers downstream, and lower transmission throughput in the reverse direction upstream. Over CSA range distance, the ADSL is capable of a downstream transmission throughput of 6.433 Mbps. For longer telephone subscriber loops confirming the resistance design rule, the downstream transmission throughput is reduced to 1.544 Mbps.

ANSI document "Network and Customer Installation Interfaces: Asymmetrical Digital Subscriber Line (ADSL) Metallic Interface"[4] defines the DMT transmission specifications over the telephone subscriber loop as well as up to seven downstream channel and four upstream channel network interfaces. The DMT line code has a baud rate of 4 kHz and up to 256 subcarriers for downstream, and up to 64 subcarriers for the upstream. Depending on the channel signal-to-noise ratio, up to 11 bits can be allocated for each subcarrier. Both Trellis code and Reed-Solomon code have been introduced for ADSL to improve the transmission performance under white Gaussian and impulse noises.

CAP/QAM line codes also have been discussed in the early ADSL standardization process. Non-standard CAP/QAM line code–based ADSL systems have been used in trials and some special-purpose applications. With properly positioned passband downstream and upstream spectra and associated constellation sizes, transmission throughputs similar to that defined by the standard ADSL also can be achieved with CAP/QAM line codes. The use of Trellis code and Reed-Solomon code also is considered in conjunction with CAP/QAM line codes. An ANSI ad hoc group has been working on producing a document to define a standard for the CAP/QAM–based ADSL.

1.4.4 HDSL2 System Standards

It is expected that with some improvement on the modulation method and the addition of coding gain, the transmission throughput of HDSL can be doubled. The development of a single-pair HDSL, also called HDSL2, has been in steady progress since late 1995. Baseband multi-level line codes were the focus of the standard development; however, transmit signal spectrum shaping, with some experience gained from the development of ADSL, is considered to minimize the effect of NEXT.

A 512-state Trellis code also has been considered to bring about a coding gain of more than 5 dB. With the advancement of VLSI, the extra signal processing and coding complexity of HDSL2 is expected to be absorbed by higher-density semiconductor chips.

1.4.5 VDSL System Standards

To meet the demand of future all-purpose multimedia applications, Very-high-bit-rate Digital Subscriber Line (VDSL) has been under study since late 1995 for transmission throughputs of 13, 26, and 52 Mbps. The VDSL service range is expected to be between 1.5 to 4.5 kft. VDSL customers will be connected by short-distance copper twisted-pair loops to nearby *Optical Network Units* (ONUs) that are linked to a CO with fiber optical cables.

The VDSL transmit spectrum can occupy a bandwidth of up to 15 MHz where the Radio Frequency Interference (RFI), both ingress and egress, has become a chief concern. Under such a high transmission throughput, the requirement of delivering desired analog and digital semiconductor capabilities under a consumer product cost constraint becomes an incentive for VDSL system developers.

1.5 Chapter-by-Chapter Overview

This book is a collection of simulation/implementation techniques and reference materials for the design and development of DSL systems. It is intended for practicing engineers working in DSL and related fields. Many techniques developed for DSLs can be very useful also for next-generation communication systems, such as a high-throughput home digital network. This book also can be used as a reference for graduate students to aid in their research studies in digital communication systems.

Note

Past technical contributions of the T1E1.4 working group can be obtained from Creative Communications Consulting, P.O. Box 15189, Durham, NC 27704; telephone: 732-842-6250.

This book is divided into two parts: Part I, "Fundamentals: Transmission Environment and Signal Processing," and Part II, "DSL Systems: System and Transceiver Architectures." Part I deals with twisted-pair telephone loop channel modeling, DSL system performance simulation, and the general implementation of digital signal processing techniques. The transmission performance potential of telephone subscriber loops are examined through the calculation of channel capacity. Adaptive channel equalization, adaptive echo cancellation, and coding techniques are addressed with an emphasis on DSL-specific implementation details.

Part II deals with the specifics of developed and developing DSL systems. For each developed DSL system, initial and major standard development activities, general system performance characteristics, and key features of standard documents are discussed. The general features and related issues for developing DSL systems also are discussed. ANSI T1D1.3 and T1E1.4 working group contributions are extensively referenced.

Specifically, each chapter covers the following topics in depth:

- Chapter 2, "Telephone Subscriber Loop Environment," describes the twisted-pair telephone loop plant. Issues involved are telephone network architecture, the structure of the telephone loop plant, the loop plant design rules, the composition of twisted-pair cables, and basic voice channel transmission requirements.
- Chapter 3, "Twisted-Pair Channel Modeling," describes the channel model of the twisted-pair telephone loop. Twisted-pair cable primary parameters are examined. A two-port network and its matrix representation are used to construct a channel model based on sections of cables and other electrical components.
- Chapter 4, "Transceiver Front-End Noise Models," describes noise models for the twisted-pair telephone loop plant: crosstalk, background, and impulse noises.
- Chapter 5, "Channel Capacity," calculates channel capacities of the twisted-pair telephone loop based on channel and noise models.
- Chapter 6, "Hybrid Circuits," describes two forms of hybrid circuit that are used to connect transmitting and receiving circuits to a two-wire telephone subscriber loop. The construction of an echo path model based on the hybrid circuit and the line coupling transformer equivalent circuit also is presented.
- Chapter 7, "Analog Front-End Precision," discusses resolution requirements for ADC and DAC devices with respect to transmitting signal peak-to-average ratio and associated channel and echo path transmission characteristics.
- Chapter 8, "Channel Equalization," presents calculation techniques for the adaptive channel equalizer. Filter coefficients as well as the output signal-to-noise ratio are calculated for baud rate and fractional spaced linear and decision feedback channel equalizers. Results are given for both baseband and passband systems as well as for the DMT time domain equalizer.
- Chapter 9, "Echo Cancellation," discusses challenges of the implementation of an adaptive echo canceller for a DSL transceiver. Issues of asymmetrical echo cancellation and crosstalk cancellation also are addressed.
- Chapter 10, "Error Correction and Trellis Coding," introduces the Reed-Solomon code as a forward error correction code with background information of parity check codes and block codes. The Trellis code modulation is discussed with background information of convolution codes and Viterbi detection algorithm. Related basic implementation techniques are discussed as well.

- Chapter 11, "DSL (Digital Subscriber Lines)," discusses standard development activities, the 2B1Q line code, the expected transmission performance, and semiconductor implementation issues related to DSL.
- Chapter 12, "HDSL (High-Bit-Rate Digital Subscriber Lines)," addresses standard development activities, the 2B1Q line code, the expected transmission performance, and semiconductor implementation issues related to HDSL.
- Chapter 13, "ADSL (Asymmetrical Digital Subscriber Lines)," discusses issues related to the standard DMT line code ADSL as well as some efforts at developing a CAP/QAM line code ADSL standard.
- Chapter 14, "SHDSL (Single-Pair High-Bit-Rate Digital Subscriber Lines)," summarizes activities for the development of HDSL2.
- Chapter 15, "VDSL (Very-High-Bit-Rate Digital Subscriber Lines)," explores new issues associated with the development of VDSL, and addresses the effect of Radio Frequency Interference (RFI).

End Notes

1. ANSI T1.601-1992, "Integrated Services Digital Network (ISDN): Basic Access Interface for Use on Metallic Loops for Application on the Network Side of the NT (Layer 1 Specification)," American National Standards Institute, Inc.
2. ANSI T1.605-1991, "Integrated Services Digital Network (ISDN): Basic Access Interface for S and T Reference Points (Layer 1 Specification)," American National Standards Institute, Inc.
3. ANSI T1E1.4, "Working Group on Digital Subscriber Lines: A Technical Report on High-Bit-Rate Digital Subscriber Lines (HDSL)," T1E1.4/96-006 (April 22, 1996).
4. ANSI T1.413-1995, "Network and Customer Installation Interfaces: Asymmetrical Digital Subscriber Line (ADSL) Metallic Interface," American National Standards Institute, Inc.

CHAPTER 2

Telephone Subscriber Loop Environment

Digital Subscriber Lines (DSL) are developed based on existing telephone subscriber loops. The telephone subscriber loop environment was developed originally for the practice of carrying analog voice services and lately with the consideration of carrying digital extensions, such as *Digital Loop Carrier* (DLC), of analog voice services. The transmission characteristics of the telephone subscriber loop environment[1,2] and the proper utilization of these transmission characteristics determine the performance potential of a DSL system.

A basic knowledge of the telephone subscriber loop environment is necessary for the understanding of many technical choices for the engineering of a particular DSL system. This chapter explains the basic components and concepts of a telephone subscriber loop environment, as follows:

- *Central Offices and customer premises.* The loop plant consists of twisted-pair cables connecting a local Central Office (CO) to customer (telephone subscriber) premises (residential or small business units). The termination conditions of a subscriber loop at a CO and a premises could also affect the engineering and performance of a DSL system.
- *Subscriber loop structure and twisted-pair cables.* An individual subscriber loop consists of many different cable sections. Twisted-pair cable size, installation methodology, and grouping of subscriber loop sections could result in different degrees of exposure to *crosstalk noise* and to *radio frequency interference* (RFI).
- *Subscriber loop design rules.* A telephone subscriber loop plant followed some general design rules during its evolution. Those rules also can be used in certain degrees as guidelines for the development and deployment of DSL systems.

- *Voice channel characteristics.* A DSL system is based on the same telephone subscriber loop as a *Plain Old Telephone System* (POTS). A DSL system is sometimes designed to coexist with a POTS service on the same twisted-pair cable, offering simultaneous analog/digital services. The understanding of the POTS signaling mechanism is necessary for the design of a DSL system that coexists with a POTS.

2.1 Central Offices and Customer Premises

Today a telephone subscriber, anywhere in the world, with a telephone set connected by a twisted-pair telephone cable to a Central Office (CO) can reach another telephone subscriber whose telephone set is also connected by a twisted-pair telephone cable to another CO. Connections between each pair of telephone sets among different telephone subscribers at different locations are made indirectly through COs. COs that connect telephone subscribers are called *end COs* (Class 5).

A telephone company building is called a *wire center* and can contain several CO switching machines. The number of subscriber connections to each CO switching machine is usually limited to fewer than 10,000, constrained by the four-digit-number assignment plan for each CO. The twisted pair telephone loop connecting a subscriber to an end CO is called a *subscriber loop.* The house hosting the subscriber telephone set is called *customer premises.* Large business customers are served through *Private Branch Exchanges* (PBX).

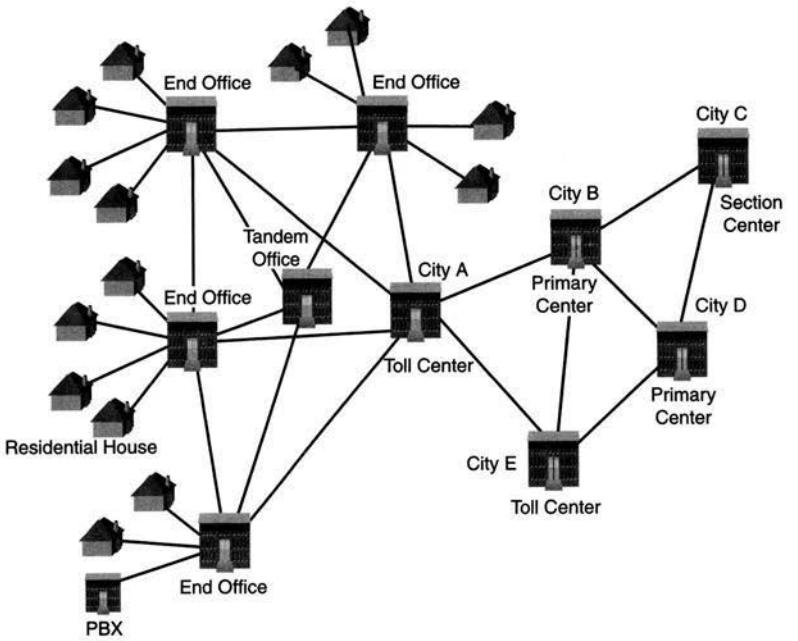
COs at a local region are connected through *interoffice trunks* or *tandem trunks* and *tandem COs* by the means of the existing and still-evolving digital hierarchy. Telephone connections beyond a local region are made possible through *toll centers* (Class 4). Above the toll center hierarchy are the *primary center* (Class 3), the *sectional center* (Class 2), and the *regional center* (Class 1). Centers are all connected through *intertoll trunks.* Figure 2.1 depicts a model telephone network.

Analog voice channels are digitized once they are terminated at an end CO. *Digital channel banks,* which consist of subscriber loop line cards and a high-speed *Time Division Multiplexing* (TDM) bus, convert analog voice signals as well as signaling information, such as originating and destination addresses, into digital format and combine the resulting digital signal into a single-digital bit stream to be integrated into the digital hierarchy.

The current digital hierarchy has transmission rates of 64 Kbps (DS0), 1.544 Mbps (DS1), 6.312 Mbps (DS2), 44.736 Mbps (DS3), and 274.176 Mbps (DS4) in North America. These transmission throughputs are typically implemented by T1, T2, T3, and T4 carrier systems based on a variety of transmission media, such as digital radio, coaxial cable,

twisted-pair cable, and fiber-optic cable. Since the early 1980s, connections between major COs have been dominated by fiber-optic cables (nearly 95 percent).[3] The evolving higher speed digital hierarchy—*Synchronous Transport Signal* (STS)—can provide transmission throughputs of 51.84 Mbps (OC-1), 155.51 Mbps (OC-3), 466.56 Mbps (OC-9), 622.08 Mbps (OC-12), and so on.

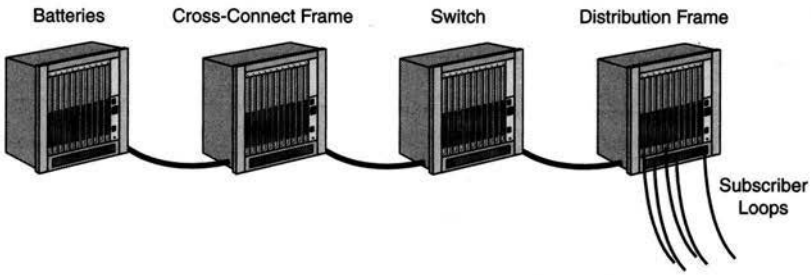
Figure 2.1 A Model Telephone Network



The major subscriber loop, or local loop, equipment in a CO consists of *main distribution frames* and a *switch machine*. *Multiplexers* are also used for the interconnection of equipment with different transmission rates conforming to a particular digital hierarchy. Subscriber loops are first terminated on distribution frames and then connected to line cards of a switch.

There are also cross-connector frames for the interconnection of switch, multiplex, and monitor equipment. *Monitor equipment* keeps electronic hardware as well as associated functions in good running condition. Most of the equipment operates directly from the battery supplies that are AC charged. Further, a lot of backup batteries are used in case of a power failure (see Figure 2.2).

Figure 2.2 Major Equipment at a CO



A switch line card supplies a DC voltage through the telephone loop to a subscriber premises to detect the on-hook and off-hook of the telephone set. Once off-hook is detected, the line card converts the dialing signal into a digital bit stream and sends it to switch equipment for further processing. For the dialed subscriber, the switch line card generates a periodic ringing signal in addition to the constant DC bias voltage for the dialed subscriber loop until the telephone is picked up and becomes off-hook. Switch line cards at both ends of an active telephone connection increase the performance of *Analog to Digital Conversion* (ADC) and *Digital to Analog Conversion* (DAC) for both subscriber loops during a telephone conversation.

The subscriber loop termination at a customer premises consists of a *Network Interface Device* (NID) from which multiple in-house wiring connections are made. An NID can be divided into two parts, as follows:

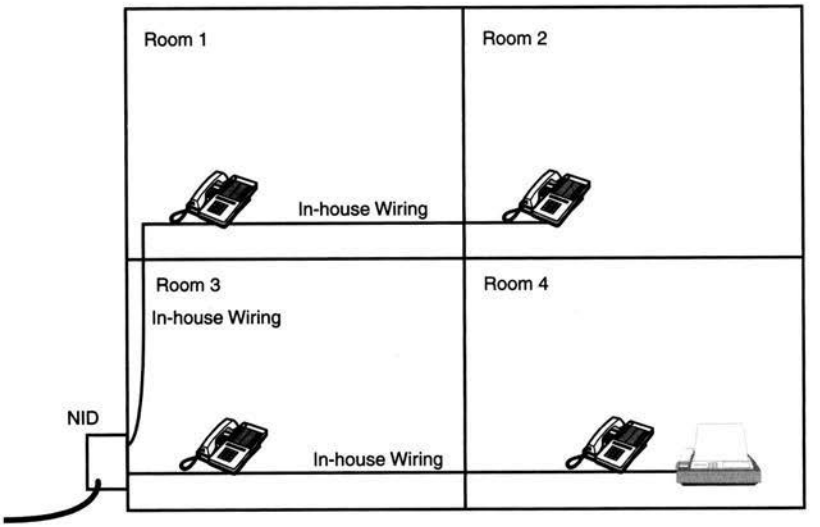
- A customer part that can be accessed by a customer to make in-house wiring connections.
- A telephone company part that is usually shielded from a customer. The telephone company part of an NID can also contain some special purpose electronics, such as a loop back circuit, for maintenance and testing.

Multiple telephone sets are connected to the telephone subscriber loop at different points in the in-house telephone wiring, which generally has a star/daisy-chain topology. Figure 2.3 shows a typical equipment and in-house wiring setup of a customer premises.

Because of the irregularity of the in-house wiring topology and sometimes poor quality of the wiring cables and their interconnections, the transmission characteristic of an in-house wiring can degrade the performance of a DSL system. Reflections could be very extensive throughout the in-house wiring. The energy loss caused by reflections can be as much as 30 dB at certain frequency regions. The inclusion of the in-house wiring has been ruled out

from the telephone subscriber loop for most DSL systems. To optimize the transmission performance, a DSL transceiver at customer premises is usually connected to the NID directly with a short and high-quality twisted-pair cable.

Figure 2.3 Premises In-House Wiring



2.2 *Subscriber Loop Structure and Twisted-Pair Cables*

A subscriber loop consists of sections (typically 500 feet long) of copper twisted pairs of cables of different gauges. The physical location of a section of a subscriber loop could be

- Aerial (hung on poles)
- Buried (directly in the ground)
- Underground (protected within a dedicated conduit)

Earlier telephone loop installations were aerial for the most part, while most recent installations, especially for new housing developments, are underground. Buried cables are used for drop wires where the extra cost of conduit installation could not be justified for each individual connection. Aerial cables are more susceptible to Radio Frequency Interference (RFI) than buried or underground cables for their effective antenna heights.

Electrical joints, also called *splices*, are usually made with hand twists without soldering to connect sections of cables together. A protective housing, which can be sealed with wax, is

used to cover cable splices, and it is usually located near a telephone pole for aerial cables or in a manhole for underground cables. A twisted-pair telephone cable with a plastic covering external to a metallic electrical sheathing can have thousands of twisted pairs organized into many binder groups.

To reduce the effect of crosstalk, binder groups within a cable have different twisting angles. Depending on the cable type, there could be 10, 25, or up to 50 twisted pairs in a binder group and up to 50 binder groups per cable. Because of the concentration, twisted-pair cables have larger *cross sections*—more twisted pairs—near the Central Office. Functionally, an individual subscriber loop can be divided into portions consisting of the following:

- *Feeder cables.* Provide links from a CO to a concentrated customer area
- *Distribution cables.* Provide links from feeder cables to potential customer sites
- *Drop wires.* Connect distribution cables to customer premises

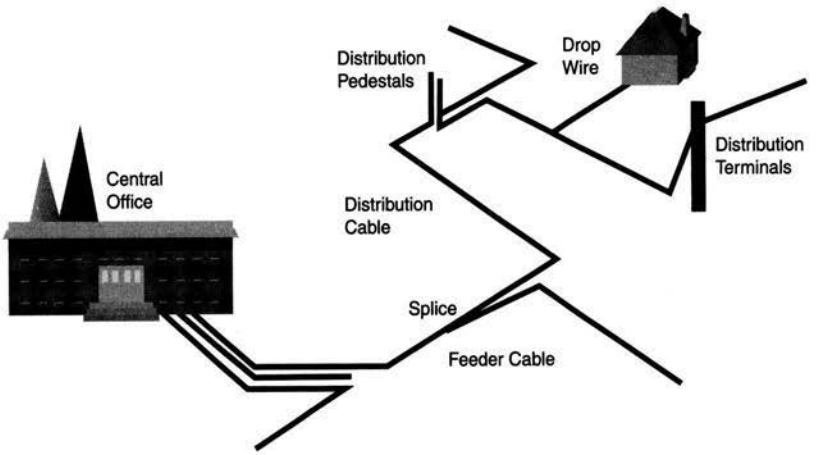
Note
Wiring inside the customer premises that connects to the drop wire at the network customer interface does not count as part of the network loop.

Connection points between feeder cables and distribution cables are commonly located in cabinets, called the *Feeder Distribution Interface* (FDI). Connection points in distribution cables are commonly located in *pedestals* for underground cables or *terminals* for aerial cables. Single aerial drop wires often consist of parallel copper wires. Recent construction uses multiple twisted pairs (two, four, or six). The drop wire is usually short and has a proportionately small effect on the loop transmission characteristics, except for potential radiation effects. The loop and drop wire could potentially pick up other high-frequency radiation noises due to the longitudinal imbalance. It could also radiate signals to other high-frequency electronic devices. Figure 2.4 shows the physical layout of cabling from a CO to the customer premises.

2.2.1 *Bridged Taps*

Because loop plant construction usually occurs ahead of customer service requests, distribution cables are usually made available to all potential customer sites. Hence, it is a common practice to connect a twisted pair from a feeder cable with more than one distribution cable pair to maximize the probability of reaching a potential customer. The unused distribution cables result in bridged taps.

Figure 2.4 General Structure of a Telephone Loop Plant



The loop plant design rules (discussed in section 2.3, "Loop Plant Design Rules"), such as *Resistance Design* and *Carrier Serving Area* (CSA), limit the total bridged tap length to minimize adverse effects, magnitude loss, and spectrum distortion on POTS (Plain Old Telephone System) transmissions.

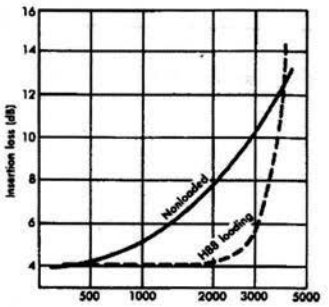
2.2.2 *Loaded Loops*

Extending the central office serving distances for the voice channel is accomplished through a procedure of installing *load coils.* Load coils are typically installed for cables with a total length (including bridged taps) exceeding 15 kft (kilofeet).

Loading arrangements are designated by a code letter that specifies the distance between loading coils and by numbers that indicate the inductance value and wire gauge. The capital letters *H, D,* and *B* indicate spacing of 6, 4.5, and 3 kft between the coils, respectively. The number in front of the letter indicates the wire gauge, and the number after the letter indicates the inductance of the coil in millihenries (mH). Therefore, the loading arrangement 19H88, for example, indicates a 19-gauge wire with a spacing distance of 6 kft and the inductance of 88 mH.

Figure 2.5 shows typical transfer functions between a loaded and a non-loaded loop based on a 12 kft, 26-gauge twisted-pair loop, for which the insertion loss is the attenuation caused by the insertion of the twisted-pair cable between a signal source and a load resistance. The physical setup of loaded loops is discussed later in section 2.3.

Figure 2.5 Insertion Losses of Loaded and Non-Loaded Loops



Note
Because its attenuation is much higher above the voice frequency, a loaded loop is not suitable for Digital Subscriber Line (DSL) systems.

2.2.3 *Twisted-Pair Loop Composition*

A telephone cable pair is made by twisting together two insulated conductors of high-purity copper. The insulation can be wood pulp formed on the conductors in a process similar to paper making (which is why sometimes it is referred to as pulp or paper cable), or it can be plastic formed by an extrusion process. *Polyolefin insulated cable* (PIC) is a general term used to describe all modern plastic insulated cables. Polyethylene is a widely used plastic insulation. Polypropylene is another commonly used plastic insulation material.

Neighboring pairs are twisted with different *pitch* (twist length) to limit electromagnetic interference (crosstalk) between them. The pairs are stranded into what are called *units,* and the units are then cabled into *cores.* The cores are covered with various types of sheaths depending on the intended use. Currently, the size of PIC cables ranges from 6 to 1,800 pairs, while the size of pulp cables ranges from 600 to 3,600 pairs. Unit sizes are 12, 13, and 25 pairs for PIC and 25, 50, and 100 pairs for pulp cables. Common wire sizes used are 19, 22, 24, and 26 gauge.

Feeder and distribution cables can contain as many as 4,200 pairs or as little as 6 pairs, all within a single sheath. In the smaller cable size, good design practice calls for using cables that are multiples of the 25-pair unit. There is very little difference between the installed cost of 6- or 12-pair cables and 25- or 50-pair cables in most applications. The extra pairs not only give the potential for growth, but also allow the allocation and use of pairs in the field to be more logical. This practice also leads to easier administration and maintenance. Feeder cables usually contain more pairs than distribution cables because of the

concentration. Feeder and distribution cable sizes are usually determined based on the projected telephone subscriber population.

Drop wires can range from one pair to hundreds or thousands of pairs, depending on the establishment to be served. Drop wires in the smaller size are not always twisted because they are usually short and do not measurably degrade transmission quality. Aerial drop wires are usually 18 or 19 gauge, while buried drop wires are usually 19, 22, or 24 gauge. High-purity copper is the most widely used conductor material for underground drop wires, while copper with special alloying (or other means for strength) is used for aerial drop wires. Specifics vary, depending on cable type.

2.3 Loop Plant Design Rules

POTS loop plant design must accomplish three goals:

- Ensure that there is sufficient direct current flow to operate station sets
- Enable DC/low-frequency call process signaling (dialing and ringing)
- Limit transmission loss and frequency roll off to acceptable levels

2.3.1 Resistance Design Rule

As mentioned in section 2.2.2, "Loaded Loops," telephone cables are designed with different gauges of wire, from 26 gauge (thin, with higher DC resistance) to 19 gauge (thicker with lower DC resistance). These different gauges are designed to have close to the same *capacitance* per unit length. It so happens that the maximum DC resistance also controls the maximum voice frequency loss and roll-off frequency.

Note
The roll-off frequency is the corner frequency beyond which the attenuation increases rapidly.

For modern switching systems, a maximum loop resistance (DC resistance) of 1500 ohms meets powering, signaling, and transmission objectives. Corresponding maximum transmission loss at 1000 Hz is about 9 dB with a roll off of 6 dB at 2800 Hz. The average loop has a DC resistance of 600 ohms with 4 dB loss at 1 KHz.

Because distances from a CO to each customer are different, distribution cables of different gauges are utilized to keep the amount of copper (and dollars) used to a minimum while meeting design guidelines. To reduce overall loop resistance, the end sections of a long subscriber loop tend to have coarser twisted pairs, whereas finer gauge twisted pairs are used closer to the central office in order to reduce the diameter of the cable in crowded ducts.

Some customers are so far away from the Central Office, however, that a direct implementation of twisted-pair cables would result in a DC resistance much higher than the specified 1500 ohms and hence a poor voice channel service quality. A procedure of installing loading coils and coarser gauge cables has been used to extend the CO serving distance for the voice channel. Inductive loading results in a loop with reduced loss within the voice band for a given gauge of cable, and acts as a lowpass filter above 3000 Hz.

Loading coils are typically installed for cables with a total length, including bridged taps, exceeding 15 kft. The first loading coil is installed at 3 kft from the CO. Loading coils are installed every 6 kft thereafter. There can be no bridged taps between loading coils in order for the *bandpass* to be flat. Bridged taps on the end sections at the CO and customer ends can be left connected, up to a total tap length of 6 kft.

Figures 2.6 and 2.7 show length distributions of all loops and non-loaded loops, respectively, according to a 1983 loop survey conducted by AT&T Bell Labs.[4]

Figure 2.6 Loop Length Distribution

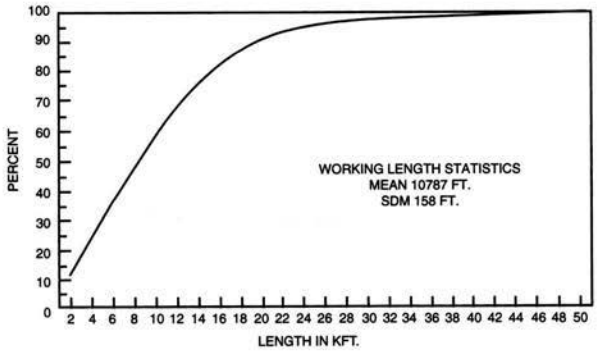
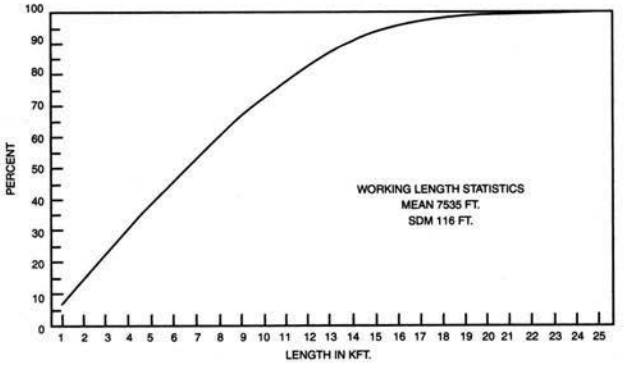


Figure 2.7 Non-Loaded Loop Length Distribution



Those loops usually consist of cable sections of different gauges and bridged taps. The length of total bridged taps is also included for the overall length of each loop. Assuming all loaded loops are longer than 15 kft, the percentage of non-loaded loops among all loops can be estimated as follows:

- Let the number of non-loaded loops less or equal to 15 kft be x.
- Let the number of non-loaded loops more than 15 kft be y.
- Let the number of loaded loops be z.

Assuming those non-loaded and loaded loops, you have the following:

$$94\% = \frac{x}{x+y} \times 100\%$$

$$79\% = \frac{x}{x+y+z} \times 100\%$$

Therefore, you have

$$\frac{x+y}{x+y+z} \times 100\% = \frac{79\%}{94\%} \times 100\% = 84\%$$

It is expected that new loops are getting shorter and the use of loading coils becomes less frequent. Therefore, the percentage of non-loaded loops should have been increased since the 1983 loop survey; however, the amount of increase could be relatively small because of the large installed telephone subscriber loop bases.

2.3.2 *DLC Systems and CSA Guidelines*

Digital Loop Carrier (DLC) systems were developed to serve customers beyond the *Resistance Design* range. Early DLC systems were based on copper twisted pairs that used the 1.544 Mbps T-carrier technology with periodic repeaters to time division multiplex 24-voice channels. Fiber-based DLC systems are now more popular. For customers near a CO, it is cheaper to connect them directly with twisted-pair cables. Depending on the cost of DLC electronics, it becomes more economical to serve customers with DLC systems beyond a certain distance. This *prove-in distance* has been decreasing as DLC electronics costs have come down because of the advancement of semiconductor and optical-electronics technologies.

The concept of *Carrier Serving Area* (CSA) engineering guidelines was introduced in the early 1980s to shorten subscriber loop length, reducing loop deployment cost and supporting all future digital services. The CSA is roughly defined as a serving distance of 9 kft for 26-gauge loops and 12 kft for 24-gauge loops from a remote terminal. CSA design guidelines can be summarized as follows:

- All loops are non-loaded only.
- For loops with 26-gauge cable (used alone or in combination with other gauge cables), the maximum allowable loop length, including bridged taps, is 9 kft.
- If all cable is coarser than 26 gauge, the maximum allowable loop length, including bridged taps, is 12 kft.
- Any single bridged tap is limited to 2 kft maximum length, and the total length of all bridged taps is limited to 2.5 kft maximum length.
- The total length of multi-gauge cable containing 26-gauge cable must not exceed the following:

$$12 - \frac{(3 \times L_{26})}{9 - L_{BTAP}} kft$$

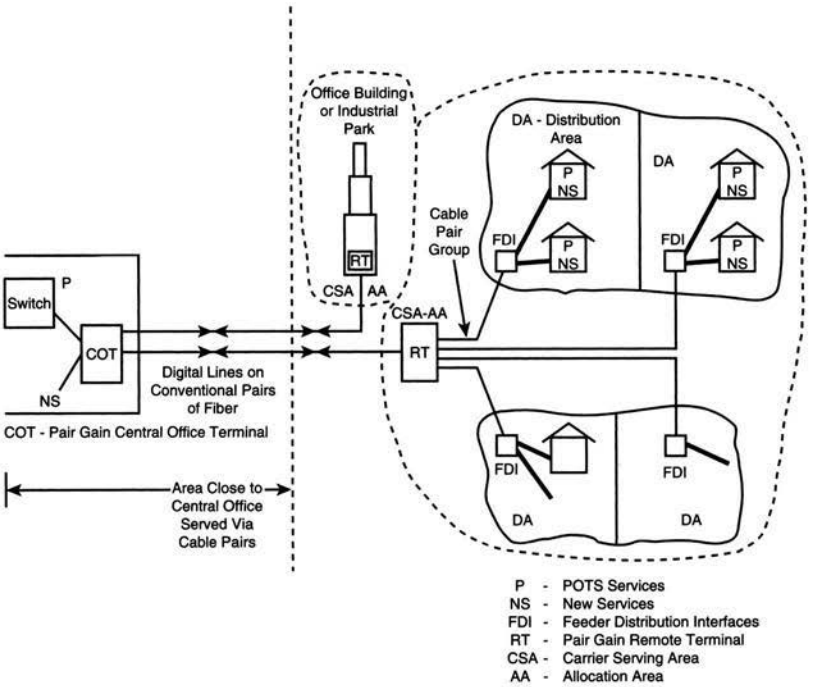
  The value L_{26} is the total length of 26-gauge cable, excluding bridged tap, and L_{BTAP} is the total length of all bridged taps.

- Although not a transmission constraint, it is suggested for administrative purposes that no more than two gauges of cables be used.

A 1991 Bellcore loop survey shows that over 60 percent of DLC loops meet the CSA guidelines.[5] In the context of DSL systems, the term CSA is applied to loops that originate from a CO as well, if they meet CSA guidelines.

A CSA is further divided into one to six *Distribution Areas* (DA), as shown in Figure 2.8. A DA is characterized by a single FDI where crossconnectors are located. A DA typically serves about 500 customers. Distribution cables emanating from an FDI usually have 1.5 to 2 pairs for all potential customer living units. On the other hand, cable pairs from a Remote Terminal (RT) to FDI are installed based on the number of real customer lines with a smaller spare ratio. This strategy is aimed at an overall minimized installation cost. The average serving distance of each DA is usually significantly shorter than that of a CSA. The Bellcore 1991 loop survey shows that most DA distribution loops are less than 6 to 8 kft in length (26 and 24 gauge, respectively).

Figure 2.8 CSA and DA



2.3.3 *T1 Line Configurations*

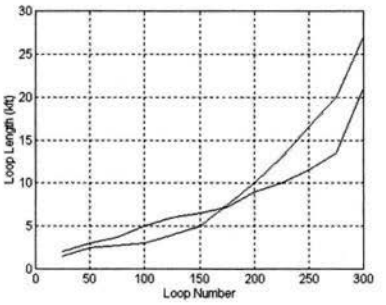
T1 lines,[6] carrying 24 DS0 channels with a transmission rate of 1.544 Mbps, are used for both DLC systems and customer private lines. The T1 technology was originally developed during the 1960s based on semiconductor transistors. A T1 line requires two twisted pairs, with each pair dedicated to one direction of transmission. T1 repeaters, where signals are received and regenerated, are placed along a T1 line at intervals of 6 kft. To minimize the effect of CO noise, the first T1 repeater is only 3 kft away from a CO. The transmission spectrum of T1 is centered around 750 KHz. The transmission power of T1 is relatively high, and a T1 transmitter could produce significant crosstalk noises to a DSL system sharing the same cable and the same frequency band.

T1 lines in the feeder cable are usually well engineered so that binder groups separate from those used for POTS are utilized. Statistically, the percentage of T1 lines in the loop plant is relatively small. Samples of customer T1 private lines are collected from two regional telephone companies.[7]

Figure 2.9 shows length distribution of these T1 lines. There are about 300 different T1 line configurations for each database. Those lines are located in different geographic areas.

Considering that only a limited number of T1 private lines have been installed (around 200,000 in the United States), this sample size is statistically significant. Some configurations have a number of T1 lines running parallel. Most T1 lines have more than one repeater.

Figure 2.9 Private T1 Line Length Distribution



The average T1 line length is 8423 feet, and the median T1 line length is 5383 feet. The average distance between repeaters is 2491 feet, and the median distance is 2487 feet. The average T1 signal loss between repeaters is about 18 dB, which is much lower than the 32 dB design requirement. It is also important to note that, on average, the T1 line multiple number is small; therefore, the number of T1 disturbers will be relatively low.

2.4 *Voice Channel Characteristics*

A DSL system might need to be designed to coexist with a POTS service on the same twisted-pair cable, assuming there is only one twisted-pair loop available to some telephone subscribers. A *Frequency Division Multiplex* (FDM) scheme is necessary to separate the voice channel from the spectrum occupied by a DSL system. The understanding of POTS voice signal level as well as dialing/ring signaling levels is required for the design of a DSL system that coexists with a POTS. Furthermore, a certain signal-to-noise ratio is to be maintained for a voice band modem to operate under out-of-band leakage energy from a DSL system.

Voice signals are digitized by line cards of switches at the end COs. The quantization and aliasing noise generated from the digitization process could be a limiting factor for the optimal performance of a voice band modem. The DSL leakage energy level in the voice band should be kept below this quantization/aliasing noise floor to minimize DSL-to-voice-band interference. The digitization process consists of sampling lowpass filter, companding, Analog to Digital Conversion (ADC), and Pulse Code Modulation (PCM). The sampling filter affects the voice channel frequency response and the amount of aliasing noise. The ADC generates equalization noise. The companding process distorts the analog voice signal such

that more digital bits are allocated to a lower magnitude signal. The companding process effectively enhances the effect of noise.

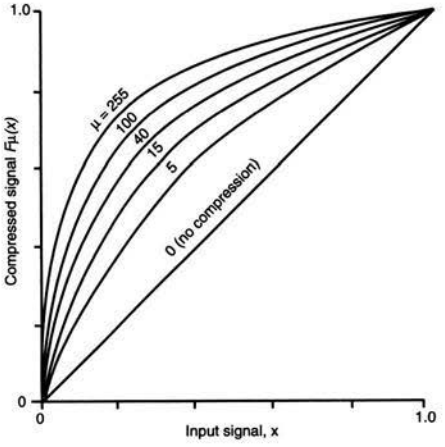
2.4.1 *Companding Methods*

The μ-law of companding is defined by the following expression:

$$F_\mu(x) = \text{sgn}(x)\frac{\ln(1+\mu x)}{\ln(1+\mu)}$$

Figure 2.10 shows how $F_\mu(x)$ changes as a function of μ. Note that for small x, $F_\mu(x)$ approaches a linear function, while for large x, $F_\mu(x)$ approaches a logarithmic function.

Figure 2.10 Logarithmic Companding Characteristics



Although the μ-law of companding has found acceptance in the North American and Japanese digital networks, the standard companding law in Europe is the A-law, which is defined by the following expressions:

$$F_A(x) = \text{sgn}(x)\frac{1+\ln A|x|}{1+\ln A} \quad \frac{1}{A} \le |x| \le 1$$

$$F_A(x) = \text{sgn}(x)\frac{A|x|}{1+\ln A} \quad 0 \le |x| \le \frac{1}{A}$$

Note that for small x, $F_A(x)$ is truly logarithmic for $|x|>1/A$ and truly linear for $|x|<1/A$.

2.4.2 *Voice Channel Attenuation and Phase Delay*

The attenuation and phase delay of a typical voice channel, 3002 line as defined by the traditional Bell system telephony practice, are shown in Figures 2.11 and 2.12, respectively. In Figure 2.11, attenuation values between the two dashed lines are considered acceptable. In Figure 2.12, a phase delay value lower than the dashed line is also considered acceptable. These characteristics are mainly due to the effects of sampling lowpass filter, Digital to Analog Conversion (DAC) reconstruction lowpass filter, and line coupling transformers connection subscriber loops to switches. In addition, the voice signal can be attenuated by up to 22 dB due to subscriber loop (0–4 dB), interoffice trunk (6–12 dB), and CO (0–6 dB) losses.

Figure 2.11 Attenuation of a Voice Channel

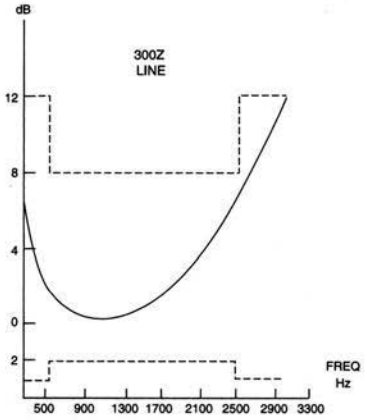
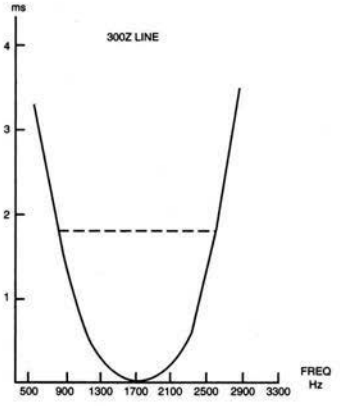


Figure 2.12 Phase Delay of a Voice Channel



The signal power in a voice channel can be measured in dBrn, which is defined as the dB ratio to a reference noise power of 10^{-12} Watt. The voice band signal power is often measured in dBrnc, which is the same dB ratio as defined for dBrn, but with the inclusion of a message-waiting filter. A message-waiting filter has the frequency response similar to our hearing system to de-emphasize energy contribution from lower and higher frequency regions of a 3.3 KHz voice band. For a relatively flat signal, the inclusion of the message-waiting filter could reduce the power by about 2 dB.

For a good voice channel, the required noise level is about 23 dBrnc, which is about 25 dBrn, to achieve a good quality voice transmission for a voice channel loss of about 10 dB. Equivalently, the required voice channel noise level is about 25— –90=— –65 dBm, in which 0 dBrn is equivalent to –90 dBm, which is defined as the dB ratio to a reference noise power of 10^{-3} Watt. The noise power density level is then the following for a 3 KHz voice channel:

$$10\log_{10}\left(10^{\frac{-65}{10}}/3000\right) \approx -100 dBm/Hz$$

Regulations limit the total voice channel transmit signal power level to less than –9 dBm. On the other hand, a mean voltage of about 0.25 volts on a load impedance of 600 ohms generates a total power of –9.8 dBm. This is equivalent to a flat transmit power density level of –44.57 dBm/Hz for a bandwidth of 3 KHz.

2.4.3 *Voice Channel Signaling Tones*

The voice channel relies on signaling tones to establish a telephone connection. Tone dials provide address information during dialing; however, tone dial signals might be high in power. Without proper filtering, tone dial signals could saturate the ADC of a DSL system. Tone dials contain a dual tone multifrequency (DTMF) signal generator with a four-row by three-column push-button pad. Each push-button corresponds to two tones in a two-of-eight scheme.

Figure 2.13 shows the tone frequencies corresponding to each key. The tone frequencies are chosen in such a way that their harmonics and distortion products will not interfere with other DTMF, call progress, or signaling tones. The signal levels applied to the loop at the telephone instrument are 14 to 4 dBm per frequency with a maximum *twist* (level difference between the two tones) of 4 dB.

There are also dial, busy, ringback, and receiver off-hook tones. Parameters of the Precision Tone Plan tones are summarized in Table 2.1.

Figure 2.13 The Dual Tone MultiFrequency (DTMF) Scheme

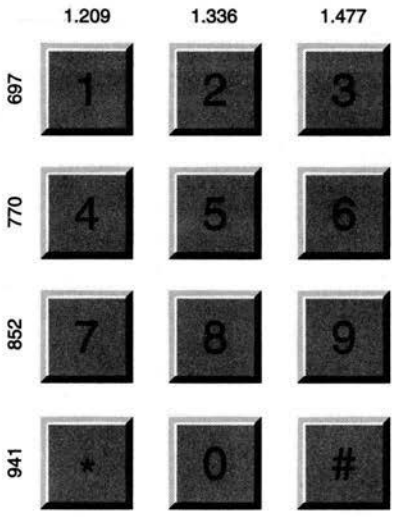


Table 2.1 Common Call Progress Tone Plans

Tone	Tone Frequency	Level per Frequency	Voltage per Frequency	Interruption Rate
Dial	350+440 Hz	–13 dBm	0.17 volts	Continuous
Busy tone	480+620 Hz	–24 dBm	0.049 volts	60 IPM
Ringback	440+480 Hz	–19 dBm	0.087 volts	2 s on and 4 off
Receiver off-hook tone	1400+2060+ 2450+2600 Hz	–6 to 3 dBm	0.39–1.09 volts	Continuous or interrupted

The called telephone is alarmed by a ringing signal. The frequencies normally used for ringing range from 16 Hz to 66 2/3 Hz. They are arranged in relationships and are given such names as ***harmonic***, ***decimonic***, ***synchromonic***, and ***single frequency***, as shown in Table 2.2.

Table 2.2 Common Ringing Schemes

Ringing Scheme	Frequencies (Hz)
Decimonic	20, 30, 40, 50, 60
Harmonic	16 2/3, 25, 33 1/3, 50, 66 2/3
Synchromonic	16, 30, 42, 54, 66
Single frequency	20 (or any above)

The ringing voltage applied to the loop by the CO line circuit varies from a nominal 105 volts at 16 Hz to 140 volts at 66 2/3 Hz. The AC ringing signal is also biased by a DC voltage, usually 48 volts, to enable the CO to detect called party answer by sensing a DC current. Each telephone ringer presents an AC coupled load of between 5000 and 10000 ohms to the loop. Ring voltage can drop to as low as 40 volts on a long loop with a large number of ringers attached.

When the call is answered and the telephone set is picked up off the hook, the ringing voltage can generate an impulse with an amplitude as high as the peak of the ringing signal. This impulse could have an amplitude as high as 150 volts. Impulses can also be generated by a telephone set with a mechanical rotary dialer. A rotary dialer can generate about 10 pulses per second with a peak-to-peak voltage variation of less than 48 volts.

With the general understanding of a telephone subscriber loop and its role in an end-to-end telephone connection, you are ready to explore in more detail the transmission characteristics of DSL systems. Characteristics of a DSL system transmission channel are related to loop distance, cable type, background noise, and noise to and from other coexisting systems. A DSL system is usually engineered with accurate channel and noise models in conjunction with extensive simulation studies.

End Notes

1. Members of the technical staff, Bell Telephone Laboratories, *Transmission Systems for Communications*, Fifth Edition (Bell Telephone Laboratories, Inc., 1982).
2. W. D. Reeve, *Subscriber Loop Signaling and Transmission Handbook, Analog* (IEEE Press, 1992).
3. T. H. Wu, *Fiber Network Service Survivability* (Artech House, 1992).
4. "ISDN Basic Access Digital Subscriber Lines," *Bellcore Technical Reference,* TR-TSY-000393, Issue 1 (May 1988).
5. "Generic Requirements for High-Bit-Rate Digital Subscriber Lines," *Bellcore Technical Advisory*, TA-NWT-001210, Issue 1 (October 1991).
6. H. Cravis and T. V. Crater, "Engineering of T1 Carrier Systems Repeated Lines," *Bell System Tech J.,* vol. 42 (March 1996): 431–486.
7. W. Y. Chen and D. L. Waring, "Applicability of ADSL to Support Video Dial Tone in the Copper Loop," *IEEE Communications Magazine,* vol. 32, no. 5 (May 1994): 102–109.

CHAPTER 3

Twisted-Pair Channel Modeling

The twisted-pair telephone loop transmission channel modeling has played an important role in the engineering of DSL systems. Following a tradition of ensuring a better than 95 percent rate of success for first time installations, DSL systems have been designed for satisfactory operations in worst-case transmission conditions.

For channel modeling, worst-case telephone loop configurations are first obtained through extensive loop surveys. The transmission characteristics of these worst-case loops are then simulated with channel impulse responses derived from twisted-pair cable primary parameters available through accurate measurements. With accurate channel models, computer simulation studies can be carried out to understand the transmission performance potential of the telephone subscriber loop plant under different system assumptions.

With channel models in conjunction with noise models (presented in Chapter 4, "Transceiver Front-End Noise Models"), advanced transceiver architectures and signal processing algorithms can be tested for the telephone loop plant environment effectively and efficiently. This chapter explains the basic concepts and techniques of twisted-pair channel modeling, as follows:

- *Primary and secondary parameters of twisted-pair cables.* The transmission characteristics of a twisted-pair cable can be accurately specified by primary parameters as defined for a distributed equivalent circuit of a transmission line. The secondary parameters have often been used for performance analysis of ideal transmission lines; however, both primary and secondary parameters of twisted-pair cables are frequency dependent.
- *Two port network ABCD parameters.* ABCD parameters of a two-port network equivalent circuit can be obtained for a twisted-pair cable from its secondary parameters. To construct accurate channel models for twisted-pair telephone loops, each cable section is

represented by its ABCD parameters. The ABCD parameters of the twisted-pair telephone loop are then obtained by cascading all cable sections in series. A general purpose electronic circuit can also be divided into a few two-port networks to simplify required transmission performance analysis.

- *Channel transfer function, insertion loss, and impulse response.* The transfer function of a twisted-pair telephone loop can be calculated from its ABCD parameters. The insertion loss, which is a slight variation of the transfer function, has been used as the channel model for DSL system performance simulation studies. The corresponding impulse response is used in simulation studies to generate a received signal at the input of a DSL transceiver.
- *Extended twisted-pair primary constants.* Some basic twisted-pair cable primary parameters are listed in Tables 3.2, 3.3, and 3.4 at the end of this chapter. The frequency range of these parameters has been extended from 5 MHz to 20 MHz based on the frequency relationships of these parameters discussed early in the initial sections of this chapter.

3.1 Primary and Secondary Parameters of Twisted-Pair Cables

A specific telephone subscriber loop model can be constructed according to twisted-pair cable primary constants.[1,2] In general, twisted cable primary constants R, L, and G are variables of frequency, while shunt capacitance C can be considered as fixed without losing too much accuracy. Figures 3.1, 3.2, and 3.3 show frequency characteristics of the series resistance R, series inductance L, and shunt conductance G, respectively, for a 26-gauge PIC cable at the temperature of 70 degrees Fahrenheit.

Figure 3.1 The Series Resistance of the 26-Gauge PIC Cable

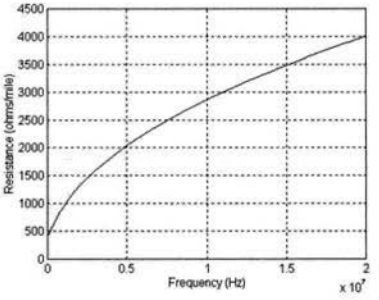


Figure 3.2 The Series Inductance of the 26-Gauge PIC Cable

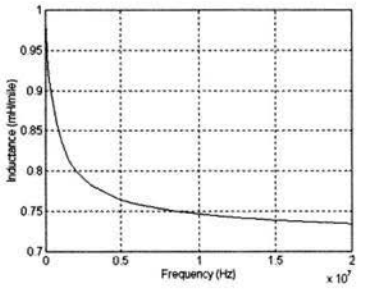
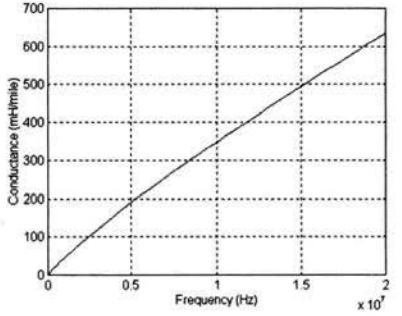


Figure 3.3 The Shunt Conductance of the 26-Gauge PIC Cable

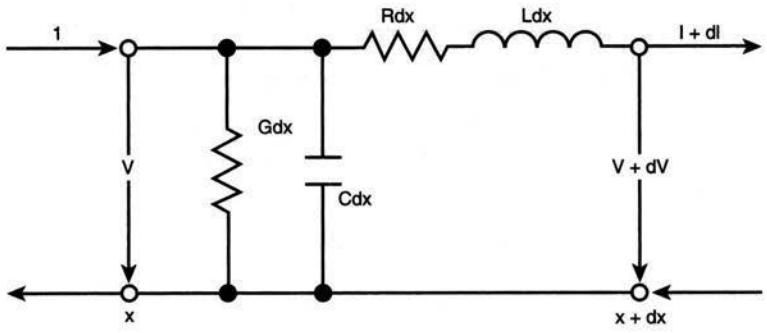


Values of these primary constants are expressed in terms of per unit distance. This kind of description is consistent with the distributed equivalent circuit of a transmission line. Figure 3.4 shows a unit component of such a distributed equivalent circuit. The equivalent circuit of an ideal transmission line consists of many of these units, with identical and frequency-independent primary constants, connected in a cascade. A twisted-pair cable can also be represented with this kind of distributed equivalent circuit, except these primary constants are frequency dependent.

These primary parameters can be measured directly or indirectly with wide bandwidth and high precision test equipment; however, some data fitting might be necessary due to the sensitivity of these measurements. Data fitting can be based on some general frequency relationships of these primary parameters. The series resistance as represented in Figure 3.1 is approximately proportional to the square root of frequency:

$$R(f) = a + b\sqrt{f}$$

Figure 3.4 The Transmission Line Equivalent Circuit



The values for *a* and *b* are empirically obtained by comparing them with measurements. The series inductance as represented in Figure 3.2 is approximately proportional to the inverse of the square root of frequency:

$$L(f) = c + \frac{d}{\sqrt{f}}$$

The values for *c* and *d* are also empirically obtained. The shunt conductance as represented in Figure 3.3 is approximately proportional to the frequency. In general, these series resistance, series inductance, and shunt conductance fittings are only valid for a limited frequency range.

These methods of primary parameter fitting can also be used to estimate twisted-pair cable parameters at frequencies that exceed existing measurements.[3] By fitting measurements from 1 MHz to 5 MHz, for example, you can obtain estimated series resistance and inductance for frequencies up to 20 MHz.

According to these primary constants, you can find twisted-pair cable secondary parameters, characteristic impedance:

$$Z_0(s) = \sqrt{\frac{R(f) + sL(f)}{G(f) + sC(f)}}$$

The complex frequency of $s=j2nf$ is introduced for the complex characteristics impedance and the propagation constant:

$$\gamma(s)=\sqrt{\left(G(f)+sC(f)\right)\left(R(f)\right)+sL(f)\right)}$$

As expected, both the characteristic impedance and propagation constant of a loop constructed with twisted-wire pairs are functions of frequency.

A loop is perfectly terminated if it is terminated with its characteristic impedance. For a perfectly terminated loop with length d, the transfer function is given by

$$H(d,s)=e^{-d\gamma(s)}=e^{-d\alpha(f)}e^{-jd\beta(f)}$$

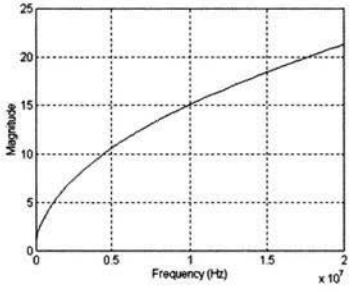
The values are as follows:

$\gamma(s)$ is a complex function of frequency f.

$\alpha(f)$ and $\beta(f)$ are both real functions of frequency f.

Figures 3.5 and 3.6 show the real part and the imaginary part, respectively, of the propagation constant.

Figure 3.5 The Real Part of the Propagation Constant for 26-Gauge PIC Cable

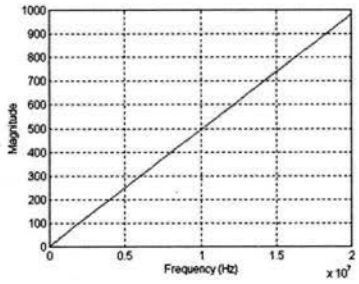


At high frequency, $f>250\ kHz$, the twisted-pair transfer function can be simplified as follows:

$$H(d,f)=e^{-d\left(k_1\sqrt{f}+k_2 f\right)}e^{-jdk_3 f}$$

The value for d is assumed to be in units of mile, and f is in units of Hertz.

Figure 3.6 The Imaginary Part of the Propagation Constant for 26-Gauge PIC Cable



The proportional constants k_1 and k_2 can be estimated by minimizing the mean square fitting error between real parts of the simplified model and $\alpha(f)$, while k_3 can be easily identified by comparing it with the imaginary parts. For real parts, you have

$$\varepsilon_i^2 = \left(k_1\sqrt{f_i} + k_2 f_i - \alpha_i(f_i)\right)^2$$

for different frequency points. Taking partial derivatives of the error sum at different frequencies and making them equal to zeros results in the following:

$$k_1 \sum_{i=1}^{n} f_i + k_2 \sum_{i=1}^{n} f_i^{1.5} = \sum_{i=1}^{n} f_i^{0.5}\alpha_i(f_i)$$

$$k_1 \sum_{i=1}^{n} f_i^{1.5} + k_2 \sum_{i=1}^{n} f_i^{2} = \sum_{i=1}^{n} f_i\alpha_i(f_i)$$

Values of k_is for different gauge of twisted pairs are summarized in Table 3.1.

Table 3.1 Parameters for a Simplified Cable Model

Gauge	k_1 ($\times 10^{-3}$)	k_2 ($\times 10^{-8}$)	k_3 ($\times 10^{-5}$)
22	3.0	0.035	4.865
24	3.8	–0.541	4.883
26	4.8	–1.709	4.907

When the channel attenuation or loss is expressed in units of dB, you have[4]

$$L_{dB}(d,f) = -20\log_{10}|H(d,f)| = \frac{20}{\ln 10} d\alpha(f) \approx 8.686 d\alpha(f)$$

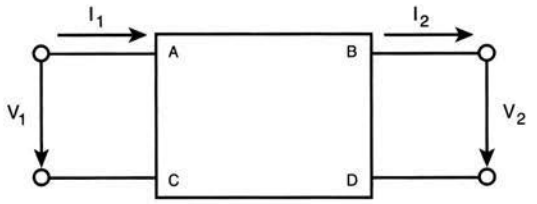
The loss value in dB units is proportional to the length of a cable. Supposing that the loss is 20 dB at a particular frequency for a 5 kft loop, the loss would be 30 dB for a 7.5 kft loop of the same gauge at the same frequency.

3.2 Two-Port Networks and ABCD Parameters

The simplified twisted-pair cable transfer function based on the propagation constant $H(d,f) = e^{-d\alpha(f)}e^{-jd\beta(f)}$ is only good for a single gauge twisted pair with perfect terminations at both ends. A subscriber loop, however, usually consists of many sections of different gauge, with bridged taps, and terminated with a resistive impedance. The transfer function of a telephone subscriber loop is not a simple product of transfer functions of these twisted-pair cable sections because of impedance mismatches. To accurately represent a subscriber loop channel, the concept of a two-port network and its ABCD parameter representation is normally used for the analysis of DSL systems.

An electronic circuit usually has an input port and an output port. The function of the electronic circuit is to produce a desired output signal based on a certain input signal. A twisted-pair cable section or a twisted-pair telephone subscriber loop also has an input port and an output port. The function of an electronic circuit or the transfer function of a twisted-pair telephone loop can be determined according to its input/output current/voltage relationships. Figure 3.7 shows the model of a two-port network that can represent an electronic circuit or a twisted-pair telephone loop.

Figure 3.7 A Standalone Two-Port Network



V_1 and I_1 are input port voltage and current, respectively. V_2 and I_2 are output port voltage and current, respectively. Input port voltage and current and output port voltage and current are related by ABCD parameters of the two-port network.

For a standalone two-port network, the input and output voltage and current relationship is represented as follows:

$$V_1 = AV_2 + BI_2$$

$$I_1 = CV_2 + DI_2$$

or in matrix format as

$$\begin{bmatrix} V_1 \\ I_1 \end{bmatrix} = \begin{bmatrix} A & B \\ C & D \end{bmatrix} \begin{bmatrix} V_2 \\ I_2 \end{bmatrix}$$

in which these ABCD parameters are defined as

$$A = \frac{V_1}{V_2}\bigg|_{I_2=0}$$

$$B = \frac{V_1}{I_2}\bigg|_{V_2=0}$$

$$C = \frac{I_1}{V_2}\bigg|_{I_2=0}$$

$$D = \frac{I_1}{I_2}\bigg|_{V_2=0}$$

ABCD parameters for a simple two-port network consisting of a series impedance, as shown in Figure 3.8, can be derived as follows:

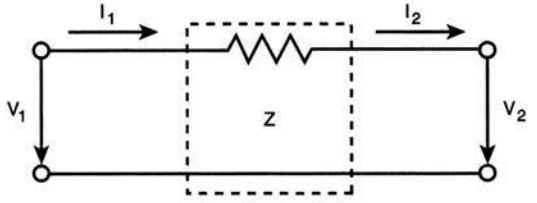
$$A = \frac{V_1}{V_2}\bigg|_{I_2=0} = 1$$

$$B = \frac{V_1}{I_2}\Big|_{V_2=0} = Z$$

$$C = \frac{I_1}{V_2}\Big|_{I_2=0} = 0$$

$$D = \frac{I_1}{I_2}\Big|_{V_2=0} = 1$$

Figure 3.8 A Series Impedance as a Two-Port Network



Therefore, the ABCD parameter matrix for a series impedance Z as a two-port network is as follows:

$$\begin{bmatrix} A & B \\ C & D \end{bmatrix} = \begin{bmatrix} 1 & Z \\ 0 & 1 \end{bmatrix}$$

ABCD parameters for another simple two-port network consisting of a shunt impedance, as shown in Figure 3.9, can be derived as follows:

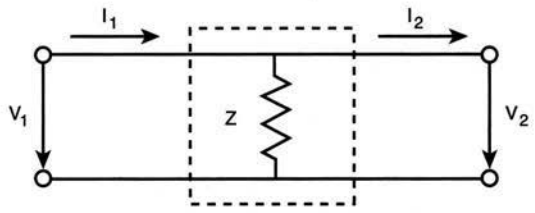
$$A = \frac{V_1}{V_2}\Big|_{I_2=0} = 1$$

$$B = \frac{V_1}{I_2}\Big|_{V_2=0} = 0$$

$$C = \frac{I_1}{V_2}\Big|_{I_2=0} = \frac{1}{Z}$$

$$D = \frac{I_1}{I_2}\Big|_{V_2=0} = 1$$

Figure 3.9 A Shunt Impedance as a Two-Port Network



Therefore, the ABCD parameter matrix for a shunt impedance Z is

$$\begin{bmatrix} A & B \\ C & D \end{bmatrix} = \begin{bmatrix} 1 & 0 \\ Z^{-1} & 1 \end{bmatrix}$$

ABCD parameters of a twisted-pair cable are complex and frequency dependent, and they are related to characteristic impedance $Z_o(s)$ and propagation constant $\gamma(s)$, as follows:

$$A(s) = D(s) = \cosh \gamma(s)d$$

$$B(s) = Z_0(s) = \sinh \gamma(s)d$$

$$C(s) = \frac{1}{Z_0(s)} \sinh \gamma(s)d$$

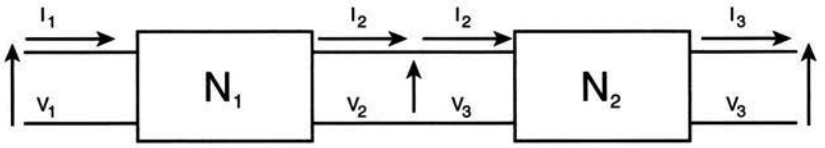
The value for d is the length of the twisted-pair cable.

Many electronic circuits can be divided into a few simpler two-port networks. These simpler two-port networks are usually connected either in series or in parallel. A twisted-pair telephone loop consists of many twisted-pair cables in series. The use of twisted-pair ABCD parameters is convenient because each section of a twisted-pair subscriber loop can be described by its own ABCD parameters, and the ABCD parameters of the whole subscriber loop are the matrix product of individual ABCD matrices.

3.2.1 *Two-Port Networks in Series*

You can obtain the ABCD parameters of two two-port networks in series by equating the voltage and current of the first two-port network to that of the following network, as shown in Figure 3.10, and deriving the relationship between input voltage and current of the first two-port network to output voltage and current of the following network.

Figure 3.10 Two Two-Port Networks in Series



For two two-port networks in series, the input and output voltage and current relationship is represented as follows:

$$\begin{bmatrix} V_1 \\ I_1 \end{bmatrix} = \begin{bmatrix} A_1 & B_1 \\ C_1 & D_1 \end{bmatrix} \begin{bmatrix} V_2 \\ I_2 \end{bmatrix}$$

$$\begin{bmatrix} V_2 \\ I_2 \end{bmatrix} = \begin{bmatrix} A_2 & B_2 \\ C_2 & D_2 \end{bmatrix} \begin{bmatrix} V_3 \\ I_3 \end{bmatrix}$$

and

$$\begin{bmatrix} V_1 \\ I_1 \end{bmatrix} = \begin{bmatrix} A_1 & B_1 \\ C_1 & D_1 \end{bmatrix} \begin{bmatrix} A_2 & B_2 \\ C_2 & D_2 \end{bmatrix} \begin{bmatrix} V_3 \\ I_3 \end{bmatrix}$$

Therefore, the ABCD parameter matrix for two two-port networks in series is

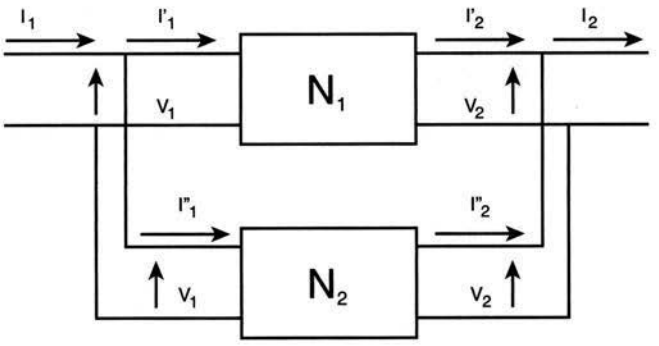
$$\begin{bmatrix} A & B \\ C & D \end{bmatrix} = \begin{bmatrix} A_1 & B_1 \\ C_1 & D_1 \end{bmatrix} \begin{bmatrix} A_2 & B_2 \\ C_2 & D_2 \end{bmatrix} = \begin{bmatrix} A_1A_2 + B_1C_2 & A_1B_2 + B_1D_2 \\ C_1A_2 + D_1C_2 & C_1B_2 + D_1D_2 \end{bmatrix}$$

3.2.2 *Two-Port Networks in Parallel*

You can obtain the ABCD parameters of two two-port networks in parallel by equating the input and output voltages of the two-port networks, as shown in Figure 3.11, and deriving

the relationship between the input voltage and combined input current, as well as between the output voltage and combined output current of these two two-port networks.

Figure 3.11 Two Two-Port Networks in Parallel



Voltage and current relationships of two two-port networks in parallel are represented as

$$\begin{bmatrix} V_1 \\ I'_1 \end{bmatrix} = \begin{bmatrix} A_1 & B_1 \\ C_1 & D_1 \end{bmatrix} \begin{bmatrix} V_2 \\ I'_2 \end{bmatrix}$$

$$\begin{bmatrix} V_1 \\ I''_1 \end{bmatrix} = \begin{bmatrix} A_2 & B_2 \\ C_2 & D_2 \end{bmatrix} \begin{bmatrix} V_2 \\ I''_2 \end{bmatrix}$$

$$I_1 = I'_1 + I''_1$$

$$I_2 = I'_2 + I''_2$$

Combining

$$V_1 = A_1 V_2 + B_1 I'_2$$

and

$$V_1 = A_2 V_2 + B_2 I''_2$$

results in the following:

$$V_1 = \frac{A_1 B_2 + A_2 B_1}{B_1 + B_2} V_2 + \frac{B_1 B_2}{B_1 + B_2} I_2$$

You also have

$$I_1 = (C_1 + C_2)V_2 + D_1 I'_2 + D_2 I''_2$$

which can be expressed as

$$B_2 I_1 = B_2(C_1 + C_2)V_2 + D_2(A_1 - A_2)V_2 + (B_1 D_2 + B_2 D_1)I'_2$$

or

$$B_1 I_1 = B_1(C_1 + C_2)V_2 + D_1(A_2 - A_1)V_2 + (B_1 D_2 + B_2 D_1)I''_2$$

by using

$$A_1 V_2 + B_1 I'_2 = A_2 V_2 + B_1 I''_2$$

Combining these two expressions together results in the following:

$$I_1 = \frac{(B_1 + B_2)(C_1 + C_2) + (D_1 - D_2)(A_2 - A_1)}{B_1 + B_2} V_2 + \frac{B_1 D_2 + B_2 D_1}{B_1 + B_2} I_2$$

Therefore, the ABCD parameter matrix for two two-port networks in parallel is

$$\begin{bmatrix} A & B \\ C & D \end{bmatrix} = \frac{1}{B_1 + B_2} \begin{bmatrix} A_1 B_2 + B_1 A_2 & B_1 B_2 \\ (B_1 + B_2)(C_1 + C_2) - (A_1 - A_2)(D_1 - D_2) & B_1 D_2 + D_1 B_2 \end{bmatrix}$$

The special case of two identical two-port networks in parallel is represented as

$$A_p = A$$

$$B_p = \frac{B}{2}$$

$$C_p = 2C$$

$$D_p = D$$

in which A, B, C, and D are the ABCD parameters of each individual two-port network, and A_p, B_p, C_p, and D_p are ABCD parameters of two two-port networks in parallel.

3.3 Channel Transfer Function and Impulse Response

The ABCD matrix information of a twisted-pair telephone loop can be easily converted into its input impedance or cable transfer function. Corresponding calculations can be put into a computer program[5] to generate channel models in conjunction with a few tables of twisted-pair cable primary parameters. The input impedance of a twisted-pair loop with a terminal impedance of $Z_t(s)$ is expressed as

$$Z_i(s) = \frac{A(s) + \dfrac{B(s)}{Z_t(s)}}{C(s) + \dfrac{D(s)}{Z_t(s)}}$$

in which $A(s)$, $B(s)$, $C(s)$, and $D(s)$ are complex frequency dependent ABCD parameters of a twisted-pair telephone loop. When the other end of the twisted-pair loop is left open, you have the following:

$$Z_{i,o}(s) = \frac{A(s)}{C(s)}$$

This is also the impedance of a bridged tap. A bridged tap can be considered as a two-port network with only a shunt impedance. Therefore, the ABCD parameters of a bridged tap are as follows:

$$\begin{bmatrix} 1 & 0 \\ \dfrac{C_{bridge}(s)}{A_{bridge}(s)} & 1 \end{bmatrix}$$

The values $A_{bridge}(s)$ and $D_{bridge}(s)$ are parts of frequency-dependent ABCD parameters of the section of twisted-pair cable connected as a bridged tap.

The transfer function of a twisted-pair loop with a source impedance of $Z_s(s)$ and a terminal impedance of $Z_t(s)$ is

$$H(s)=\frac{Z_t(s)}{Z_s(s)\big(C(s)Z_t(s)+D(s)\big)+A(s)Z_t(s)+B(s)}$$

When the effect of source impedance is excluded, that is $Z_s(s)=0$, you have the following:

$$H(s)=\frac{1}{A(s)+\dfrac{B(s)}{Z_t(s)}}$$

Following earlier practices of the Bell System[6], the insertion loss, which is defined as

$$H_{INS}(s)=\frac{Z_s(s)+Z_t(s)}{Z_s(s)\big(C(s)Z_t(s)+D(s)\big)+A(s)Z_t(s)+B(s)}$$

has been used as the channel model for DSL system performance simulation studies.[7] The use of insertion loss avoids the signal loss caused by the voltage division between source and loop input impedance while still including the effect of the source impedance or the voltage division between source and termination impedance when the loop is very short. For an example of a zero length or null loop, that is, for

$$\begin{bmatrix} A & B \\ C & D \end{bmatrix}=\begin{bmatrix} 1 & 0 \\ 0 & 1 \end{bmatrix}$$

the transfer function is

$$H(s)=\frac{Z_t(s)}{Z_s(s)+Z_t(s)}$$

while the insertion loss is

$$H_{INS}(s)=\frac{Z_s(s)+Z_t(s)}{Z_s(s)+Z_t(s)}=1$$

Figures 3.12 and 3.13 show real and imaginary parts, respectively, of the input impedance for the 9 kft 26-gauge twisted-pair loop with a terminal resistance of 100 ohm.

Figure 3.12 The Real Part of the Input Impedance of the 9 kft 26-Gauge Twisted-Pair Loop

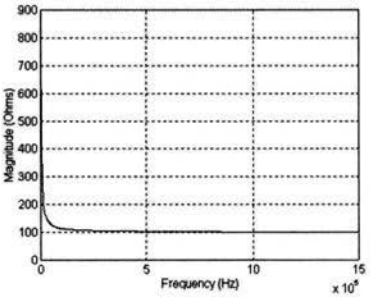


Figure 3.13 The Imaginary Part of the Input Impedance of the 9 kft 26-Gauge Twisted-Pair Loop

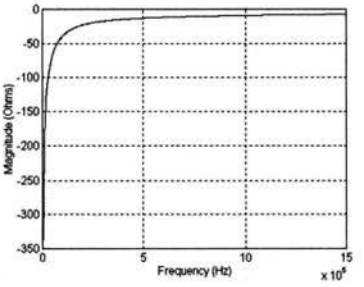
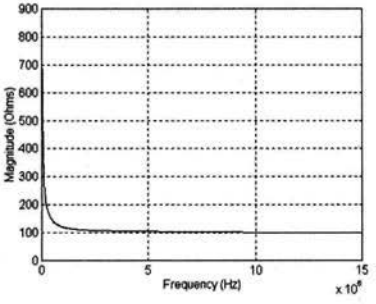


Figure 3.14 shows the magnitude of the input impedance for the 9kft 26-gauge twisted-pair loop with a terminal resistance of 100 ohms.

Figure 3.14 The Input Impedance of the 9 kft 26-Gauge Twisted-Pair Loop



Figures 3.15 and 3.16 show the magnitude and phase, respectively, of the insertion loss for the 9 kft 26-gauge twisted-pair loop.

Figure 3.15 The Magnitude of the Insertion Loss for the 9 kft 26-Gauge Loop

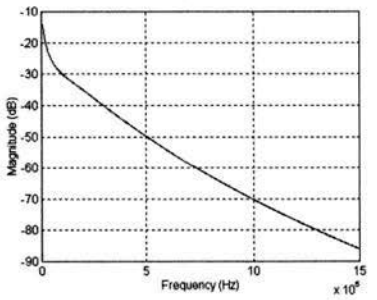


Figure 3.16 The Phase of the Insertion Loss for the 9 kft 26-Gauge Loop

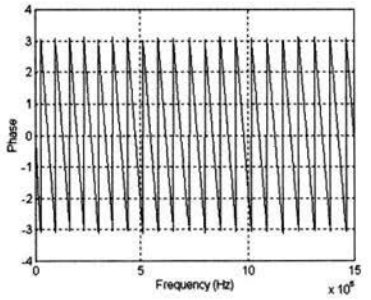


Figure 3.17 shows the corresponding impulse response of the 9kft 26-gauge twisted-pair loop.

Figure 3.17 The Impulse Response of the 9 kft 26-Gauge Loop

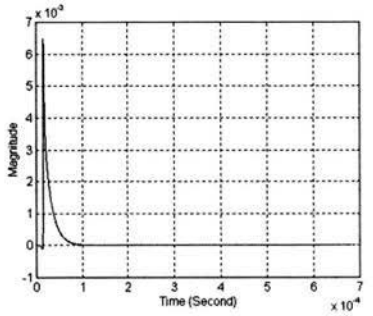


Figure 3.18 shows the configuration of a twisted-pair subscriber loop with bridged taps.

Figure 3.18 The Configuration of a Subscriber Loop with Bridged Taps

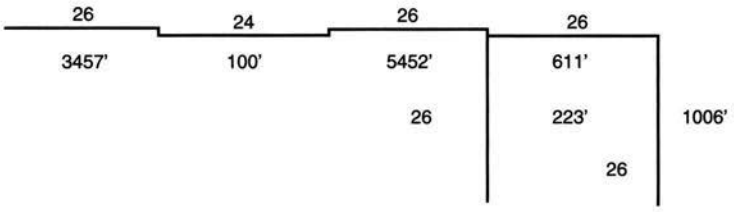


Figure 3.19 shows the magnitude of the input impedance at both ends of the loop.

Figure 3.19 The Input Impedance of a Twisted-Pair Loop with Bridged Taps

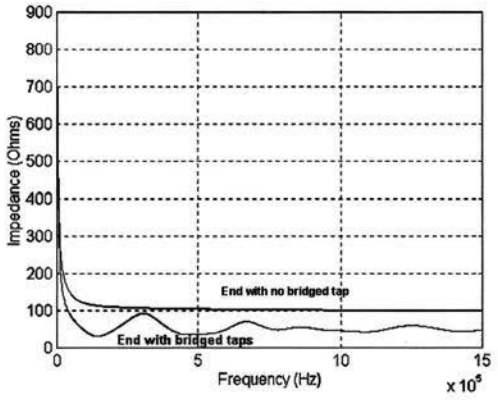
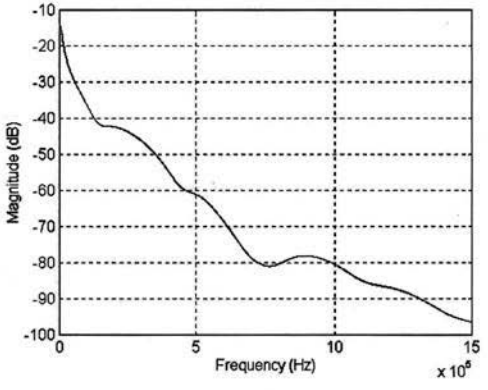


Figure 3.20 shows the magnitude of the transfer function for the loop in both directions.

Figure 3.20 The Transfer Function of a Twisted-Pair Loop with Bridged Taps



The input impedance is different at each end of a twisted-pair loop with bridged taps, while the insertion loss for the same twisted-pair loop with bridged taps and the same source and terminal impedance are the same in different directions. This can be explained as follows: The ABCD parameters of a two-port network at the reverse direction are related to those of the same two-port network at the forward direction as

$$\begin{bmatrix} A_r & B_r \\ C_r & D_r \end{bmatrix} = \begin{bmatrix} D_f & B_f \\ C_f & S_f \end{bmatrix}$$

Therefore the input impedance of a twisted-pair telephone loop at the reverse direction is

$$Z_{ri}(s) = \frac{A_r(s) + \dfrac{B_r(s)}{Z_t(s)}}{C_r(s) + \dfrac{D_r(s)}{Z_t(s)}} = \frac{D_f(s) + \dfrac{B_f(s)}{Z_t(s)}}{C_f(s) + \dfrac{A_f(s)}{Z_t(s)}} \neq Z_{fi}(s) = \frac{A_f(s) + \dfrac{B_f(s)}{Z_t(s)}}{C_f(s) + \dfrac{D_f(s)}{Z_t(s)}}$$

The input impedance at different ends are different because $A_f(s)$ $D_f(s)$ for twisted-pair telephone loops with random bridged taps. On the other hand, the insertion loss at the reverse direction of a twisted-pair telephone loop with bridged taps and the same source and terminal impedance, $Z(s)$, is:

$$H_{INS_r}(s) = \frac{2Z(s)}{C_r(s)Z^2(s) + (D_r(s) + A_r(s))Z(s) + B_r(s)} = \frac{2Z(s)}{C_f(s)Z^2(s) + (A_f(s) + D_f(s))Z(s) + B_f(s)} = H_{INSf}(s)$$

The insertion loss at different directions of a twisted-pair telephone loop with random bridged taps could be the same as long as source and terminal impedance are the same.

3.4 *Extended Twisted-Pair Primary Constants*

Tables 3.2, 3.3, and 3.4 list the frequency-dependent primary parameters for 22-gauge, 24-gauge, and 26-gauge PIC twisted-pair cables, respectively, at a temperature of 70° F. More detailed data can be found in DSL standard documents that are cited in Chapter 1, "Introduction," as well as the references at the end of this chapter.

Parameters are listed in the following tables with a log frequency scale. Some data fitting is necessary when using these tables to construct channel models. Primary parameters have been extended from 5 MHz to 20 MHz according to frequency relationships discussed in

section 3.1, "Primary and Secondary Parameters of Twisted-Pair Cables," earlier in this chapter. The use of different fitting methods could cause some small discrepancies in the resulting channel models.

Table 3.2 22-Gauge PIC Cable at 70 Degrees F

Frequency (Hz)	R (ohm/Mile)	L (mH/Mile)	G (μ–Mho/ Mile)	C (μF/ Mile)
1	174.27	0.9861	0.000	0.083
5	174.27	0.9861	0.001	0.083
10	174.27	0.9861	0.001	0.083
15	174.27	0.9861	0.001	0.083
20	174.27	0.9861	0.002	0.083
30	174.27	0.9861	0.003	0.083
50	174.27	0.9861	0.005	0.083
70	174.27	0.9861	0.006	0.083
100	174.27	0.9861	0.009	0.083
150	174.27	0.9860	0.013	0.083
200	174.27	0.986	0.017	0.083
300	174.28	0.9860	0.024	0.083
500	174.29	0.9858	0.040	0.083
700	174.29	0.9857	0.054	0.083
1000	174.31	0.9856	0.076	0.083
1500	174.34	0.9853	0.110	0.083
2000	174.37	0.9850	0.145	0.083
3000	174.44	0.9844	0.211	0.083
5000	174.62	0.9833	0.341	0.083
7000	174.83	0.9821	0.467	0.083
10000	175.22	0.9804	0.652	0.083
15000	176.06	0.9778	0.954	0.083
20000	177.11	0.9744	1.248	0.083
30000	179.86	0.9672	1.824	0.083
50000	187.64	0.9491	2.943	0.083
70000	197.71	0.9372	4.032	0.083
100000	215.55	0.9237	5.630	0.083
150000	247.57	0.9055	8.229	0.083
200000	277.95	0.8898	10.772	0.083
300000	333.39	0.8642	15.744	0.083

Frequency (Hz)	R (ohm/Mile)	L (mH/Mile)	G (μ–Mho/ Mile)	C (μF/ Mile)
500000	421.57	0.8309	25.396	0.083
700000	493.24	0.8123	34.796	0.083
1000000	583.59	0.7950	48.587	0.083
1500000	707.91	0.7783	71.014	0.083
2000000	812.72	0.7681	92.958	0.083
3000000	988.53	0.7557	135.865	0.083
5000000	1267.31	0.7429	219.158	0.083
7000000	1493.93	0.7367	300.284	0.083
10000000	1779.64	0.7309	419.297	0.083
15000000	2172.76	0.7254	612.834	0.083
20000000	2504.18	0.7222	802.205	0.083

Table 3.3 24-Gauge PIC Cable at 70 Degrees F

Frequency (Hz)	R (ohm/Mile)	L (mH/Mile)	G (μ–Mho/ Mile)	C (μF/ Mile)
1	277.19	0.9861	0.000	0.083
5	277.19	0.9861	0.001	0.083
10	277.19	0.9861	0.002	0.083
15	277.19	0.9861	0.003	0.083
20	277.19	0.9861	0.004	0.083
30	277.19	0.9861	0.005	0.083
50	277.19	0.9861	0.008	0.083
70	277.19	0.9861	0.011	0.083
100	277.19	0.9861	0.016	0.083
150	277.20	0.9860	0.022	0.083
200	277.20	0.9860	0.028	0.083
300	277.20	0.9860	0.040	0.083
500	277.21	0.9859	0.063	0.083
700	277.22	0.9858	0.084	0.083
1000	277.23	0.9857	0.115	0.083
1500	277.25	0.9854	0.164	0.083

continues

Table 3.3 Continued

Frequency (Hz)	R (ohm/Mile)	L (mH/Mile)	G (μ–Mho/ Mile)	C (μF/ Mile)
2000	277.28	0.9852	0.210	0.083
3000	277.34	0.9848	0.299	0.083
5000	277.48	0.9839	0.466	0.083
7000	277.66	0.9829	0.625	0.083
10000	277.96	0.9816	0.853	0.083
15000	278.58	0.9793	1.213	0.083
20000	279.35	0.9770	1.558	0.083
30000	281.30	0.9723	2.217	0.083
50000	286.82	0.9577	3.458	0.083
70000	294.29	0.9464	4.634	0.083
100000	308.41	0.9347	6.320	0.083
150000	337.22	0.9204	8.993	0.083
200000	369.03	0.9087	11.550	0.083
300000	431.55	0.8885	16.436	0.083
500000	541.69	0.8570	25.633	0.083
700000	632.08	0.8350	34.351	0.083
1000000	746.04	0.8146	46.849	0.083
1500000	902.84	0.7947	66.665	0.083
2000000	1035.03	0.7825	85.624	0.083
3000000	1256.77	0.7676	121.841	0.083
5000000	1608.38	0.7523	190.021	0.083
7000000	1894.20	0. 7449	254.644	0.083
10000000	2254.56	0.7380	347.294	0.083
15000000	2750.38	0.7314	494.193	0.083
20000000	3168.38	0.7275	634.737	0.083

Table 3.4 26-Gauge PIC Cable at 70 Degrees F

Frequency (Hz)	R (ohm/Mile)	L (mH/Mile)	G (μ–Mho/ Mile)	C (μF/ Mile)
1	440.75	0.9861	0.000	0.083
5	440.75	0.9861	0.001	0.083

Frequency (Hz)	R (ohm/Mile)	L (mH/Mile)	G (μ–Mho/ Mile)	C (μF/ Mile)
10	440.75	0.9861	0.002	0.083
15	440.76	0.9861	0.003	0.083
20	440.76	0.9861	0.004	0.083
30	440.76	0.9861	0.005	0.083
50	440.76	0.9861	0.008	0.083
70	440.76	0.9861	0.011	0.083
100	440.76	0.9861	0.016	0.083
150	440.76	0.9861	0.022	0.083
200	440.76	0.9860	0.028	0.083
300	440.76	0.9860	0.040	0.083
500	440.77	0.9859	0.063	0.083
700	440.78	0.9859	0.084	0.083
1000	440.79	0.9858	0.115	0.083
1500	440.81	0.9856	0.164	0.083
2000	440.83	0.9854	0.210	0.083
3000	440.88	0.9850	0.299	0.083
5000	441.01	0.9843	0.466	0.083
7000	441.15	0.9836	0.625	0.083
10000	441.39	0.9825	0.853	0.083
15000	441.87	0.9907	1.213	0.083
20000	442.45	0.9789	1.558	0.083
30000	443.88	0.9753	2.217	0.083
50000	447.81	0.9660	3.458	0.083
70000	453.09	0.9546	4.634	0.083
100000	463.39	0.9432	6.320	0.083
150000	485.80	0.9306	8.993	0.083
200000	513.04	0.9212	11.550	0.083
300000	575.17	0.9062	16.436	0.083
500000	699.61	0.8816	25.633	0.083
700000	812.95	0.8614	34.351	0.083
1000000	956.65	0.8381	46.849	0.083
1500000	1154.38	0.8146	66.665	0.083
2000000	1321.07	0.8001	85.624	0.083

continues

Table 3.4 Continued

Frequency (Hz)	R (ohm/Mile)	L (mH/Mile)	G (μ–Mho/ Mile)	C (μF/ Mile)
3000000	1600.68	0.7823	121.841	0.083
5000000	1267.31	0.7638	190.021	0.083
7000000	2044.07	0.7552	254.643	0.083
10000000	2858.90	0.7469	347.294	0.083
15000000	3484.14	0.7391	494.193	0.083
20000000	4011.24	0.7344	634.737	0.083

End Notes

1. "Some Transmission Characteristics of Telephone Cables Used in the Loop Plant," *IBM T1D1 Contribution,* T1D1.3/86-003 (January 24, 1986).

2. "ISDN Basic Access Digital Subscriber Lines," *Bellcore Technical Reference,* TR-TSY-000393, Issue 1 (May 1988).

3. W. Y. Chen, "Twisted-Pair Channel Models for VDSL," *Texas Instruments T1E! Contribution,* T1E1.4/96-134 (April 9, 1996).

4. J. J. Werner, "The HDSL Environment," *IEEE JSAC,* vol. 9, no. 6 (August 1991): 785–800.

5. D.G. Messerschmitt, "A Transmission Line Simulator Written in C," *IEEE Transcript on Selected Areas in Communications* (January 1984).

6. *Transmission Systems for Communications,* Fifth Edition (Bell Telephone Laboratories, 1982): 267.

7. "A Technical Report on High-Bit-Rate Digital Subscriber Lines (HDS)," *Texas Instruments T1E1 Contribution,* T1E1.4/96-006, Working Draft (April 22, 1996).

CHAPTER 4

Transceiver Front-End Noise Models

Noise is the combination of irrelevant signals coming from intelligent sources, such as other transmission systems, and non-intelligent sources, such as a microwave oven. When the noise occurs in the frequency band of communication interest, the strength of the noise could affect the quality of communication.

In a busy restaurant, for example, conversation is difficult without raising your voice because the noise floor has been raised significantly by other loud conversations. On the other hand, casual conversation is discouraged in a movie theater to keep the quality of the sound high. For telecommunication, the combination of a high signal level and a low noise level could result in an effective transmission system.

For a DSL system, the strength of a received signal is determined by the strength of the signal from the corresponding transmitter and the attenuation of the telephone subscriber loop. The effectiveness of the received signal, however, is judged relative to the noise level at the front end of a DSL transceiver. Besides the limitation of a transceiver hardware noise floor, there are three types of noise that affect the performance of a DSL system:

- *Crosstalk noise.* Crosstalk noise comes from adjacent telephone subscriber loops of the same or different types of transmission systems. This can also be divided as *Near End Crosstalk* (NEXT) and *Far End Crosstalk* (FEXT) noises. The effect of crosstalk noise is similar to conversation in a noisy restaurant in that raising your voice (transmit signal strength) alone sometimes cannot make the communication any better because others are doing the same.
- *Impulse noise.* Impulse noises are random impulses with magnitudes that are so high that their presence can be associated with receiver detection errors. The impulse noise can be from poor quality CO switching equipment or household electronics, such as a light dimmer.

- *Background noise.* Background noise exists in the telephone loop plant at a level that is a little stronger than the thermal or semiconductor noise level. This background noise can be caused by the combination of the background radio noise and noise generated by electrical and electronic devices and picked up by the telephone loop plant for its great exposure. Radio noises related to specific sources, such as AM medium and short wave radio stations, are discussed later in Chapter 15, "VDSL (Very-High-Bit-Rate Digital Subscriber Lines)."

The severity of a particular noise can be measured from its power level or its power density level. The magnitude of background noise can be in the range of 10 to 30 of micro-volts. The noise power is usually expressed in units of *dBm*, which is defined as follows:

$$P = 10 \times \log_{10} \frac{v^2}{R \times P_m} = 10 \times \log_{10} \frac{v^2}{100 \times 0.001}$$

The value for v is the average voltage of the noise, R=100 is the receiver input impedance, and P_m=0.001 is the reference of one milli-Watt.

The noise power density is usually expressed in units of *dBm/Hz*, which is defined as follows:

$$PSD = 10 \times \log_{10} \frac{v^2}{R \times P_m \times B} = 10 \times \log_{10} \frac{v^2}{0.1 \times B}$$

The value for B is the bandwidth of noise or of particular interest in unit of *Hertz*. For an example, the background noise power density is about *−140 dBm/Hz* while the receiver front-end electronics thermal noise power density could be lower than *−150 dBm/Hz*.

4.1 Crosstalk Noise

As discussed in Chapter 3, "Twisted-Pair Channel Modeling," telephone subscriber loops are organized in binder groups of 10, 25, or 50 pairs. Many binder groups share a common physical and electrical shield in a cable. Due to capacitive and inductive coupling, there is crosstalk between each twisted pair even though pairs are well insulated at DC. The effect of crosstalk is minimized by adapting different twist distances among different pairs in a binder group. Binder groups are also twisted such that no two groups are adjacent for long runs. For DSL systems, in which the signal bandwidth is well beyond the voice frequency, the crosstalk could become a limiting factor to the achievable transmission throughput.

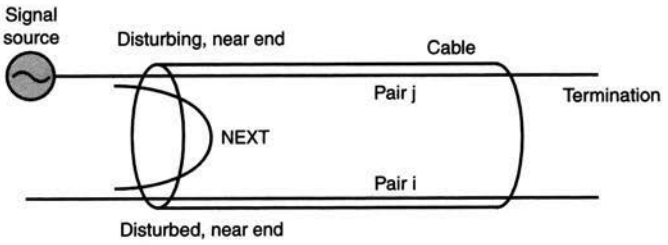
In addition to Near End Crosstalk (NEXT) and Far End Crosstalk (FEXT) noises, described in the list at the beginning of this chapter, there is also *self crosstalk,* which is initiated from adjacent transmitters of the same type of DSL system. Further, there is *foreign crosstalk,* which is initiated from other DSL or twisted-pair systems.

The severity of crosstalk could be related to the system installation scale, that is, the total number of disturbers in the same twisted pair cable. Crosstalk coupling loss models have been developed for NEXT and FEXT with the consideration of different number of disturbers. These crosstalk coupling loss models are based on twisted pairs within the same cable of significant length, usually longer than 1 kilofeet. The effect of crosstalk could be different if only a portion of twisted pairs are within the same cable.

4.1.1 NEXT Coupling Configurations

NEXT is defined as the crosstalk effect between a receiving path and a transmitting path of DSL transceivers at the same end of two different subscriber loops within the same twisted-pair cable. The NEXT noise at the receiver front end of a particular DSL transceiver is caused by signals transmitted by other transceivers at the same end of the twisted cable. Specifically, a near-end transceiver *i* would experience NEXT noise from the near-end transceiver *j* if the two transceivers share the same frequency spectrum within the same twisted-pair cable, as indicated by Figure 4.1.

Figure 4.1 The Principles of NEXT

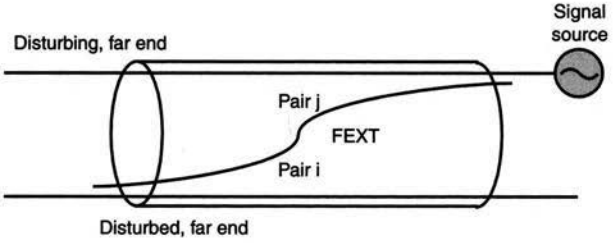


Self-NEXT is defined as NEXT caused by other transceivers of the same type. Self-NEXT has been considered a limiting factor for the transmission performance of DSL and HDSL systems when transmissions in opposite directions occupy the same spectrum, and the separation of transmitted and received signals is achieved through adaptive echo cancellation. *Foreign-NEXT* is defined as NEXT caused by other transceivers of different types. Transceivers of other types could have different transmission spectrums and different signal transmission levels. ADSL can experience foreign-NEXT from HDSL, and vice versa.

4.1.2 FEXT Coupling Configurations

FEXT is defined as the crosstalk effect between a receiving path and a transmitting path of DSL transceivers at opposite ends of two different subscriber loops within the same twisted-pair cable. The FEXT noise at the receiver front end of a particular DSL transceiver is caused by signals transmitted by other transceivers at the opposite end of the twisted cable. Specifically, a near-end transceiver *i* would experience FEXT noise from the far-end transceiver *j* if they share the same frequency spectrum within the same twisted-pair cable, as indicated by Figure 4.2.

Figure 4.2 The Principles of FEXT



There is also *self-FEXT* from the same types of transceivers and *foreign-FEXT* from different types of transceivers. The effect of self-NEXT might dominate that of self-FEXT when both exist for such systems as DSL and HDSL. There is always self-FEXT unless all transceivers are synchronized and sending the same data sequence.

When self-NEXT is absent (through the arrangement of *Frequency Division Multiplex* (FDM) systems between transmissions in opposite directions, for example), the effect of self-FEXT could dominate that of background noise in certain frequency regions. For an FDM system, such as ADSL, the dominant noise component could be different at different frequency regions. It could be self-FEXT, foreign-NEXT, or background noises.

4.1.3 Distribution of Crosstalk Coupling Losses

The coupling mechanism of crosstalk has been studied since the early 1900s.[1] It was discovered that the crosstalk is mainly due to the unbalance of coupling capacitance of a twisted-pair cable. The effect of NEXT was seriously considered during the system engineering of the T1 system.[2] FEXT was also considered during T1 transmission engineering efforts but was classified as a minor factor compared with NEXT.

The study of transmission issues related to T1 systems established a first step in dealing with NEXT modeling for simulations. The study not only tried to model NEXT loss with mean

and standard deviation, but also initiated the use of 1 percent worst-case NEXT value for overall system requirements. The reason is that people were expecting better than 95 percent satisfactory T1 service at an error ratio of less than 10^{-6}.

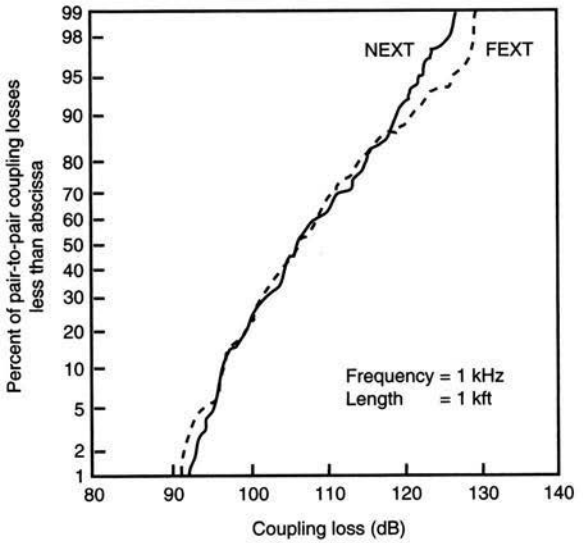
Note

The 95 percent satisfactory service rate for initial installation without the involvement of technicians for field visits has been a common industry practice to keep the cost of providing telecommunication service in control.

The use of the 1 percent worst case for transmission engineering would allow multiple spans of T1 systems in an end-to-end service connection and also provide room for some unforeseen impairments.

Crosstalk loss is defined as the attenuation for a disturbing signal to pass through the coupling mechanism arriving at a disturbed receiver. There are different crosstalk losses for NEXT and FEXT. Crosstalk losses from one pair to another pair are different for different pair-to-pair combinations. The crosstalk loss values can differ by up to 40 dB at a single frequency and have a nearly Gaussian distribution.[3,4] Figure 4.3 shows the distribution of NEXT loss at a frequency of 1 KHz.

Figure 4.3 The Distribution of NEXT and FEXT Losses



The 1 percent worst-case crosstalk loss shown at the bottom of the graph in Figure 4.3 is about 40 dB less than that of the 99 percent case. There are only 1 percent crosstalk losses with values that are lower than that of the 1 percent worst case.

There are lots of measurements and calculations involved in the statistical analysis of crosstalk losses, even for a single frequency. There could be 1,225 different NEXT values at a particular frequency for a 50-pair binder group, assuming the pair-to-pair NEXT is symmetrical. The measured NEXT losses can be approximated with a gamma or a truncated Normal distribution on log scale.

The truncated Normal distribution has a better physical meaning because the number of NEXT pairs is limited. In practice, you might be concerned about NEXT from more than one disturber, in which case you need to calculate a power sum for multiple disturbers. In a 50-pair group, you have 50, 3.16×10^{15}, and 4.1×10^{11} different power sum NEXT values for 49 disturbers, 24 disturbers, and 10 disturbers, respectively. The computation of power sums for 24 and 10 disturbers is usually carried out by a computer because of the large number of calculations required.

4.1.4 *The Unger NEXT and Simplified NEXT/FEXT Models*

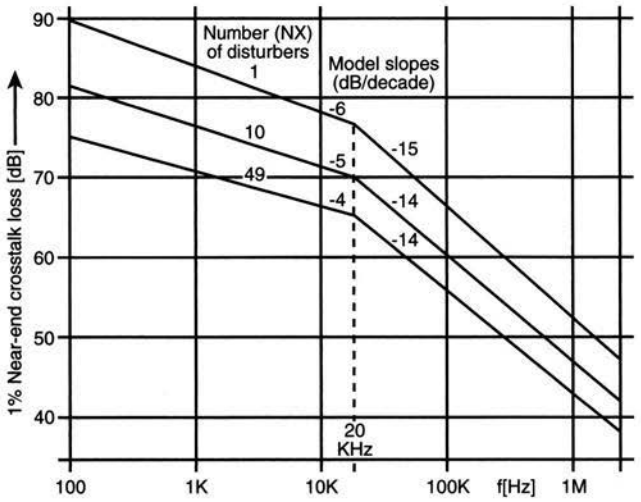
Because of the work load, measurements of NEXT have only been made for a few particular frequencies. A NEXT model that covers a broad frequency range was necessary for the study of DSL transmission performance. J.H.W. Unger of Bellcore constructed a distributed, cross-coupling computer program with many simulated twisted pairs to model the crosstalk process based on the unbalanced-coupling capacitance principle. The coupling capacitance parameters were calibrated by comparing simulated results with real measurements at available frequencies. The NEXT effect was then simulated for the broad range of frequencies. These simulated results also represented the effect of a different number of disturbers.

Simulation results were summarized as the Unger 1985 model illustrated in Figure 4.4.[5] This Unger model was developed based on a 50-pair 18 kft. 22-Gauge PIC cable terminated with characteristic impedance at both ends for the 1 percent worst-case NEXT. The Unger model is very close to that used by an earlier study.[6]

The piece-wise linear (log-log scale) Unger NEXT model has loss values of 57 dB, 61 dB, and 67 dB for 49 disturbers, 10 disturbers, and 1 disturber, respectively, at a frequency of 80 KHz. A simplified 49 disturber NEXT model, which has 57 dB of loss at 80 KHz and a linear (log-log scale) slope of –15 dB/decade, has also been used and can be expressed as

$$NEXT_{49} = \frac{1}{1.134\times10^{13}} f^{\frac{3}{2}}$$

Figure 4.4 Unger NEXT Model



The value f is in units of *Hertz*, and the $NEXT_{49}$ value is a unit-less ratio, which can be expressed in dB by taking the base 10 Log of the $NEXT_{49}$ ratio and then multiplying it by 10.

This simplified NEXT model can also be generalized for N disturbers as

$$NEXT_N = \left(\frac{N}{49}\right)^{0.6} \frac{1}{1.134 \times 10^{13}} f^{\frac{3}{2}}$$

Notice that the loss difference between 1 disturber and 49 disturbers is about 10 dB. You can assume this general scaling factor is due to the physical arrangement of twisted pairs under the 1 percent worst-case condition. In other words, when you are dealing with 1 percent worst case, you are only interested in the disturbing pairs that are closest to the disturbed pair. Therefore, the additional group of disturbing pairs causes less disturbances because it is further away from the original group of disturbing pairs.

This leads to a generalized expression dealing with multiple disturber groups.[7] Assuming that N^1 is the number of disturbers for the first dominant disturbing pair group and N^2 is the number of disturbers for the second disturbing pair group, you have the following formulation:

$$NEXT_{N_1} = \left(\frac{N_1}{49}\right)^{0.6} \frac{1}{1.134 \times 10^{13}} f^{\frac{3}{2}}$$

$$NEXT_{N_2} = \left(\frac{N_1 + N_2}{49N_1}\right)^{0.6} \frac{1}{1.134 \times 10^{13}} f^{\frac{3}{2}}$$

In other words, two groups of disturbers that have different disturbing signal spectra should use two slightly different NEXT models to take into account the physical structure of the twisted-pair cable. This relationship between different types of disturber groups is consistent with the measurements.[8]

A simplified 49 disturber FEXT loss model can be expressed as

$$FEXT_{49} = kdf^2 |H(f)|^2$$

The values are as follows:

- k=8 × 10^{-20} is empirically derived from the FEXT measurements.
- d is the loop length in feet.
- f is the frequency in Hz.
- $H(f)$ is the transfer function of the loop.

Due to the similarity between NEXT and FEXT distribution, the same power sum scale for NEXT can also be applied to FEXT, in which case you have the following:

$$FEXT_N = \left(\frac{N}{49}\right)^{0.6} kdf^2 |H(f)|^2$$

These NEXT/FEXT models can be used in conjunction with the transmit signal power density to obtain crosstalk noise power density at the front end of a DSL receiver. For example, the NEXT power density at the front end of a DSL receiver can be expressed as

$$PSD_{NEXT}(f) = S(f)NEXT_N(f) = \left(\frac{N}{49}\right)^{0.6} \frac{S(f) \times f^{\frac{3}{2}}}{1.134 \times 10^{13}}$$

The value $S(f)$ is the power density of the transmit signal.

The FEXT power density at the front end of a DSL receiver can be expressed as

$$PSD_{FEXT}(f) = S(f)FEXT_N(f) = S(f) \times \left(\frac{N}{49}\right)^{0.6} kdf^2 |H(f)|^2$$

These 1 percent worst-case NEXT models have been based on the exact collocation of transmitters and receivers. This is generally true for transceivers located at a CO, but not for transceivers at customer premises. At the subscriber end, transceivers are very likely to be distributed at different customer premises apart from each other. In addition, the collocation assumption might not be true when considering NEXT or FEXT from other digital systems, such as T1 lines. Up to 5.5 dB of additional loss has been considered for the T1 NEXT by other studies.[9,10]

4.2 *Impulse Noise*

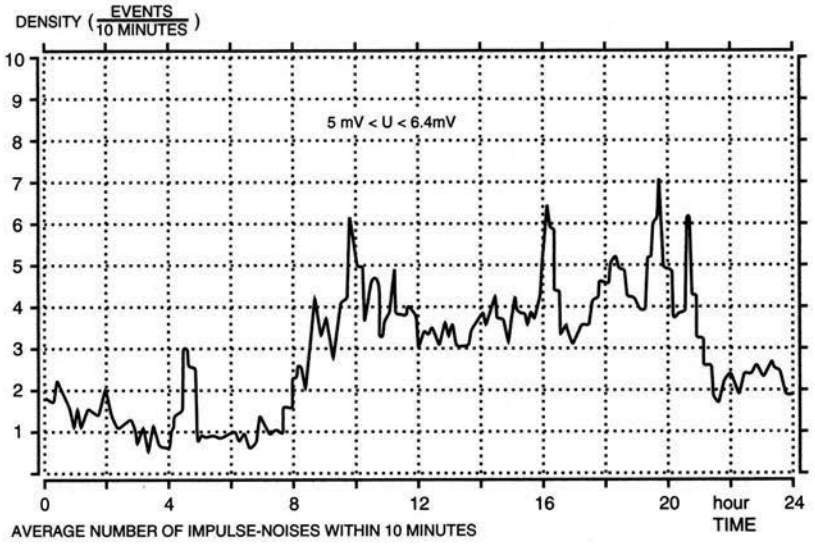
Unlike crosstalk noise—whose cause can be identified—the origin of impulse noise is more difficult to locate. Impulse noise could come directly through some connections to the telephone subscriber loop or come from the influence of an electromagnetic field.

Impulse noise is characterized as a random pulse waveform whose amplitude is much higher compared with the Gaussian-like background noise. According to some survey results, the amplitude of impulse noise is usually between 5 and 20 mV, and the frequency of impulses is between 1 and 5 per minute.[11] Also, the duration of the impulse waveform lasts from 30 to 150 microseconds. It was believed that impulse energy was concentrated at below 40 KHz; however, this might be caused by the bandwidth of impulse measuring equipment.

Characteristics of impulse noise could be quite different at other locations.[12,13] It has been a continuous effort to better understand the characteristics and effects of the impulse noise during the development of many DSL systems. Impulse noise is a major impairment for ADSL, especially due to the heavy ADSL subscriber loop loss. According to a Bellcore study, a majority of impulses would cause a receiver detection error, compared with the very weak received ADSL signal.

A NYNEX impulse noise study shows that impulse noises with amplitudes between 10 and 40 mV occur at about 10 times per minute on average.[14,15] A Deutsche Bundespost impulse noise study exposed that impulse noises were somehow related to daily activities (see Figure 4.5).[16]

Figure 4.5 Frequency of Impulses During a Day



The Deutsche Bundespost impulse noise study also indicated that the probability density function of the amplitude u of impulse noise can be approximated by

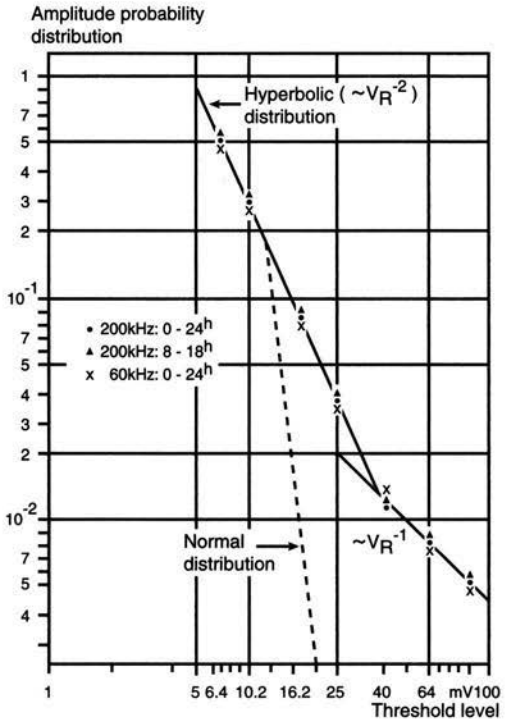
$$p(u) = \frac{u_0^2}{u^3}$$

over an amplitude range of 5 to 40 mV, in which u_0=5 mV. Thus, the probability that the magnitude of the amplitude u exceeds some value u_t is described as follows:

$$P(|u| > u_t) = \left(\frac{u_0}{u_t}\right)^2$$

This hyperbolic distribution model is derived from impulse measurements, as expressed in Figure 4.6.

Figure 4.6 Impulse Noise Amplitude Distribution



It was also suggested by the Deutsche Bundespost impulse noise study that above 40 mV, the amplitude probability distribution is modeled by

$$P(|u| > u_t) = \frac{u_1}{u_t}$$

in which u_1=0.625 mV.

Two impulse noise wave forms have been suggested by Bellcore for an ADSL impulse noise performance test, as shown in Figures 4.7 and 4.8.[17] The impulse noise waveform #1 has more high frequency components compared with the impulse noise waveform #2. Both are real impulse waveforms collected from a field impulse noise survey.

Figure 4.7 Test Impulse Noise Waveform #1

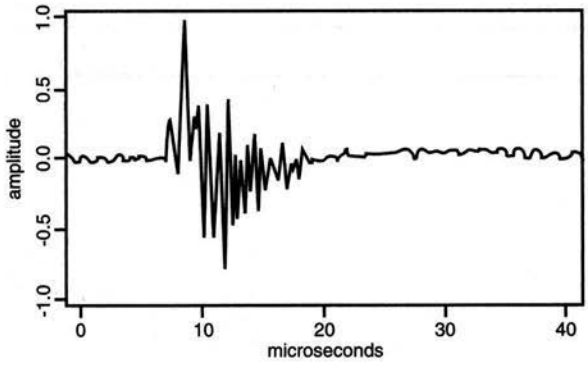
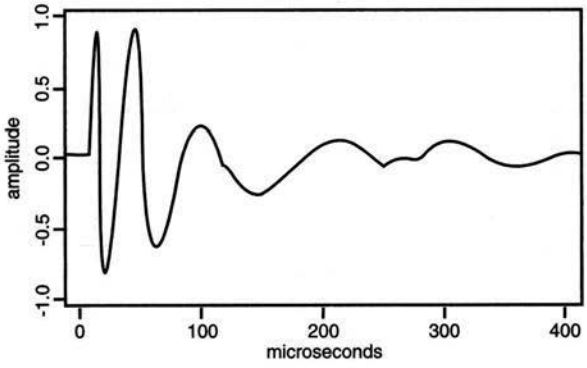


Figure 4.8 Test Impulse Noise Waveform #2



Amplitudes of the waveforms depicted in Figures 4.7 and 4.8 are normalized and adjusted during a test to see the threshold at which these waveforms can cause error. The threshold can then be converted to the estimated probability that a second will be erred, as follows:

$$E = 0.0037\,P(u > u_{e1}) + 0.0208\,P(u > u_{e2})$$

The value u_{e1} = 25 mV, and the value u_{e2} = 40 mV.[18]

While crosstalk and background noises impose a limit on transmission throughput over the twisted-pair telephone subscriber loop, the error caused by impulse noise can be corrected with forward error correction codes. The required error correction coding overhead could reduce the transmission throughput a little.

4.3 *Background and Receiver Front-End Thermal Noise*

By avoiding the effect of NEXT and FEXT, the loop plant noise level or the receiver front-end noise level becomes a limiting factor for the performance of a DSL system. During the standardization process of Asymmetrical Digital Subscriber Lines (ADSL), Bellcore conducted a background noise survey at two New Jersey locations. Table 4.1 summarizes the average background noise power density levels for three frequency bands.

Table 4.1 Residential Background Power Density Level (dBm/Hz)

Location	8–100 KHz	100–500 KHz	500 KHz–2MHz
1	–150	–148	–133
2	–136	–153	–146

The analysis of transmission performance over the twisted-pair telephone subscriber loop has been based on the assumption of a received signal over a Gaussian noise. The probability density of the background noise is very close, but not a Gaussian distribution. The histograms of the background noise are very similar to Gaussian density, except that they have short tails. Therefore, the Gaussian noise assumption is still valid.

Based on results from the Bellcore noise survey, the background noise level for the twisted-pair telephone loop plant has been assumed to be –140 dBm/Hz. This assumed that the loop plant background noise level is higher than the thermal noise of a receiver front-end electronic circuit. On the other hand, the circuit noise can easily exceed the –140 dBm/Hz background noise level if the proper design and implementation techniques have not been applied.

The receiver front-end noise level can be made close to that defined by the thermal noise and the noise figure of the first analog amplifier—assuming the interference from the transceiver electronic circuits can be avoided by a good hardware design. For the thermal noise, you have the following formulation:

$$v_{ns}^2 = kTR_s\Delta f$$

Assuming that input and output are both matched to source resistance R_s [19] for $k = 1.37 \times 10^{-23}$, $T = 290°\text{K}$, and $\Delta f = 1MHz$, you have the thermal noise power

$$\frac{v_{ns}^2}{R_s} = -65\,dBmV$$

as compared to the 0 dBmV defined by the power of 1 millivolts on a 75 ohms impedance. This is corresponding to a noise power density of –174 dBm/Hz. The received signal level becomes strong enough for analog-to-digital conversion at the output of the receiver amplifier. The noise power at the output of the receiver amplifier is the sum of the thermal noise, the amplifier gain, and the amplifier noise figure, ranging from 3 to 7 dB in dB units. In other words, the equivalent receiver front-end noise power density level can be made as low as about –160 dBm/Hz.

End Notes

1. S. H. Lin, "Statistical Behavior of Multipair Crosstalk," *Bell Systems Technical Journal,* vol. 59, no. 6 (July/August 1980): 955–974.

2. S. H. Lin, "Statistical Behavior of Crosstalk Power Sum with Dominant Components," *Bell Systems Technical Journal,* vol. 60, no. 7 (September 1981): 1363–1374.

3. J. H. W. Unger, "Near-End Crosstalk Model for Line Code Studies," *Bellcore T1D1 Contribution,* T1D1.3/85-244 (November 12, 1985).

4. S. V. Ahamed, P. P. Bohn, and N. L. Gottfried, "A Tutorial on Two-Wire Digital Transmission in the Loop Plant," *IEEE Trans. Commun.*, vol. COM-29, no. 11 (November 1981): 1554–1564.

5. This relationship was first suggested by a personal note from J. Bingham of Amati in the middle of 1993.

6. M. Elder and W. Y. Chen, "Effects of NEXT and FEXT in the Same Cable," *BNR and Bellcore Joint T1E1 Contribution,* T1E1.4/93-220 (August 1993).

7. J. Bingham and W. Y. Chen, "NEXT from T1 to ADSL and Vice Versa," *Amati and Bellcore Joint Contribution,* T1E1.4/93-178 (August 1993).

8. W. Y. Chen and D. L. Waring, "Applicability of ADSL to Support Video Dial Tone in the Copper Loop," *IEEE Communications Magazine,* vol. 32, no. 5 (May 1994): 102–109.

9. Bingham and Chen, "NEXT from T1 to ADSL and Vice Versa."

10. Chen and Waring, "Applicability of ADSL to Support Video Dial Tone in the Copper Loop": 102–109.

11. J. J. Werner, "Impulse Noise in the Loop Plant," *Proc. IEEE ICC '90,* Atlanta, Georgia (April 16–19, 1990): 1734–1737.

12. W. Henkel and T. Kessler, "Statistic Description and Modeling of Impulse Noise on the German Telephone Network," *Electron. Lett.*, vol. 30, no. 12 (June 9, 1994): 935–936.

13. J. W. Cook, "Wideband Impulse Noise Survey of the Access Network," *BT Tech. J.*, vol. 11 (1993): 155–162.

14. "NYNEX Loop Performance Survey Final Report," *Bellcore Special Report SR-TSY-0025* (October 1986).

15. R. A. McDonald, "Report on Bellcore Impulse Noise Study," *Bellcore T1D1 Contribution,* T1D1.3/87-256 (July 27, 1987).

16. K. Szechenyi, "On the NEXT and Impulse Noise Properties of Subscriber Loops," *Proc. GLOBECOM '89,* Dallas, Texas (November 27–30, 1989): 1569–1573.

17. K. Kerpez and C. Valenti, "Impulse Noise Testing for ADSL Transceiver," *Bellcore T1E1 Contribution,* T1E1.4/93-034 (March 10, 1993).

18. ANSI T1.413.

19. M. S. Ghausi, *Electronic Circuits* (Van Nostrand Reinhold Company, 1971).

CHAPTER 5

Channel Capacity

Channel capacity is defined as the maximum throughput over a particular transmission channel. Specifically, if the throughput of a transmission system is less than the channel capacity, the transmission can be made error free in conjunction with some specific modulation and coding techniques. Channel capacity can be compared with the capacity of a solid container with a certain shape. The maximum capacity of a particular container can be reached if it is filled with liquid; however, to hold solid objects with specific shapes, the maximum capacity of the container can never be reached.

The data sequence sent through a transmission channel can be compared with solid objects with specific shapes. The task of telecommunication systems engineering is similar to finding the best way to pack solid objects such that the utilization of the container (channel) capacity is maximized.

Channel capacity is a good indication of the transmission potential for a particular channel. You can obtain a conservative estimate of the twisted-pair loop plant transmission potential by considering the worst-case channel capacity of the telephone subscriber loop plant. Channel capacity is also a good reference when judging the transmission efficiency of a particular transceiver architecture.

Although early transmission systems are not very efficient, performance of DSL systems can be engineered as close as only a few dBs away from the channel capacity. The channel capacity of a telephone subscriber loop is determined by the transmit signal level, the channel attenuation, and the receiver front-end noise level. For the self-NEXT dominated condition, channel capacity is only related to the channel attenuation. Specifically, channel capacity is

based on the signal-to-noise ratio, which could be frequency dependent on a particular telephone subscriber loop.

This chapter presents the basic concepts and calculations of channel capacity for the twisted-pair telephone subscriber loop channel as follows:

- *Signal-to-noise ratio.* Because of the frequency dependence of the attenuation of a twisted-pair cable and the crosstalk coupling function, the SNR of a twisted-pair telephone subscriber loop is also frequency dependent. For a particular telephone subscriber loop, the SNR can be different, depending on the noise environment that can be arranged through system considerations.
- *Channel capacity calculations.* Specifically, the calculation of channel capacity can be further divided into topics, as follows:
  - *Basic channel capacity concept.* For a flat (frequency-independent) channel, the channel capacity is the product of the channel bandwidth and the base 2 log of 1 plus the SNR.
  - *Channel capacity for a twisted-pair telephone subscriber loop with frequency-dependent SNR.* The channel capacity of a twisted-pair telephone loop is the integration of the base 2 log of 1 plus the frequency-dependent SNR. If calculated over the frequency of interest, this channel capacity provides a good reference for the targeted transmission performance of a DSL system.
  - *Differential channel capacity.* By taking the derivative of the channel capacity at a certain frequency, the differential channel capacity gives a good indication of the transmission performance potential for each frequency region of a particular channel.
  - *Channel capacity with implementation constraints.* A 6 dB performance margin, which is achieved through raising the noise level by 6 dB, is usually required for the performance simulation study and confirmation test of DSL systems to compensate for some non-categorized channel impairments. The SNR is normally limited by the dynamic range of a particular hardware implementation. These practical engineering and implementation constraints can also be included in the channel capacity calculation to provide a more realistic reference.

Channel capacity calculations in this chapter are based on 26-gauge twisted-pair loops with lengths of 1 mile, 2 miles, and 3 miles. Corresponding self-NEXT and self-FEXT models are based on 49 disturbers.

5.1 Signal-to-Noise Ratio

The frequency-dependent SNR at a receiver front end is related to the received signal power spectrum density and the noise power spectrum density. The received signal power spectrum density, $S(f)$, is determined by the transmit power spectrum density, $Q(f)$, and the twisted-pair loop channel transfer function, $H(f)$, as shown in the following expression:

$$S(f) = Q(f)|H(f)|^2 = Q(f)e^{-2d\left(k_1\sqrt{f}+k_2 f\right)}$$

The simplified channel model derived in Chapter 3, "Twisted-Pair Channel Modeling," has been used for this expression:

$$|H(f)| = e^{-d\left(k_1\sqrt{f}+k_2 f\right)}$$

The higher the received signal power, the higher the transmission throughput; however, the effectiveness of the received signal power is relative to the noise power also present at the input of a receiver. There are NEXT, FEXT, loop plant background, analog-to-digital conversion quantization, and other electronic hardware noises, as discussed in Chapter 4, "Transceiver Front-End Noise Models."

The strength of a white noise of power density W can be described by its total power σ^2 within a particular bandwidth of B. For the simplified channel model, the received signal-to-white-noise ratio is expressed as

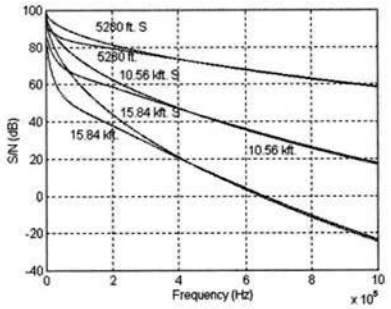
$$\frac{S(f)}{W} = \frac{Q(f)|H(f)|^2}{W} = \frac{P}{\sigma^2}e^{-2d\left(k_1\sqrt{f}+k_2 f\right)}$$

The transmit signal density is assumed to be white with a bandwidth of B and P and is the total power of the transmit signal. Figure 5.1 shows signal-to-noise ratios under the white noise condition for primary constant-based and simplified channel models assuming a transmit power density of –40 dBm/Hz and a white noise power density of –140 dBm/Hz.

In Figure 5.1, "5280 ft. S." stands for the 5280 ft., or 1 mile, simplified channel model, while "5280 ft." stands for the primary constants-based channel model. Similar notation applies to loops of other lengths in the same figure and subsequent figures. Simplified channel models produce fewer losses at a low frequency region, below about 300 KHz, and therefore result in higher signal-to-noise ratios. The 3 mile, 15840 ft., 26-gauge

twisted-pair loops have 0 dB signal-to-noise ratio at the frequency of about 650 KHz. The shorter 1 mile and 2 mile loops have usable bandwidths up to 1 MHz and beyond.

Figure 5.1 Signal-to-White-Noise Ratio for Twisted-Pair Loops



5.1.1 NEXT Signal-to-Noise Ratios

The NEXT noise power spectral density is determined by the transmit power spectral density and the NEXT coupling transfer function. The NEXT power spectral density is expressed as follows:

$$N_N(f) = Q(f)NEXT(f) = Q(f)\frac{1}{1.134\times10^{13}}f^{-\frac{3}{2}}$$

Under the self NEXT condition in which the same transmit power spectrum affects both received signal and noise power, the received signal-to-noise ratio is expressed as

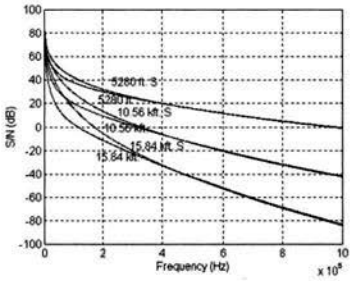
$$\frac{S(f)}{N_N(f)} = \frac{Q(f)|H(f)|^2}{Q(f)NEXT(f)} = \frac{e^{-2d\left(k_1\sqrt{f}+k_2f\right)}f^{-\frac{3}{2}}}{1.134\times10^{-13}}$$

In practice, especially at a low frequency region where the NEXT noise power density is very small, you need to consider the effect of white background noise. By including the background noise power density, the received signal-to-noise ratio becomes

$$\frac{S(f)}{N_N(f)+W} = \frac{Q(f)|H(f)|^2}{Q(f)NEXT(f)+W} = \frac{e^{-2d\left(k_1\sqrt{f}+k_2f\right)}}{1.134\times10^{-13}f^{\frac{3}{2}}+\frac{\sigma^2}{P}}$$

Figure 5.2 shows signal-to-noise ratios under the self-NEXT-plus-white-noise condition for primary-constant-based and simplified channel models

Figure 5.2 Signal-to-Self-NEXT-Plus-White-Noise Ratio for 26-Gauge Twisted-Pair Loops



Under the self-NEXT condition, the 3 mile and 2 mile, 26-gauge twisted-pair loops have 0 dB signal-to-noise ratio at the frequency of about 110 KHz and 320 KHz, respectively, while the shortest 1 mile loop has usable bandwidth of about 970 KHz.

5.1.2 *FEXT Signal-to-Noise Ratios*

The FEXT noise power spectral density is determined by the transmit power spectral density and the FEXT coupling transfer function, as follows:

$$N_F(f) = Q(f)FEXT(f) = Q(f)|H(f)|^2 kdf^2$$

Under the self-FEXT condition where the same transmit power spectrum affects both received signal and noise power, the received signal-to-noise ratio is expressed as

$$\frac{S(f)}{N_F(f)} = \frac{Q(f)|H(f)|^2}{Q(f)FEXT(f)} = \frac{1}{kdf^2}$$

The values are as follows:

$k = 8 \times 10^{-20}$.

d is in unit of ft.

f is in unit of Hz.

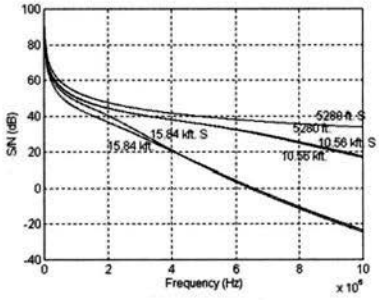
The channel model becomes irrelevant when channel transfer functions are the same for the channel model and for the FEXT model.

In practice, especially at a low-frequency region and a high-frequency region where the FEXT noise power density is very small, you need to consider the effect of white background noise. By including the background noise power density, the received signal-to-noise ratio becomes

$$\frac{S(f)}{N_F(f)+W}=\frac{Q(f)|H(f)|^2}{Q(f)FEXT(f)+W}=\frac{1}{kdf^2+\dfrac{\sigma^2}{P}e^{2d\left(k_1\sqrt{f}+k_2 f\right)}}$$

Figure 5.3 shows signal-to-noise ratios under the self-FEXT-plus-white-noise condition for primary-constant-based and simplified channel models

Figure 5.3 Signal-to-Self-FEXT-Plus-White-Noise Ratio for 26-Gauge Twisted-Pair Loops



The usable bandwidth for the longest 3 mile, 26-gauge loop is around 650 KHz, which is the same as for the white noise only case. However, the signal-to-noise ratios have been reduced to below 50 dB at frequencies beyond 150 KHz also in comparison with the white noise only case. The usable bandwidths for shorter loops are beyond 1 MHz.

5.2 *Channel Capacity Calculations*

The transmission throughput of a DSL system is limited by the characteristics of the twisted-pair channel and the noise environment at the receiver front end, no matter what kind of transceiver structure is involved. Specifically, the transmission throughput of a DSL system is limited by the channel capacity for the particular loop and noise combination. Many studies have been carried out for the channel capacity of the twisted-pair telephone subscriber loop.[1]

5.2.1 *Basic Concepts of Channel Capacity*

The efficiency of a practical transmission system can be judged by how many bits per Hertz it can carry. For a simple *Quadrature Amplitude Modulation* (QAM) line code with a baud rate of 1 Hertz, the following expression describes this number of bits per Hertz efficiency:

$$C_{QAM} = \log_2\left(1+\frac{3}{\Delta^2}\frac{S}{N}\right)$$

The values are as follows:

S is the received signal power.

N is the receiver front-end noise power.

Δ^2 is related to the desired error rate.

C_{QAM} is in unit of number of bits per symbol or per Hertz for this special example.

In other words, the transmission efficiency of a QAM system is determined by the transmission channel signal-to-noise ratio and the desired error rate. For a desired error rate of 10^{-7}, you can find the value of Δ to be 5.333, according to the Gaussian distribution:

$$10^{-7} = \frac{2}{\sqrt{2\pi}}\int_{\Delta}^{\infty} e^{-\frac{x^2}{2}}\,dx$$

Table 5.1 summarizes Δ values for other error rates.

Table 5.1 Δ and Error Rates

Error Rate	10^{-2}	10^{-3}	10^{-4}	10^{-5}	10^{-6}	10^{-7}
Δ	2.577	3.287	3.891	4.418	4.892	5.333

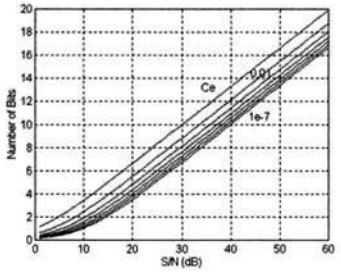
Figure 5.4 shows the relationship between the number of bits and the signal-to-noise ratio under different error rates for a QAM line code.

The top curve in Figure 5.4 is the channel capacity. The next lower curve represents the QAM transmission efficiency at an error rate of 10^{-2}. Lower curves are for error rates of 10^{-3}, 10^{-4}, 10^{-5}, 10^{-6}, respectively, and the bottom curve is for the error rate of 10^{-7}. A lower error rate requires a higher signal-to-noise ratio to achieve a certain number of bits per

Hertz; however, the maximum number of bits per Hertz is limited by the following expression, referred to as the channel capacity at a bandwidth of 1 Hertz when $\Delta = \sqrt{3}$:

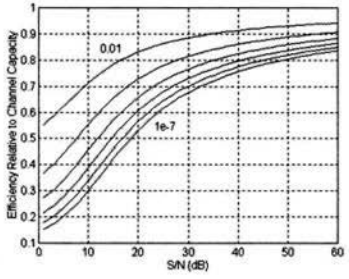
$$C_e = \log_2\left(1 + \frac{S}{N}\right)$$

Figure 5.4 QAM Transmission Efficiency



The corresponding error rate is 0.0833. There is an SNR difference of 9.77 dB between error rates of 0.0833 and 10^{-7}. The expression of C_e is the general form of calculation channel capacity. Figure 5.5 shows ratios of QAM transmission efficiency to the channel capacity for different error rates and different SNRs.

Figure 5.5 Efficiency Relative to Channel Capacity



The top curve in Figure 5.5 represents the ratio of QAM transmission efficiency at an error rate of 10^{-2} to channel capacity. Lower curves are ratios for error rates of 10^{-3}, 10^{-4}, 10^{-5}, 10^{-6}, respectively, and the bottom curve is for the ratio of QAM transmission efficiency at an error rate of 10^{-7} to channel capacity. The transmission throughput is only half of the

channel capacity at SNRs of 7.5 dB, 12 dB, 15 dB, 17 dB, and 18.5 dB and error rates of 10^{-3}, 10^{-4}, 10^{-5}, 10^{-6}, and 10^{-7}, respectively. The transmission efficiency is relatively high for a QAM line code at a high signal-to-noise ratio.

The channel capacity for a bandwidth of B with a flat signal and noise spectra is

$$C = B\log_2\left(1+\frac{S}{N}\right)$$

Table 5.2 summarizes the channel capacities of the voice band for different SNRs assuming a bandwidth of 4 KHz with flat signal and noise spectra.

Table 5.2 Voice Band Channel Capacity

S/N (dB)	10	20	30	40	50	60
Channel Capacity (kbps)	13.84	26.63	39.87	53.15	66.44	79.73

5.2.2 *Channel Capacity for Frequency-Dependent SNR*

For frequency-dependent received signal and noise power spectra with a bandwidth of B, the integral channel capacity is expressed as

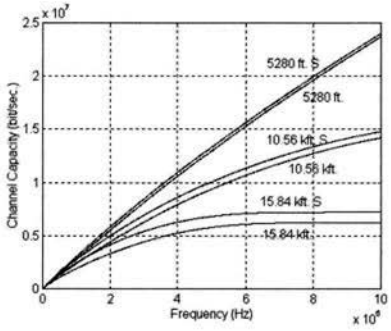
$$C = \int_0^B \log_2\left(1+\frac{S(f)}{N(f)}\right)$$

For the receiver front-end white noise limited condition, the channel capacity is expressed as

$$C = \int_0^B \log_2\left(1+\frac{S(f)}{N(f)}\right)df = \int_0^B \log_2\left(1+\frac{P}{\sigma^2}e^{-2d\left(k_1\sqrt{f}+k_2 f\right)}\right)df$$

Figure 5.6 shows channel capacities under the white noise condition for primary-constant-based and simplified channel models assuming a transmit power density of −40 dBm/Hz and a white noise power density of −140 dBm/Hz.

Figure 5.6 White Noise Channel Capacity for 26-Gauge Twisted-Pair Loops



Channel capacities are all higher than 6 Mbps under the background white noise condition for 1 mile, 2 mile, and 3 mile 26-gauge loops.

For the self-NEXT limited condition, the channel capacity is expressed as

$$C = \int_0^B \log_2\left(1 + \frac{S(f)}{N_N(f)}\right) df = \int_0^B \log_2\left(1 + \frac{e^{-2d\left(k_1\sqrt{f} + k_2 f\right)} f^{-\frac{3}{2}}}{1.134 \times 10^{-13}}\right) df$$

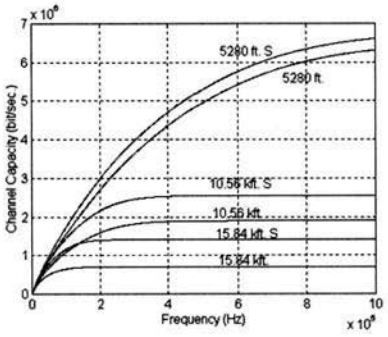
For the self-NEXT-plus-receiver-front-end-white-noise-limited condition, the channel capacity is expressed as follows:

$$C = \int_0^B \log_2\left(1 + \frac{S(f)}{N_N(f) + W}\right) df = \int_0^B \log_2\left(1 + \frac{e^{-2d\left(k_1\sqrt{f} + k_2 f\right)}}{1.134 \times 10^{-13} f^{\frac{3}{2}} + \frac{\sigma^2}{P}}\right) df$$

Figure 5.7 shows channel capacities under the self-NEXT-plus-white-noise condition for primary constant based and simplified channel models also assuming a transmit power density of −40 dBm/Hz and a white noise power density of −140 dBm/Hz.

Under the self-NEXT-plus-white-noise condition, channel capacities are below 1 Mbps and 2 Mbps for 3 mile and 2 mile 26-gauge twisted-pair loops, while the 1 mile 26-gauge loop has a channel capacity of beyond 6 Mbps.

Figure 5.7 NEXT-Plus-White-Noise Channel Capacity for the 26-Gauge Twisted-Pair Loops



For the self -FEXT-limited condition, the channel capacity is expressed as

$$C = \int_0^B \log_2\left(1 + \frac{S(f)}{N_F(f)}\right)df = \int_0^B \log_2\left(1 + \frac{1}{klf^2}\right)df$$

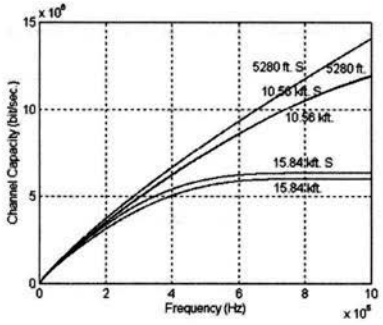
For the self-FEXT-plus-receiver-front-end-white-noise-limited condition, the channel capacity is expressed as

$$C = \int_0^B \log_2\left(1 + \frac{S(f)}{N_F(f) + W}\right)df = \int_0^B \log_2\left(1 + \frac{1}{klf^2 + \frac{\sigma^2}{P}e^{2d\left(k_1\sqrt{f} + k_2 f\right)}}\right)df$$

Figure 5.8 shows channel capacities under the self-FEXT-plus-white-noise condition for primary-constant-based and simplified channel models, also assuming a transmit power density of –40 dBm/Hz and a white noise power density of –140 dBm/Hz.

Under the self-FEXT-plus-white-noise condition, the channel capacity of the 3 mile 26-gauge loop is about 6 Mbps, which is the same as the white noise only case, while the shorter 2 mile and 3 mile loops have channel capacities above 10 Mbps.

Figure 5.8 FEXT-Plus-White-Noise Channel Capacity for the 26-Gauge Twisted-Pair Loop

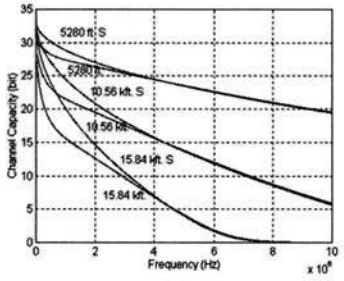


You can examine the contribution of an individual frequency region to the overall channel capacity by taking derivative of the channel capacity to obtain the differential channel capacity. The receiver-front-end-white-noise-limited condition is expressed as

$$\frac{dC}{dB} = \log_2\left(1+\frac{S(f)}{W}\right) = \log_2\left(1+\frac{P}{\sigma^2}e^{-2d\left(k_1\sqrt{f}+k_2 f\right)}\right)$$

The differential channel capacity is just the base 2 logarithm of receiver front-end signal-to-noise ratio. Figure 5.9 shows differential channel capacities under the white noise condition for primary-constant-based and simplified channel models assuming a transmit power density of −40 dBm/Hz and a white noise power density of −140 dBm/Hz. The maximum differential channel capacity is $\log_2\left(1+1\times10^{10}\right) \approx 33.2$ bits. The differential channel capacity becomes 1 bit when the signal-to-noise ratio is 1.

Figure 5.9 White Noise Differential Channel Capacity



For the self-NEXT-limited condition, the differential channel capacity is expressed as

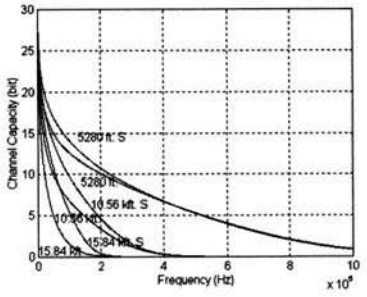
$$\frac{dC}{dW} = \log_2\left(1+\frac{S(f)}{N_N(f)}\right) = \log_2\left(1+\frac{e^{-2d\left(k_1\sqrt{f}+k_2 f\right)} f^{-\frac{3}{2}}}{1.134\times10^{-13}}\right)$$

For the self-NEXT-plus-receiver-front-end-white-noise-limited condition, the differential channel capacity is expressed as

$$\frac{dC}{dW} = \log_2\left(1+\frac{S(f)}{N_N(f)+W}\right) = \log_2\left(1+\frac{e^{-2d\left(k_1\sqrt{f}+k_2 f\right)}}{1.134\times10^{-13} f^{\frac{3}{2}}+\frac{\sigma^2}{P}}\right)$$

Figure 5.10 shows differential channel capacities under the self-NEXT-plus-white-noise condition for primary-constant-based and simplified channel models, also assuming a transmit power density of −40 dBm/Hz and a white noise power density of −140 dBm/Hz.

Figure 5.10 NEXT-Plus-White-Noise Differential Channel Capacity



Under the self-NEXT-limited condition, the majority of the frequency region where the channel is usable has a differential channel capacity of fewer than 10 bits. The channel is almost closed at about 200 KHz and 400 KHz for 3 mile and 2 mile loops, respectively.

For the self-FEXT-limited condition, the differential channel capacity is expressed as

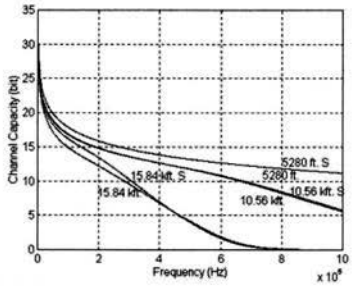
$$\frac{dC}{dB} = \log_2\left(1+\frac{S(f)}{N_F(f)}\right) = \log_2\left(1+\frac{1}{klf^2}\right)$$

For the self-FEXT-plus-receiver-front-end-white-noise-limited condition, the differential channel capacity is expressed as

$$\frac{dC}{dB} = \log_2\left(1+\frac{S(f)}{N_F(f)+W}\right) = \log_2\left(1+\frac{1}{klf^2+\frac{\sigma^2}{P}e^{2d\left(k_1\sqrt{f}+k_2 f\right)}}\right)$$

Figure 5.11 shows differential channel capacities under the self-FEXT-plus-white-noise condition for primary-constant-based and simplified channel models, also assuming a transmit power density of −40 dBm/Hz and a white noise power density of −140 dBm/Hz.

Figure 5.11 FEXT-and-White-Noise Differential Channel Capacity



Under the self-FEXT-limited condition, there are big portions where the differential channel capacity is larger than 5 bits. These 1 mile and 2 mile loops have a usable bandwidth beyond 1 MHz, while the 3 mile loop has a usable bandwidth of about 650 KHz.

5.2.3 *Channel Capacity with Implementation Constraints*

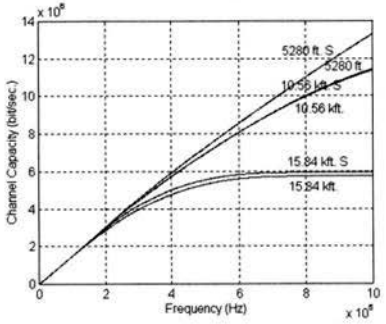
The channel capacity can be used as a reference for a DSL system design. With advanced modulation and coding techniques, the transmission throughput of a DSL system can be brought to within 2 to 6 dB of the channel capacity. You can further take some practical and test-procedural constraint into account to obtain a conditional channel capacity as a more practical design reference.

You observed from the previous calculations, for example, the high channel capacity of the self-FEXT-plus-white-noise-limited conditional is partially a contribution of the high signal-to-noise ratio (larger than 60 dB) at the low-frequency region. In practice, these high signal-to-noise ratios might not be realized due to the receiver hardware dynamic range.

One of the practical limitations of the SNR at the very low-frequency region is the transformer, which blocks DC and creates a high-pass filter that greatly reduces the SNR at very low frequency.

Figure 5.12 shows channel capacities under the same self-FEXT-plus-white-noise condition for primary-constant-based and simplified channel models except with a constraint of a hardware dynamic range of less than, for example, 45.15 dB. This effect is emulated by limiting the differential channel capacity to less or equal to 15 bits for all frequencies. As the figure indicates, channel capacities can be reduced by 10–15 percent due to hardware dynamic range.

Figure 5.12 FEXT Channel Capacity with 45.15 dB Hardware Dynamic Range

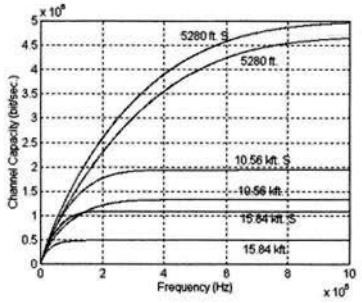


Many DSL systems were designed with a 6 dB performance margin reserved for non-characterized loop and system impairments. Figure 15.13 shows channel capacities under the same self-NEXT-plus-white-noise condition for primary-constant-based and simplified channel models with the addition of a 6 dB performance margin. The effect of the 6 dB performance margin is emulated by reducing the signal-to-noise ratio by a factor of 4 at all frequencies. The additional 6 dB performance margin can reduce the channel capacity by more than 20 percent.

Similar channel capacities can be calculated for 22-gauge and 24-gauge twisted-pair loops. You can find the distance scaling factor between different gauges of loops for the simplified channel model. Ignoring the effect of k_2s, you have the following:

$$d_{22} = d_{26}\frac{k_{1,26}}{k_{1,22}} = d_{26}\frac{4.8}{3.0} = 1.6d_{26}$$

Figure 5.13 NEXT Channel Capacity with 6 dB Noise Margin



Therefore, the channel capacities of a 5280 ft. 26-gauge simplified channel model are equivalent to those of a 8448 ft. 22-gauge simplified channel model. Similarly, you have

$$d_{24} = d_{26}\frac{k_{1,26}}{k_{1,24}} = d_{26}\frac{4.8}{3.8} = 1.26\,d_{26}$$

in which the simplified channel models are as follows for 26-gauge and 24-gauge twisted-pair cables, respectively:

$$H(d,f) = e^{-d\left(k_{1,26}\sqrt{f}+k_{2,26}f\right)}$$

$$H(d,f) = e^{-d\left(k_{1,24}\sqrt{f}+k_{2,24}f\right)}$$

This means that the channel capacities of a 5280 ft. 26-gauge simplified channel model is equivalent to those of a 6669 ft. 24-gauge simplified channel model.

End Notes

1. I. P. Auer, "Channel Capacity of Subscriber Loops Considering Near-End Crosstalk as the Dominant Source of Noise," Bellcore internal memorandum (June 1988). I. Kalet and S. Shamai-Shitz, "On the Capacity of a Twisted-Wire Pair: Gaussian Model," *IEEE Trans. Commun.*, vol. 38, no. 3 (March 1990): 379–383. J. T. Aslanis and J. M. Cioffi, "Achievable Information Rates on Digital Subscriber Loops: Limiting Information Rates with Crosstalk Noise," *IEEE Trans. Common.*, vol. 40, no. 2 (February 1992): 361–372. J. J. Werner, "The HDSL Environment," *IEEE JSAC*, vol. 9, no. 6 (August 1991): 785–800.

CHAPTER 6

Hybrid Circuits

For half-duplex telegraphs of early days, transmission was carried out only in one direction over one pair of two-wire cables at a given time. The transmission direction can be regulated through some handshake protocol whenever a transceiver at one end has data to transmit. The transmission direction can also be time divided: transceivers at both ends are synchronized and take turns transmitting. This is sometimes called *Time Division Multiplex* (TDM) or *Time Division Duplex* (TDD), respectively. For a telephone conversation, a real-time, full-duplex system, in which telephone subscribers at both ends can talk and listen simultaneously, is preferred to emulate a more natural situation.

Real-time, full-duplex transmission of voice signals can be accomplished using a hybrid circuit, which connects a microphone and an earphone to a two-wire telephone subscriber loop. A hybrid circuit is basically an electrical bridge. There is little signal from the transmit path coming back to the receiving path when the electrical bridge is balanced. The balance condition, however, requires the impedance match to the telephone subscriber loop. This condition cannot really be satisfied because the input impedance of a telephone loop is not exactly fixed, due to bridged taps and temperature variation.

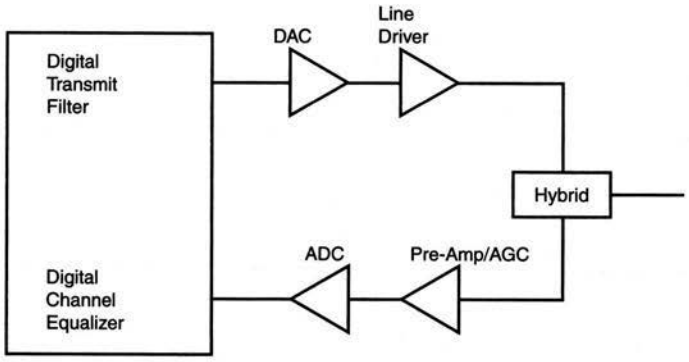
This small amount of impedance mismatch is tolerable for voice applications. In fact, the echo, which is caused by impedance mismatch of a hybrid circuit, of someone's own talk is usually perceived as an "alive" indication for a telephone connection.

For real-time, full-duplex data transmission applications, the amount of hybrid echo should be minimized; otherwise, the echo could interfere with the received signal. Although some telephone set hybrid circuits rely on voltage parities from different windings of one or two magnetic cores to cancel the transmit signal, hybrid circuits used for DSL systems are based on the balance of resistive networks to minimize the amount of echo.

DSL transceivers typically consist of both a single-ended and a differential hybrid circuit. Both circuits can be simplified to some resistive networks. DSL hybrid circuits also usually have a coupling transformer, which is mainly used for the purpose of longitudinal signal isolation and surge protection. Both wires of a telephone loop can pick up some substantial noises through the open electromagnetic field; however, the only difference between these two longitudinal signals appears after a transformer. A coupling transformer can also reduce the severity of some longitudinal surge voltage or current.

Because a hybrid is an analog circuit, it is connected to the rest of a DSL transceiver through a *Digital to Analog Converter* (DAC) in the transmitting path and an *Analog to Digital Converter* (ADC) in the receiving path. Figure 6.1 shows the typical structure of an *Analog Front End* (AFE) that connects the digital portion of a DSL transceiver to the telephone subscriber.

Figure 6.1 The General Structure of an Analog Front End



The transmit signal to a DAC is usually coming from digital transmit shaping filters, and the received signal from an ADC usually goes to channel equalizers. A hybrid circuit can provide some limited amount of transmission loss from the transmitting path to the receiving path, depending on the impedance balance condition. There is usually a line drive between the DAC and the hybrid circuit for supplying sufficient voltage and current onto the twisted-pair loop with certain line impedance.

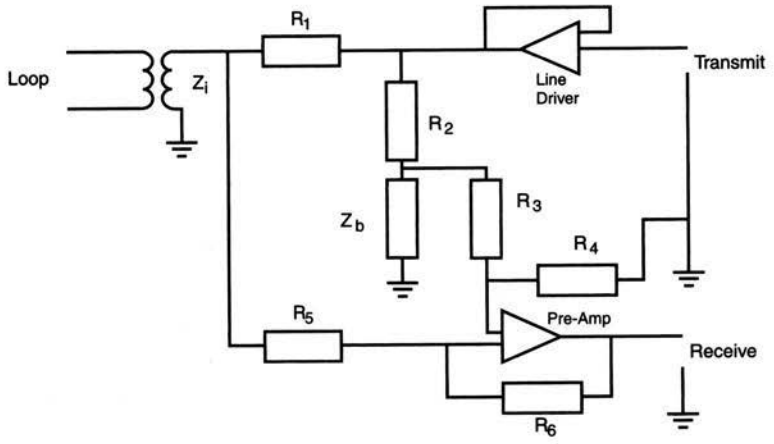
There is usually also a pre-amplifier with automatic gain control between the hybrid circuit and the ADC to raise the received signal level to that suitable for the input dynamic range of the ADC. There are typically two types of hybrid circuits used for Digital Subscriber Line (DSL) transceivers: single-ended hybrid circuits and differential hybrid circuits. This chapter explains the structure, functionality, and components of these two types of hybrid circuits and related concepts, as follows:

- *Single-ended hybrid circuits.* Single-ended hybrid circuits can be simplified into a classical electrical bridge with four branches. The transmitting path and the receiving path are connected at two diagonal ports, while the twisted-pair telephone loop is used as one of these branches through the coupling transformer.
- *Differential hybrid circuits.* Differential hybrid circuits can be simplified into a balance circuit of six resistors with six joints. The transmitting path, the receiving path, and the twisted-pair telephone loop are cross-connected through a coupling transformer to six joints of this balance network. A differential hybrid circuit is suitable for using a differential line driver.
- *Transformer equivalent circuits.* A line coupling transformer can be represented with a T-equivalent circuit for transformer design and system performance analysis. The ABCD parameters of the transformer equivalent circuit are also derived to be used in conjunction with ABCD parameters of the twisted-pair telephone subscriber loop.
- *Echo path model.* A realistic echo path model can be obtained by combining the equivalent circuit of the line coupling transformer, the balance network, and the input impedance of the loop. The echo path model can be used to assess the echo level and as a reference for the design of an echo canceller.

6.1 Single-Ended Hybrid Circuits

Figure 6.2 shows a single-ended hybrid circuit.

Figure 6.2 Single-Ended Hybrid Circuit



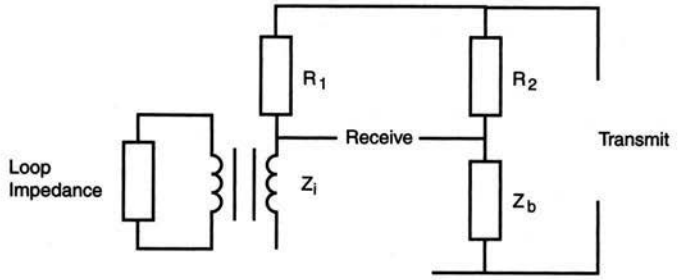
An electrical bridge connects the transmit line driver, the receive preamplifier, and the line transformer. The four branches of the electrical bridge are as follows:

- R_1
- R_2
- The equivalent twisted-pair loop impedance Z_i
- The balance impedance Z_b

The impedance seen by the twisted loop through the transformer is R_1 plus the line driver output impedance R_l. Because the output impedance of the line driver is usually negligible compared with R_1, the termination impedance for the twisted loop is approximately equal to R_1. The signal is received through R_3 and R_5 by the pre-amplifier, while R_4 and R_6 are resistors required as part of a differential feedback circuit.

The single-ended hybrid circuit can be simplified to an electrical bridge with the transformer and attached loop impedance as one of four branches, as shown in Figure 6.3.

Figure 6.3 Simplified Equivalent Circuit for Single-Ended Hybrid



The balance condition occurs when the signal loss from the transmitting path to the receiving path (also called the *echo return loss*) becomes infinity. A balance condition for a single-ended hybrid circuit is reached when you have

$$\frac{Z_i}{R_1 + Z_i} = \frac{Z_b}{R_2 + Z_b}$$

If $R_1 = Z_i$, then $Z_b = R_2$.

The echo path is defined as from the transmit port to the receive port. The echo path transfer function for the single-ended hybrid is

$$H_{ec}(f) = \frac{Z_i(f)}{R_1 + Z_i(f)} - \frac{Z_b(f)}{R_2 + Z_b(f)}$$

Note
You should be aware that the perfect balance condition cannot be achieved if only fixed resistors are used for the bridge network.

Zero line driver impedance and infinite pre-amplifier input impedance have been assumed in the previous expression of the echo path transfer function. A more accurate echo path transfer function can be obtained through the use of two-port network equivalent circuits and associated ABCD parameters. The two-port network ABCD matrix for this single-ended hybrid echo path is as follows:

$$\begin{bmatrix} A & B \\ C & D \end{bmatrix} = \begin{bmatrix} \dfrac{(R_1 + Z_i(f))(R_2 + Z_b(f))}{Z_i(f)R_2 - Z_b(f)R_1} & \dfrac{R_1R_2(Z_i(f) + Z_b(f)) + Z_i(f)Z_b(f)(R_1 + R_2)}{Z_i(f)R_2 - Z_b(f)R_1} \\ \dfrac{R_1 + R_2 + Z_i(f) + Z_b(f)}{Z_i(f)R_2 - Z_b(f)R_1} & \dfrac{(R_1 + R_2)(Z_i(f) + Z_b(f))}{Z_i(f)R_2 - Z_b(f)R_1} \end{bmatrix}$$

For $R_1 = R_2 = R$, we have

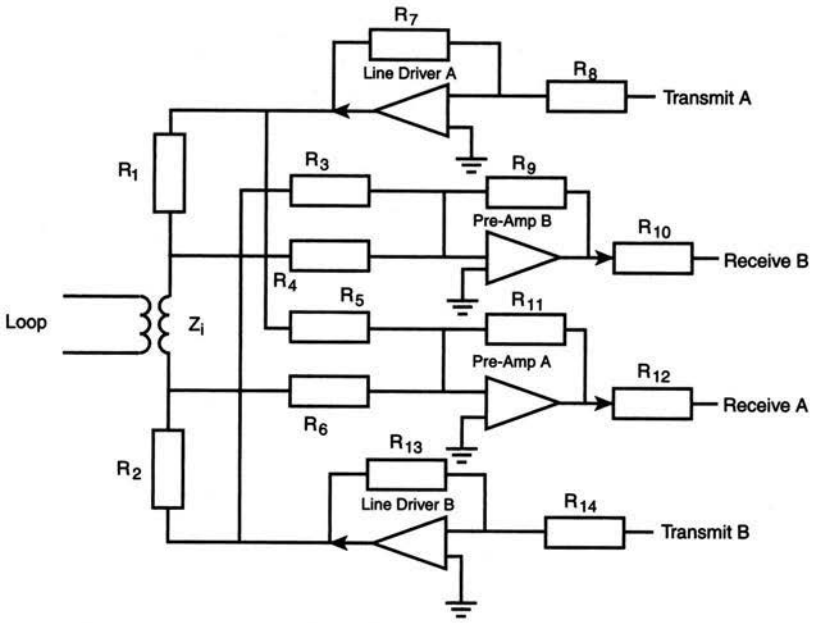
$$\begin{bmatrix} A & B \\ C & D \end{bmatrix} = \begin{bmatrix} \dfrac{R\left(1 + \dfrac{Z_i(f)}{R}\right)\left(1 + \dfrac{Z_b(f)}{R}\right)}{Z_i(f) - Z_b(f)} & \dfrac{R(Z_i(f) + Z_b(f)) + 2Z_i(f)Z_b(f)}{Z_i(f) - Z_b(f)} \\ \dfrac{2 + \dfrac{Z_i(f)}{R} + \dfrac{Z_b(f)}{R}}{Z_i(f) - Z_b(f)} & \dfrac{2(Z_i(f) + Z_b(f))}{Z_i(f) - Z_b(f)} \end{bmatrix}$$

You can also study the effect of line driver output and pre-amplifier input impedance using the ABCD matrix of the echo path. The single-ended hybrid circuit is suitable for a single output line driver. A differential output line driver requires a *differential hybrid circuit.*

6.2 *Differential Hybrid Circuits*

Figure 6.4 shows a differential hybrid circuit.

Figure 6.4 Differential Hybrid Circuit

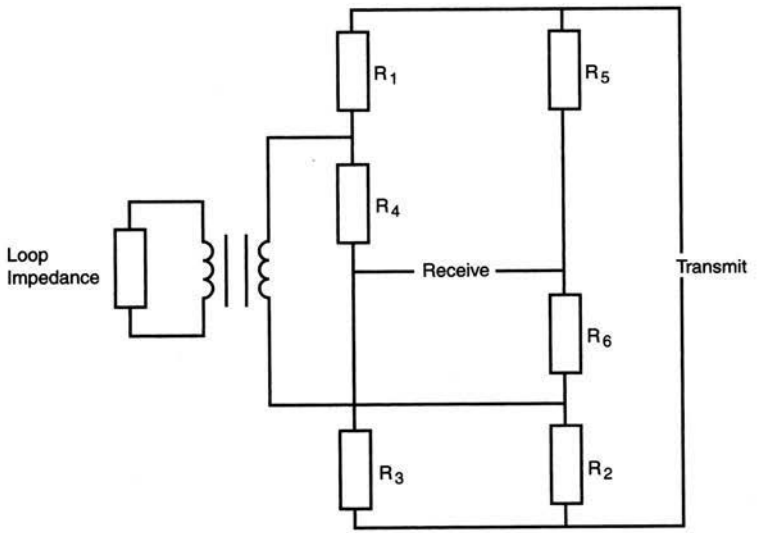


Outputs of a pair of differential line drivers are connected to joint points of $R_1 - R_4$ and $R_2 - R_3$. Inputs of a pair of differential pre-amplifiers are connected to joint points of $R_3 - R_4$ and $R_5 - R_6$. Notice that resistors R_3 and R_4 are effectively connected to the opposite phases of the line drivers, as are resistors R_5 and R_6.

The proper selection of resistor values can minimize the amount of transmitting signal coming back to the receiving path. The impedance seen by the twisted-pair loop through the transformer between one lead of the transformer and the ground is R_1 plus the line driver output impedance R_l. The impedance between the other lead of the transformer and the ground is R_2 plus the line driver output impedance R_l. Because the output impedance of the line driver is usually negligible, the termination impedance for the twisted loop is approximately equal to $R_1 + R_2$.

The balance resistive network of the differential hybrid can also be simplified to an electrical bridge with the transformer and its attached twisted-pair loop impedance connected in the middle of two branches, as shown in Figure 6.5.

Figure 6.5 Simplified Equivalent Circuit for Differential Hybrid



For the differential drive hybrid, we normally let $R_1 = R_2$, $R_3 = R_5$, and $R_4 = R_6$ through the choice of design. The balance condition for the differential drive hybrid is then reached when

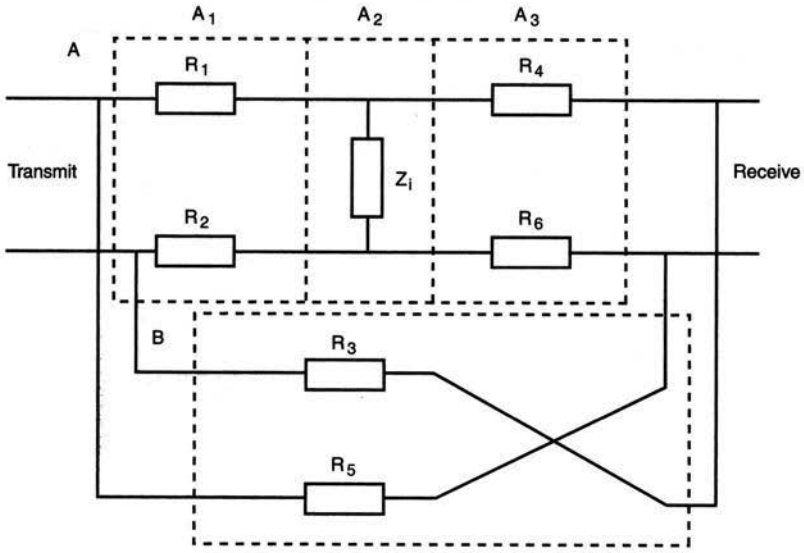
$$\frac{R_1}{R_1 + Z_i(f)} = \frac{R_3 - R_4}{R_3 + R_4}$$

choosing $R_1 = \frac{1}{2} Z_i(f)$ for termination impedance matching results in $R_3 = 2R_4$. The general echo path transfer function for the differential hybrid is as follows:

$$H_{ec}(f) = \frac{1}{2R_1 + Z_i(f)} \left[R_1 + \left(Z_i(f) + R_1 \right) \frac{R_4 - R_3}{R_4 + R_3} \right]$$

To consider the effect of line driver and preamplifier impedances, the use of two-port network equivalent circuits and associated ABCD parameters is required. To derive the ABCD matrix for the echo path of a differential hybrid circuit, we further arrange the simplified differential hybrid circuit into two two-port networks in parallel, as shown in Figure 6.6.

Figure 6.6 A Two-Port Network Parallel Representation of the Differential Hybrid Circuit



The two-port network A consists of three element two-port networks. The ABCD matrix for the two-port network A_1 is

$$\begin{bmatrix} A & B \\ C & D \end{bmatrix}_{A_1} = \begin{bmatrix} 1 & R_1 + R_2 \\ 0 & 1 \end{bmatrix}$$

The ABCD matrix for the two-port network A_2 is

$$\begin{bmatrix} A & B \\ C & D \end{bmatrix}_{A_2} = \begin{bmatrix} 1 & 0 \\ \frac{1}{Z_i} & 1 \end{bmatrix}$$

The ABCD matrix for the two-port network A_3 is

$$\begin{bmatrix} A & B \\ C & D \end{bmatrix}_{A_3} = \begin{bmatrix} 1 & R_4 + R_6 \\ 0 & 1 \end{bmatrix}$$

The ABCD matrix for the two-port network A is

$$\begin{bmatrix} A & B \\ C & D \end{bmatrix}_A = \begin{bmatrix} A & B \\ C & D \end{bmatrix}_{A_1} \begin{bmatrix} A & B \\ C & D \end{bmatrix}_{A_2} \begin{bmatrix} A & B \\ C & D \end{bmatrix}_{A_3}$$

$$= \begin{bmatrix} 1 + \dfrac{R_1 + R_2}{Z_i} & R_1 + R_2 + R_4 + R_6 + \dfrac{(R_1 + R_2)(R_4 + R_6)}{Z_i} \\ \dfrac{1}{Z_i} & 1 + \dfrac{R_4 + R_6}{Z_i} \end{bmatrix}$$

The ABCD matrix for the two-port network B is

$$\begin{bmatrix} A & B \\ C & D \end{bmatrix}_B = -\begin{bmatrix} 1 & R_3 + R_5 \\ 0 & 1 \end{bmatrix}$$

For $R_1 = R_2$, $R_3 = R_5$, and $R_4 = R_6$, we have

$$\begin{bmatrix} A & B \\ C & D \end{bmatrix}_A = \begin{bmatrix} 1 + \dfrac{2R_1}{Z_i} & 2R_1 + 2R_4 + \dfrac{4R_1R_4}{Z_i} \\ \dfrac{1}{Z_i} & 1 + \dfrac{2R_4}{Z_i} \end{bmatrix}$$

and

$$\begin{bmatrix} A & B \\ C & D \end{bmatrix}_B = \begin{bmatrix} 1 & 2R_3 \\ 0 & 1 \end{bmatrix}$$

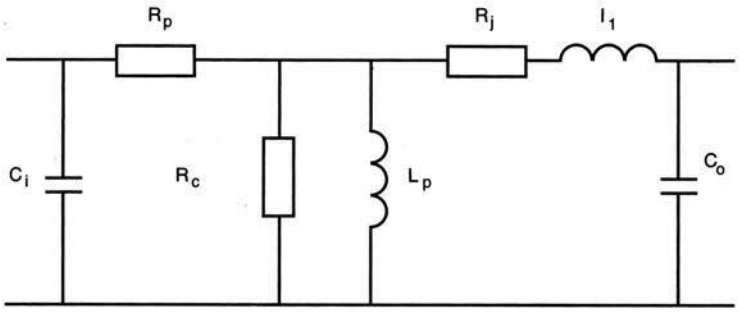
The two-port network ABCD matrix for this differential hybrid echo path is

$$\begin{bmatrix} A & B \\ C & D \end{bmatrix} = \begin{bmatrix} \dfrac{-\dfrac{R_3\left(1+\dfrac{2R_1}{Z_i}\right)+R_1+R_4+\dfrac{2R_1R_4}{Z_i}}{R_1-R_3+R_4+\dfrac{2R_1R_4}{Z_i}}}{} & \dfrac{-\dfrac{2R_3\left(R_1+R_4+\dfrac{2R_1R_4}{Z_i}\right)}{R_1-R_3+R_4+\dfrac{2R_1R_4}{Z_i}}}{} \\ \dfrac{\dfrac{1}{Z_i}\left(R_1-R_3+R_4+\dfrac{2R_1R_4}{Z_i}\right)-2\left(1+\dfrac{R_1}{Z_i}\right)\left(1+\dfrac{1R_4}{Z_i}\right)}{R_1-R_3+R_4+\dfrac{2R_1R_4}{Z_i}} & \dfrac{R_3\left(1+\dfrac{2R_4}{Z_i}\right)+R_1+R_4+\dfrac{2R_1R_4}{Z_i}}{R_1-R_3+R_4+\dfrac{2R_1R_4}{Z_i}} \end{bmatrix}$$

6.3 *Transformer Equivalent Circuits*

The transfer function of a transformer connecting the twisted-pair loop to the hybrid circuit can be determined according to its equivalent circuit. Figure 6.7 shows a typical transformer equivalent circuit.[1]

Figure 6.7 Simplified Hybrid or Transformer Equivalent Circuit



Key parameters for the transformer equivalent circuit include the following:

R_p—The resistance of the primary coil

R_s—The resistance of the secondary coil

R_c—The core resistance

L_p—The primary inductance

L_l—The leakage inductance

C_i—The input capacitance

C_o—The output capacitance

The ABCD matrix of the transformer equivalent circuit is

$$\begin{bmatrix} A & B \\ C & D \end{bmatrix} = \begin{bmatrix} 1 & 0 \\ sC_i & 1 \end{bmatrix} \begin{bmatrix} 1 & R_p \\ 0 & 1 \end{bmatrix} \begin{bmatrix} 1 & 0 \\ \frac{1}{R_c} + \frac{1}{sL_p} & 1 \end{bmatrix} \begin{bmatrix} 1 & R_s + sL_l \\ 0 & 1 \end{bmatrix} \begin{bmatrix} 1 & 0 \\ sC_o & 1 \end{bmatrix}$$

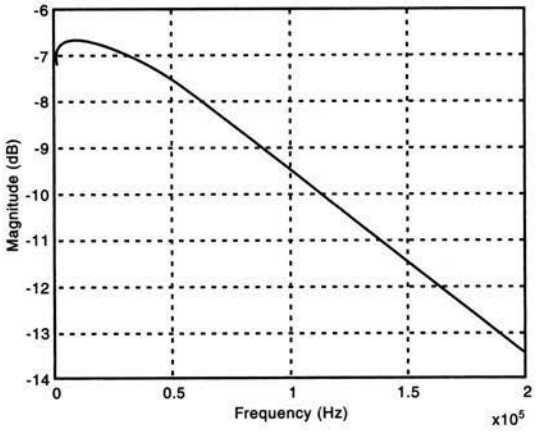
6.3.1 *ISDN Transformer Equivalent Circuit Parameters*

Transformer equivalent circuit parameters for a typical Basic Rate Access ISDN (Integrated Services Digital Network) channel, also called Digital Subscriber Line (DSL) transceiver, are as follows:

$R_p = 8\ \Omega$
$R_s = 12\ \Omega$
$R_c = 150\ k\Omega$
$L_p = 28.5\ mH$
$L_l = 28\ \mu H$
$C_i = 22\ pF$
$C_o = 22\ pF$

Figure 6.8 shows the frequency response of a transformer designed for an ISDN transceiver with source and termination impedances of 135 ohms.

Figure 6.8 Transfer Function of an ISDN Transformer



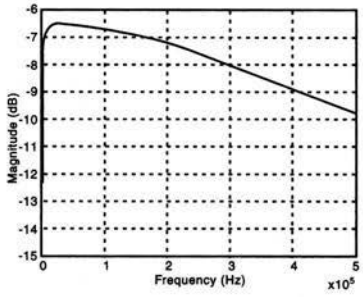
6.3.2 HDSL Transformer Equivalent Circuit Parameters

Transformer equivalent circuit parameters for a typical High-bit-rate Digital Subscriber Line (HDSL) transceiver are as follows:

$R_p = 1.8\ \Omega$
$R_s = 2.5\ \Omega$
$R_c = 50\ k\Omega$
$L_p = 3\ mH$
$L_l = 29\ \mu H$
$C_i = 35\ pF$
$C_o = 35\ pF$

Figure 6.9 shows the frequency response of a transformer designed for an HDSL transceiver with source and termination impedances of 135 ohms.

Figure 6.9 Transfer Function of an HDSL Transformer



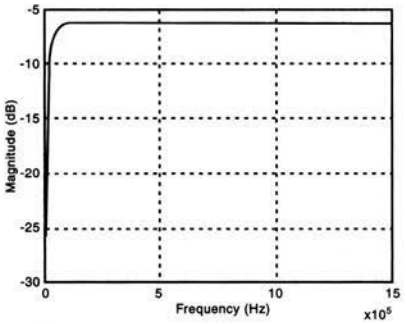
6.3.3 ADSL Transformer Equivalent Circuit Parameters

Transformer equivalent circuit parameters for a typical Asymmetrical Digital Subscriber Line (ADSL) transceiver are as follows:

$R_p = 1.32\ \Omega$
$R_s = 1.12\ \Omega$
$R_c = 50\ k\Omega$
$L_p = 407.5\ \mu H$
$L_l = 5.4\ \mu H$
$C_i = 35\ pF$
$C_o = 35\ pF$

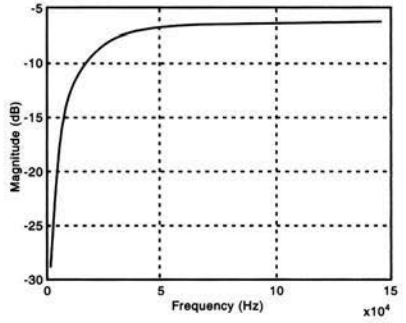
Figure 6.10 shows the frequency response of a transformer designed for an ADSL transceiver with source and termination impedances of 100 ohms.

Figure 6.10 Transfer Function of an ADSL Transformer



The low frequency portion of the transfer function is enlarged in Figure 6.11.

Figure 6.11 Transfer Function of an ADSL Transformer at Low Frequencies



Among these DSL transformers, the one for ISDN has the narrowest bandwidth, and the one for ADSL has the widest bandwidth. The bandwidth of a DSL transformer depends on the primary inductance: The larger the primary inductance, the narrower the bandwidth. On the other hand, a smaller primary inductance leads to a higher low-corner frequency, as shown in Figure 6.11. The selection of low- and high-corner frequencies are interrelated with the current transformer technologies.

6.4 *Echo Path Model*

Because of the impedance mismatch, there is always echo of transmitted signal to a DSL receiver front end coming back from the hybrid circuit. The knowledge of the magnitude of the echo is necessary to determine the dynamic range of receiver front-end analog circuits.

A total characterization of the echo path transfer function is required for the design of an echo canceller.

Transmission at opposite directions of a DSL system can also be achieved through using different frequency bands. This is sometimes called *Frequency Division Multiplex* (FDM) or *Frequency Division Duplex* (FDD). A hybrid circuit with high echo return loss is also preferred for an FDM or FDD DSL system to relax the requirement of band separating filters.

A realistic echo path model can be constructed based on the hybrid circuit configuration, the transformer equivalent circuit, and the input impedance of the telephone subscriber loop. The effect of transmit and receiver filters or band separating filters can also be included depending on different design reference objectives. The calculation of the echo path transfer function can be carried out using two-port network equivalent circuits and associated ABCD parameters.

The input impedance of a twisted-pair loop can be expressed by its ABCD parameters as

$$Z_i = \frac{A + \dfrac{B}{Z_t}}{C + \dfrac{D}{Z_t}}$$

The value Z_t is the termination impedance at the other end of the twisted-pair loop. We can also express the twisted-pair loop impedance with the inclusion of the transformer by recognizing

$$\begin{bmatrix} A & B \\ C & D \end{bmatrix} = \begin{bmatrix} A_T & B_T \\ C_T & D_T \end{bmatrix} \begin{bmatrix} A_l & B_l \\ C_l & D_l \end{bmatrix} = \begin{bmatrix} A_T A_l + B_T C_l & A_T B_l + B_T D_l \\ C_T A_l + D_T C_l & C_T B_l + D_T D_l \end{bmatrix}$$

in which

$_T$ denotes the transformer.

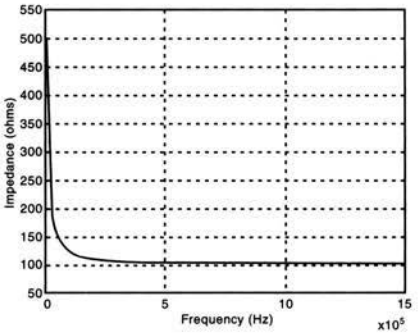
$_l$ denotes the twisted-pair loop.

The input impedance of a twisted-pair loop connected through a transformer can be expressed by its ABCD parameters as

$$Z_i = \frac{A_T A_l + B_T C_l + \dfrac{A_T B_l + B_T D_l}{Z_t}}{C_T A_l + D_T C_l + \dfrac{C_T B_l + D_T D_l}{Z_t}}$$

Figure 6.12 shows the magnitude of the input impedance of a 1 mile, 26-gauge twisted-pair loop.

Figure 6.12 Magnitude of the Input Impedance of a 1 Mile, 26-Gauge Loop



The magnitude of the input impedance converges to about 100 ohms at high frequency, while the magnitude can be at around 600 ohms or higher at voiceband.

Figure 6.13 shows the real and imaginary parts of the 1 mile, 26-gauge twisted-pair loop input impedance. The amplitude of the imaginary part is negligible at both low and high frequencies, while it can be as large as –200 ohms in between these extreme frequencies. In Figure 6.13, circles are marked at 15 kHz apart.

Figure 6.13 Real and Imaginary Parts of the Input Impedance of a 1 Mile, 26-Gauge Loop

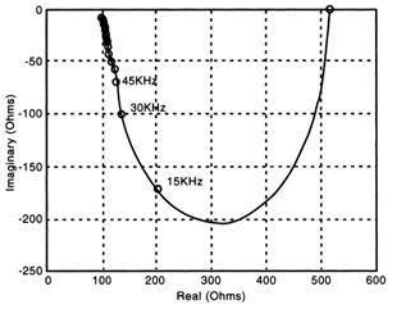


Figure 6.14 shows the magnitude of the input impedance of a twisted-pair loop with bridged taps. Originally detailed in Chapter 3, "Twisted-Pair Channel Modeling," the configuration of this loop is shown in Figure 6.15. The magnitude of the input impedance also converges to about 100 ohms at high frequency, but not always larger than 100 ohms.

Figure 6.14 Magnitude of the Input Impedance of a Loop with Bridged Taps

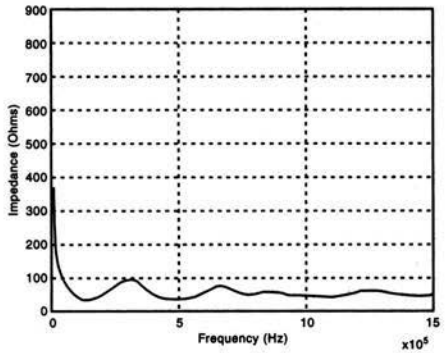


Figure 6.15 Configuration of a Subscriber Loop with Bridged Taps

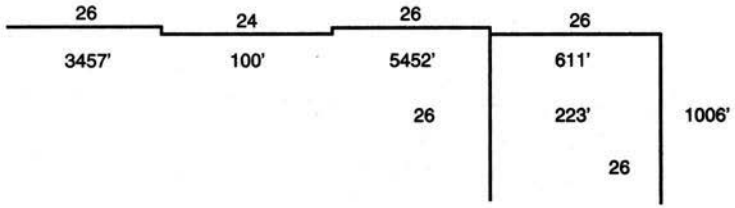


Figure 6.16 shows the real and imaginary parts of input impedance for the twisted-pair loop with bridged taps according to the configuration of Figure 6.15. The amplitude of the imaginary part is also negligible at both low and high frequencies. In Figure 6.16, circles are also marked at 15 kHz apart.

Figure 6.17 shows the magnitude of the input impedance of a 1 mile, 26-gauge twisted-pair loop with the inclusion of the transformer used for the Basic Rate Access ISDN channel, which is also called DSL. The DSL transmit signal energy is mostly concentrated at below 50 kHz.

Figure 6.16 Real and Imaginary Parts of the Input Impedance of a Loop with Bridged Taps

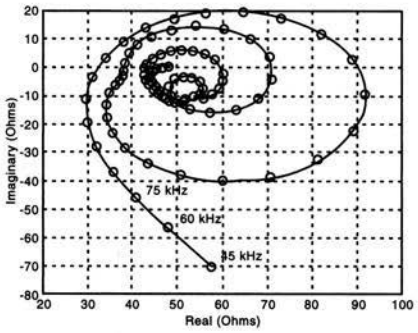


Figure 6.17 Magnitude of a 1 Mile, 26-Gauge Loop Including a DSL Transformer

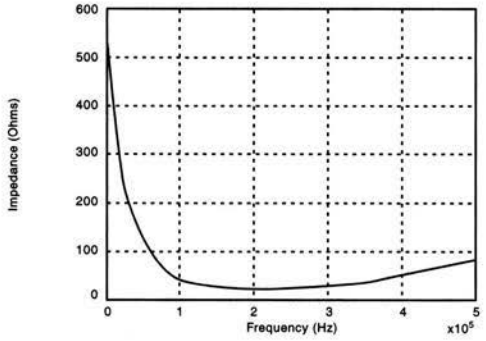


Figure 6.18 shows the real and imaginary parts of the input impedance for a 1 mile, 26-gauge twisted-pair loop with a DSL transformer. The upper portion of the curve corresponds to the low frequency part of the loop input impedance. In Figure 6.18, circles are marked at 5 kHz apart.

Figure 6.19 shows the magnitude of the input impedance of a 1 mile, 26-gauge twisted-pair loop with the inclusion of an HDSL transformer. The HDSL transmit signal energy is mostly concentrated at below 200 kHz.

Figure 6.20 shows the real and imaginary parts of the input impedance for a 1 mile, 26-gauge twisted-pair loop with an HDSL transformer. The upper portion of the curve also corresponds to the low frequency part of the loop input impedance. In Figure 6.20, circles are also marked at 5 kHz apart.

Figure 6.18 Real and Imaginary Parts of a 1 Mile, 26-Gauge Loop Including a DSL Transformer

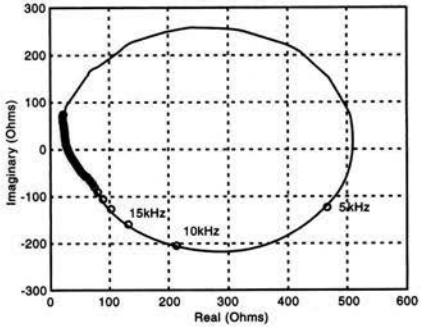


Figure 6.19 Magnitude of a 1 Mile, 26-Gauge Loop Including an HDSL Transformer

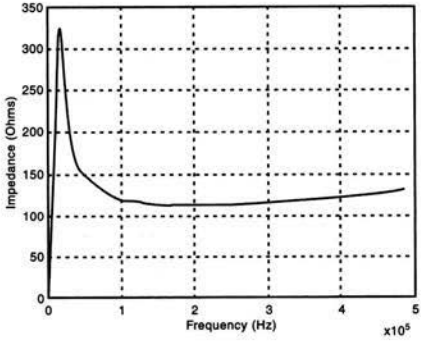


Figure 6.20 Real and Imaginary Parts of a 1 Mile, 26-Gauge Loop Including an HDSL Transformer

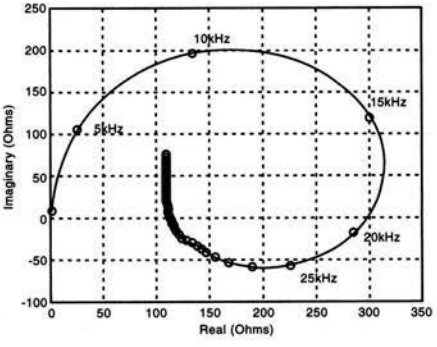


Figure 6.21 shows the magnitude of the input impedance of a twisted-pair loop with bridged taps and the inclusion of a DSL transformer. The configuration of this loop is also from Figure 6.15.

Figure 6.21 Magnitude of a Loop with Bridged Taps Including a DSL Transformer

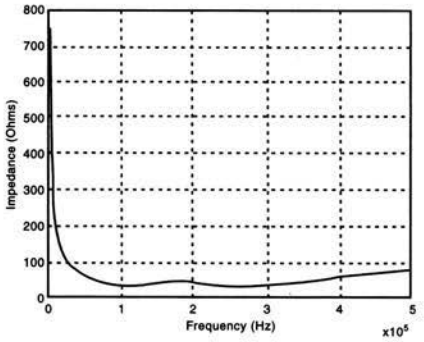


Figure 6.22 shows the real and imaginary parts of the input impedance for the twisted-pair loop with bridged taps according to the configuration of Figure 6.15 and with the inclusion of a DSL transformer. The upper portion of the curve corresponds to the low-frequency part of the loop input impedance.

Figure 6.22 Real and Imaginary Parts of a Loop with Bridged Taps Including a DSL Transformer

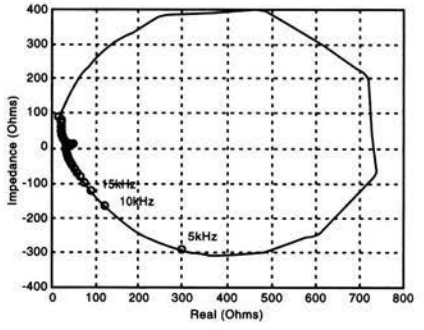


Figure 6.23 shows the magnitude of the input impedance of a twisted-pair loop with bridged taps for the configuration of Figure 6.15 and the inclusion of an HDSL transformer.

Figure 6.23 Magnitude of a Loop with Bridged Taps Including an HDSL Transformer

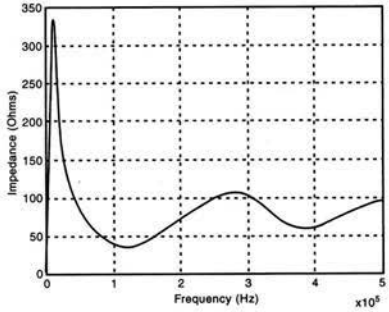


Figure 6.24 shows the real and imaginary parts of the input impedance for the twisted-pair loop with bridged taps for the configuration of Figure 6.25 and the inclusion of an HDSL transformer. The upper portion of the curve corresponds to the low frequency part of the loop input impedance.

Figure 6.24 Real and Imaginary Parts of a Loop with Bridged Taps Including an HDSL Transformer

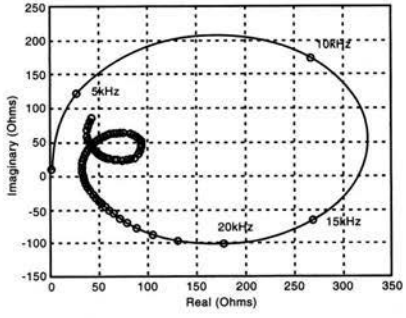
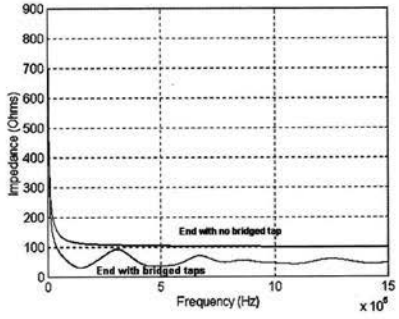


Figure 6.25 Input Impedance of a Twisted-Pair Loop with Bridged Taps

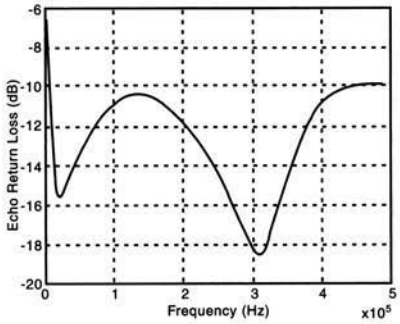


The echo path transfer function for the single-ended hybrid circuit can be calculated by letting $R_1 = 135\ \Omega$ and $R_2 = Z_b = 1000\ \Omega$ in conjunction with twisted-pair loop impedances with the inclusion of transformers. The echo path transfer function derived in section 6.1, "Single-Ended Hybrid Circuits," for the single-ended hybrid circuit can be simplified as follows:

$$H_{ec}^{s}(f) = \frac{1}{2}\frac{Z_i(f) - R_1^s}{Z_i(f) + R_1^s}$$

The superscript *s* denotes the transfer function and the resistor for the single-ended hybrid circuit to distinguish those of the differential hybrid circuits. Figure 6.26 shows the echo path transfer function for the twisted-pair loop with bridged taps and an HDSL transformer.

Figure 6.26 Echo Path Transfer Function for a Single-Ended Hybrid Circuit with a Twisted-Pair Loop of Bridged Taps and an HDSL Transformer

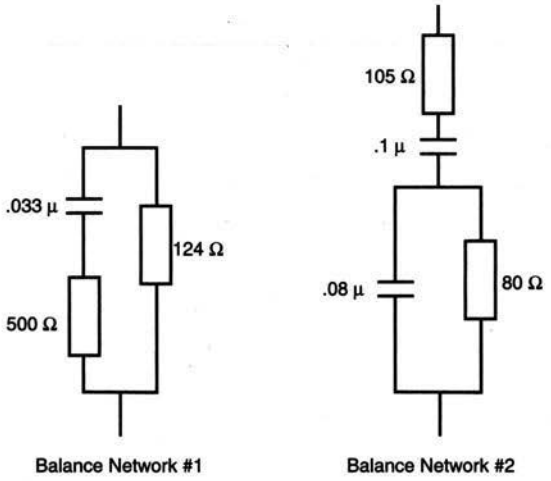


To enhance the echo return loss, Z_b can be implemented with an RC network.[2]

Note
An RC network can be used to emulate the frequency dependent input impedance of a twisted-pair telephone loop.

The RC balance network #1 in Figure 6.27 has a resistor in parallel with a serial RC network. The RC balance network #2 has a parallel RC network and a serial RC network in serial.

Figure 6.27 Two RC Balance Networks



Figures 6.28 and 6.29 show echo path transfer functions with RC balance networks #1 and #2, respectively, in conjunction with an R_2 of 100 ohms. The use of a fixed RC balance network balance is not particularly effective against telephone subscriber loops with bridged taps.

Figure 6.28 Echo Path Transfer Function for a Single-Ended Hybrid Circuit with the RC Network #1

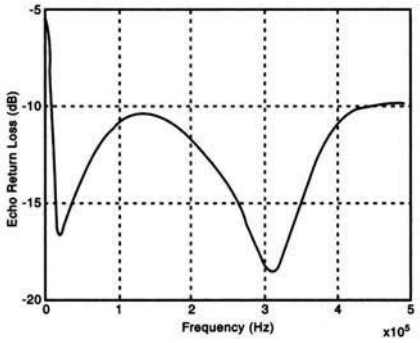
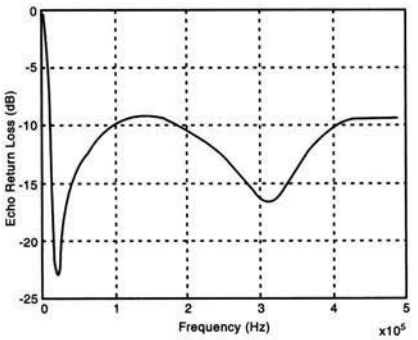


Figure 6.29 Echo Path Transfer Function for a Single-Ended Hybrid Circuit with the RC Network #2



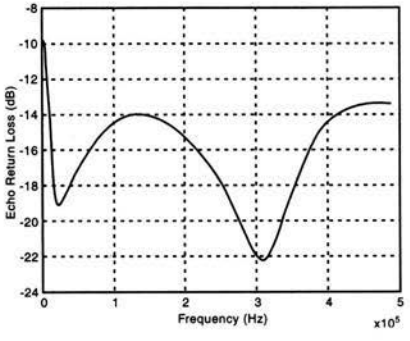
The echo path transfer function for the differential hybrid circuit can be calculated by letting $R_1 = R_2 = 67\ \Omega$ and $R_3 = 2R_4 = 2000\ \Omega$ also in conjunction with twisted-pair loop impedances with the inclusion of transformers. The echo path transfer function derived in section 6.2, "Differential Hybrid Circuits," for the differential hybrid circuit can be simplified as follows:

$$H_{ec}^{d}(f) = \frac{1}{3}\frac{2R_1^d - Z_i(f)}{2R_1^d + Z_i(f)}$$

The superscript *d* denotes the transfer function and the resistor for the differential hybrid circuit.

Figure 6.30 shows the echo path transfer function for the twisted-pair loop with bridged taps and an HDSL transformer.

Figure 6.30 Echo Path Transfer Function for a Differential Hybrid Circuit with a Twisted-Pair Loop of Bridged Taps



The transfer function has the same shape as that of a single-ended hybrid; the loss difference is due to the scaling factors of $1/2$ over $1/3$ when $R_1^s = 2R_1^d$. The loss difference is $20 \times \log_{10}(3/2) = 3.52$ dB. The performance of a differential hybrid, however, is the same as that of a single-ended hybrid circuit because the received signal through a differential hybrid circuit also experiences 3.52 dB more loss.

End Notes

1. Midcom web page at **http://www.midcom-inc.com/technotes/tn17.html**.

2. W. Y. Chen, J. L. Dixon, and D. L. Waring, "HDSL Echo Cancellation," *IEEE JSAC,* vol. 9, no. 6 (August 1991): 848–860. G. S. Moschytz and S. V. Ahamed, "Transhybrid Loss with RC Balance Circuits for Primary-Rate ISDN Transmission Systems," *IEEE JSAC,* vol. 9, no. 6 (August 1991): 951–959.

CHAPTER 7

Analog Front-End Precision

Some transmission systems can be realized with analog circuit technology only, such as transmit line driver, receiver amplifier, and threshold detector. The transmission potential cannot be fully realized, however, with the use of current analog circuit technology only. Digital processing techniques, such as adaptive channel equalization and adaptive echo cancellation, have played a very important role at maximizing the transmission efficiency of DSL systems.

On the other hand, the transmit signal still needs to be in analog format to fit the analog twisted-pair telephone loop better. Information after digital signal processing with limited precision is converted to analog format through a *Digital to Analog Converter* (DAC), and the received analog signal is converted through an *Analog to Digital Converter* (ADC) for further digital signal processing.

The precision of DAC and ADC should be fine enough to realize the potential of the analog telephone subscriber loop channel. In other words, the precision should be chosen such that the DAC and ADC quantization noise will not be a limiting factor for the transmission performance of DSL systems. The required DAC and ADC precision depends on the following:

- The transmit signal line code
- The transmit shaping filter
- The characteristics of the channel
- The attenuation of the echo path

There are baseband, passband single-carrier, and multiple-carrier line codes used for DSL systems. The four-level baseband line code, also called 2B1Q for 2 bits per quaternary, has been used for both the *Basic Rate Access ISDN channel* (also called DSL) and for HDSL.

A baseband line code usually consists of many parity symmetric and equally spaced signal levels. Passband single carrier line codes, such as *Quadrature Amplitude Modulation* (QAM) *and Carrierless AM/PM* (CAP), have also been proposed for DSL systems. A passband single carrier line code has a two-dimensional signal. The two-dimensional signal is divided into an in-phase channel and a quadrature channel implemented by the cosine and sine phases of the single carrier, respectively.

Parity symmetric and equally spaced multiple signal levels are used for both in-phase and quadrature channels. The *Discrete MultiTone* (DMT) line code is the standard for ADSL. A DMT line code consists of a multiple of single carriers implemented through the *Discrete Fourier Transform* (DFT). The number of carriers available to carry information is equal to, or slightly less than, half of the DFT size. Each carrier of a DMT line code has the same two-dimensional signal as that of a passband single carrier system.

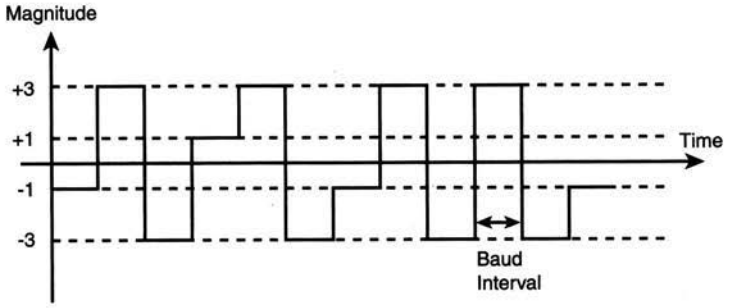
Different line codes have different peak-to-average voltage ratios. The peak-to-average voltage ratio can also be affected by transmit shaping filters for a DAC and by the channel and the echo path for an ADC. This chapter discusses issues related to the determination of DAC and ADC precision requirements including the following:

- *Peak-to-average ratio (PAR) of line codes.* PARs are calculated for baseband multiple level, passband single carrier, and DMT multiple carrier line codes. Relationships of PARs to the number of signal levels, constellation size, and the number of carriers are derived. The effect of clipping for the DMT line code is also discussed.
- *Effects of transmit filter, channel, and echo path.* The use of a transmit filter generally leads to a higher PAR. The PAR can also be increased for a signal passing through the telephone subscriber loop channel. The echo path could produce the same effect.
- *Characteristics of ADC and DAC.* The effect of ADC and DAC quantization noise and its relationship to required PAR are discussed. The effect of ADC and DAC nonlinearity is compared with that of quantization noise.
- *ADC and DAC precision requirements.* Combining PARs of different line codes and the quantization noise of ADC and DAC, precision requirements are estimated for a few practical DSL system examples.

7.1 *Transmit Signal Peak-to-Average Voltage Ratio*

A binary baseband signal can have signal levels of –1 and +1. A four-level baseband signal can have signal levels of –3, –1, +1, and +3. Figure 7.1 shows the waveform of a baseband 2B1Q line code.

Figure 7.1 A Baseband 2B1Q Line Code



For the previous and following baseband signals, the distance between adjacent signal levels is maintained to be 2. In general, an n level baseband signal can have signal levels of $-n+1$, $-n+3$, … $n-3$, $n-1$, for which n is an even number.

Assuming a load resistance of one, the average power for a binary signal is one. Using the same load resistance value assumption, the average power for a four-level signal is $\left(1^2+3^2\right)/2$. In general, the average power for an n level baseband signal is

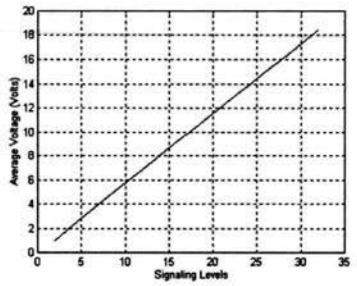
$$\frac{2}{n}\left(1^2+3^2+\ldots(n-1)^2+(n-1)^2\right)=\frac{n^2-1}{3}$$

Assuming a load resistance of one, the average voltage of this n level baseband signal is

$$\sqrt{\frac{n^2-1}{3}}$$

Figure 7.2 shows average voltage levels for different levels of baseband signals assuming a voltage of two volts between adjacent signal levels.

Figure 7.2 Average Signal Magnitude of Baseband Signal



For a peak voltage level of $(n-1)$ volts, the peak-to-average voltage ratio of an n level baseband signal is

$$(n-1)\sqrt{\frac{3}{(n^2-1)}} = \sqrt{\frac{3(n-1)}{n+1}}$$

Figure 7.3 shows peak-to-average voltage ratio (PAR) for baseband signals with different numbers of signaling levels.

Figure 7.3 Peak-to-Average Voltage Ratio of Baseband Signal

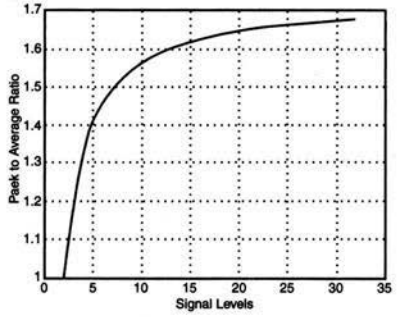
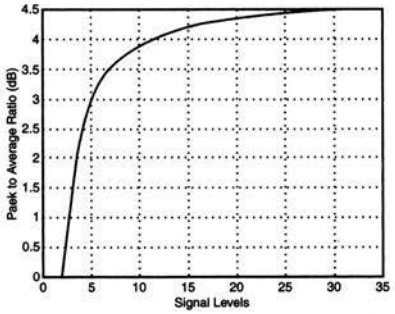


Figure 7.4 shows the same PAR in terms of dB.

Figure 7.4 Peak-to-Average Voltage Ratio (dB)



In practice, the peak transmit voltage is limited by the voltage level of a power supply. For a 5 volt power supply, the peak-to-peak voltage can be as high as 4.6 volts without introducing too much amplifier nonlinearity. Using a single-ended hybrid circuit, the peak signal level can be represented by a voltage level of 2.3 volts. Under the power supply voltage limited condition, the average transmit power for an n level baseband signal with a load resistance of 135 ohms is then

$$P_T = \frac{2.3^2}{135}\left(\frac{(n+1)}{3(n-1)}\right)$$

For an example of a four-level signal, the average transmit power is

$$P_T = \frac{2.3^2}{135}\left(\frac{5}{3\times 3}\right) = 0.02177 \text{ Watts} = 13.38 \text{ dBm}$$

Because of the increased PAR, the average transmit power for a 32-level baseband signal with the same 5 volt power supply is 2 dB lower.

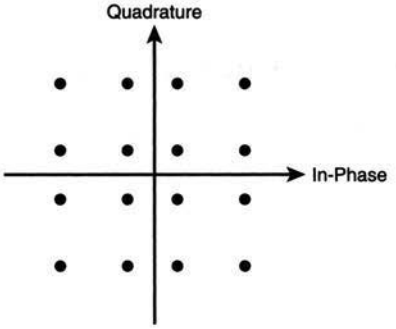
7.1.1 *PAR of Passband Single Carrier Line Codes*

A two-dimensional passband single carrier line code can be characterized by its constellation. A CAP line code is a little different compared with the QAM line code. The difference is explained in Chapter 8, "Channel Equalization." CAP and QAM line codes can, however,

share the same constellation. A QAM with a constellation size of 4 is also called *Quadrature Phase Shift Keying* (QPSK) for its four phases of the same magnitude.

Assuming a two-dimensional constellation can be represented by multiple signal levels, similar to the baseband case, in each orthogonal dimension, a 4 CAP/QAM signal can have signal levels of –1 and +1 in each dimension, but only one magnitude of $\sqrt{2}$. A 16 CAP/QAM signal can have four signal levels, –3, –1, +1, or +3, in each orthogonal dimension. Possible magnitude values for a 16 CAP/QAM signal are $\sqrt{2}$, $\sqrt{10}$, and $3\sqrt{2}$. Figure 7.5 shows a 16 CAP/QAM constellation.

Figure 7.5 A 16 CAP/QAM Constellation



In general, a 2^{2n} CAP/QAM constellation can have magnitudes of the following:

$$\sqrt{2}, \sqrt{1+3^2}, \cdots, \sqrt{1+\left(2^n-1\right)^2}, \sqrt{3^2+1}, \sqrt{3^2+3^2}, \cdots, \sqrt{3^2+\left(2^n-1\right)^2}, \cdots,$$
$$\sqrt{\left(2^n-1\right)^2+1}, \cdots, \sqrt{\left(2^n-1\right)^2+\left(2^n-1\right)^2}$$

The value n is the constellation size index, which is the number of bits in each dimension.

For $n=1$, we have a 4 CAP/QAM constellation; for $n=2$, we have a 16 CAP/QAM constellation, and so forth.

Also, by assuming a load resistance of one, the average power for a 4 CAP/QAM signal is 2. Assuming the same load resistance value, the average power for a 16 CAP/QAM signal is

$$(4\times 2+8\times 10+4\times 18)/16=10$$

In general, the average power for a 2^{2n} CAP/QAM signal is

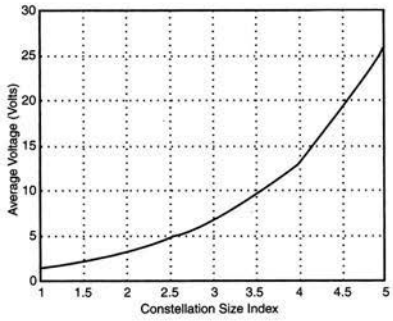
$$\left(\frac{4}{2^{2n}} \times \sum_{i=1}^{2^{n-1}} \sum_{j=1}^{2^{n-1}} \left((2i-1)^2 + (2j-1)^2\right)\right) = \frac{2}{3}\left(2^{2n}-1\right)$$

The average voltage of a 2^{2n} CAP/QAM signal in conjunction with a 1 ohm load resistance is

$$\sqrt{\frac{2}{3}\left(2^{2n}-1\right)}$$

Figure 7.6 shows average voltage levels for a passband signal with different constellation size indices.

Figure 7.6 Average Signal Magnitude of Passband Signal



A passband sinusoidal signal also has a peak-to-mean square root voltage, which corresponds to the power ratio of $\sqrt{2}$. With the consideration of the sinusoidal peak value, the peak-to-average voltage ratio of a passband signal is

$$\sqrt{\frac{6\left(2^n-1\right)}{2^n+1}}$$

Figure 7.7 shows peak-to-average voltage ratio (PAR) for passband signals of different constellation size indices.

Figure 7.7 Peak-to-Average Voltage Ratio of Passband Signal

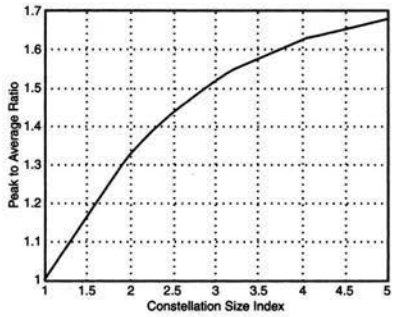
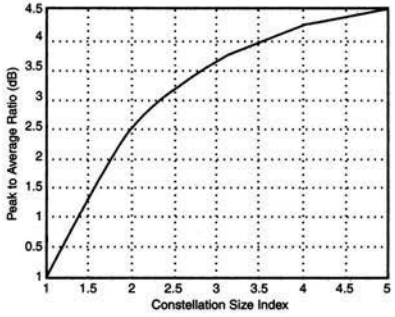


Figure 7.8 shows the same PAR in terms of dB.

Figure 7.8 Peak-to-Average Voltage Ratio in dB



Using a 5 volt power supply and a single-ended hybrid circuit, the average transmit power for an n level passband signal in conjunction with a load resistance of 135 ohms is then

$$P_T = \frac{2.3^2}{135}\frac{2^n+1}{6(2^n-1)}$$

For an example of a 16 CAP/QAM signal, the average transmit power is

$$P_T = \frac{2.3^2}{135}\left(\frac{5}{6\times 3}\right) = 0.01088 \text{ Watts} = 10.37 \text{ dBm}$$

Under the same power supply voltage, the average transmit power of a 16 CAP/QAM line code is about 3 dB less compared with a 2B1Q line code of the same transmission

throughput under the same transmission bandwidth. The 3 dB power reduction of the 16 CAP/QAM line code is partially caused by the sinusoid peak-to-average ratio of $\sqrt{2}$.

7.1.2 PAR of DMT Line Codes

A Discrete MultiTone (DMT) system consists of multiple QAM constellations, each of which has a different carrier frequency. The total average power of a DMT system is the average power sum of each carrier as expressed in the following:

$$P_{DMT} = \sum_{i=1}^{m} P_{T_i}$$

The value P_{DMT} is the total average power, m is the number of carriers, and P_{sub_i} is the average power of ith carrier of a DMT system. If peaks of all carriers can be aligned, the peak voltage of a DMT system is the peak voltage sum of all carriers. Under this assumed condition and for the particular case where the average power of each carrier is the same, you have

$$PAR_{DMT} = \frac{V_p}{\sqrt{\frac{P_{DMT}}{R}}} = \frac{\sum_{i=1}^{m} V_{pi}}{\sqrt{\frac{\sum_{i=1}^{m} P_{sub_i}}{R}}} = \frac{\sum_{i=1}^{m} V_{pi}}{\sqrt{\frac{mP_{sub}}{R}}} = \frac{1}{\sqrt{m}} \sum_{i=1}^{m} \frac{V_{pi}}{\sqrt{\frac{P_{sub}}{R}}} = \frac{1}{\sqrt{m}} \sum_{i=1}^{m} PAR_i$$

The values are as follows:

V_p is the peak voltage of the DMT system.

V_{pi} is the peak voltage of ith carrier.

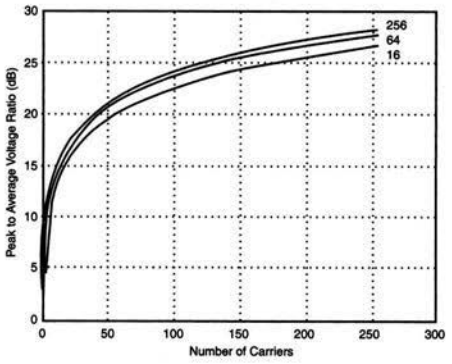
P_{sub} is the same average power for all carriers.

With the additional special condition of $PAR_i = PAR_{sub}$, for which PAR_{sub} is the same PAR for all carriers, you have

$$PAR_{DMT} = \sqrt{m} PAR_{sub}$$

Figure 7.9 shows the DMT PAR for different numbers of carriers, assuming the following: Peaks of all carriers can be aligned, average carrier powers are equal, and each carrier has constellation sizes of 16, 64, and 256, respectively.

Figure 7.9 Cosine Carrier Peak-to-Average Voltage Ratio



For a practical case where the peak of a DMT signal occurs when all carriers have the maximum amplitudes and 45 degree phase (that is, all carriers produce the top rightmost constellation point), we have

$$PAR_{DMT} = \frac{1}{\sqrt{m}} \sum_{i=1}^{m} k_i PAR_i = \frac{K_m}{\sqrt{m}} \sum_{i=1}^{m} PAR_i$$

for which k_is are modification factors associated with the addition of the next adjacent carrier, and K_ms are modification factors associated with the total number of carriers. Values of k_is and K_ms are obtained through computer simulation.

With the additional special condition of $PAR_i = PAR_{sub}$, we have

$$PAR_{DMT} = \frac{PAR_{sub}}{\sqrt{m}} \sum_{i=1}^{m} k_i = K_m \sqrt{m} PAR_{sub}$$

Figure 7.10 shows values of peak reduction factors, k_is.

Figure 7.10 Peak Reduction Factor, k_i

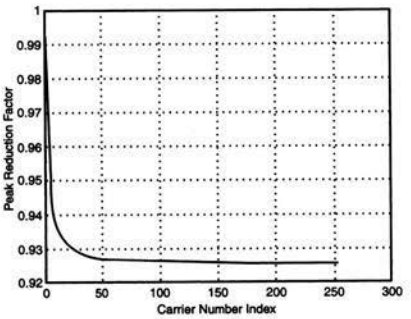
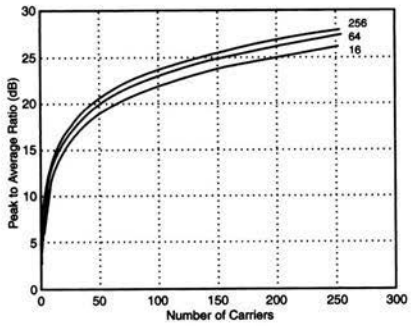


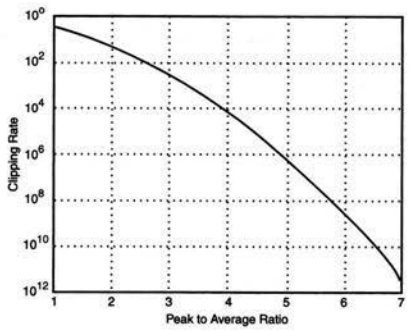
Figure 7.11 shows the DMT PAR for different numbers of carriers with modification factors, k_is, and assumes that average carrier powers are equal and each carrier has constellation sizes of 16, 64, and 256, respectively. The inclusion of peak reduction factor reduces the estimated DMT PAR by about 1 dB.

Figure 7.11 Peak-to-Average Voltage Ratio



The DMT signal approaches a Gaussian distribution when the number of carriers is larger than 20. The representation of all DMT peak values might be necessary. In other words, the clipping of a DMT signal due to the limit of available voltage value might not degrade the performance of a DMT-based transmission system. The clipping noise spreads across all carriers. The clipping noise power level is usually low compared with signal power for a clipping-to-average voltage ratio of larger than 4. Figure 7.12 shows the clipping rate of a Gaussian-distributed signal with a limiting peak-to-average voltage ratio.

Figure 7.12 Clipping Rate of a Gaussian Signal



7.2 *Transmit Filter, Channel, and Echo Path Effects*

An analog or digital transmit filter is usually used to shape the spectrum of a DSL system. The transmit filter expands the PAR. The effect of a digital *Finite Impulse Response* (FIR) filter can be analyzed by calculating the mean, the variance, and the peak value of the FIR filter output with random data as the FIR filter input. Effects of the analog transmit filter, channel, and echo path are similar to that of the digital FIR filter.

The magnitude distribution of a multi-level signal after an FIR filter can be calculated as follows. We have the FIR filter output signal as

$$x(k) = \sum_{i}^{m} h_i a_{k-i}$$

The values are as follows:

h_is are FIR filter coefficients.

The FIR filter has a total of m coefficients.

a_is are n-level data symbols with magnitudes of $-(n-1)$, $-(n-3)$, ..., -1, 1, ..., $(n-3)$, $(n-1)$.

The mean of the FIR filter output is

$$E[x(k)] = \sum_{i=1}^{m} E[h_i]E[a_{k-i}] = 0$$

for

$$E[a_{k-i}] = 0$$

The variance of the FIR filter output is

$$E[x^2(k)] = E\left[\left(\sum_{i=1}^{m} h_i a_{k-i}\right)^2\right] = \sum_{i=1}^{m} E[h_i^2]E[a_{k-i}^2] = mE[h_i^2]E[a_{k-i}^2]$$

$$= \frac{2\sum_{i=1}^{n/2}(2i-1)^2}{n}\sum_{i=1}^{m} h_i^2 = \frac{(n^2-1)\sum_{i=1}^{m} h_i^2}{3}$$

The mean square root voltage, assuming a load resistance of 1, is then

$$\sqrt{\frac{(n^2-1)\sum_{i=1}^{m} h_i^2}{3}}$$

The FIR filter output also has a peak magnitude of

$$x(k)_{MAX} = MAX(a_{k-i})\sum_{i=1}^{m}|h_i| = (n-1)\sum_{i=1}^{m}|h_i|$$

The filter output peak-to-average voltage ratio is

$$\sum_{i=1}^{m}|h_i|\sqrt{\frac{3(n-1)}{(n+1)\sum_{i=1}^{m} h_i^2}}$$

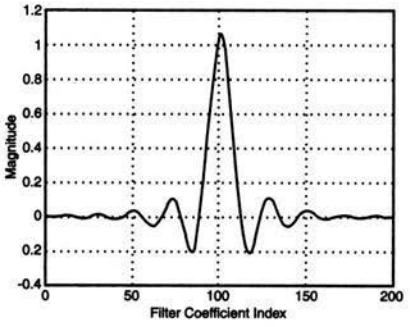
For a four-level signal, we have

$$\frac{3}{\sqrt{5}} \frac{\sum_{i=1}^{m} |h_i|}{\sqrt{\sum_{i=1}^{m} h_i^2}}$$

7.2.1 *Baseband Square Root Nyquist Shaping Filters*

For using a baseband square root Nyquist shaping filter, as shown in Figure 7.13, the peak-to-average ratio for a four-level signal after the filter is about 18 dB. The square root Nyquist shaping filter introduces the minimum signal distortion when used as a transmit and receive filter pair. The design of the square root Nyquist filter is discussed in more detail in Chapter 8 and Chapter 13, "ADSL (Asymmetrical Digital Subscriber Lines)."

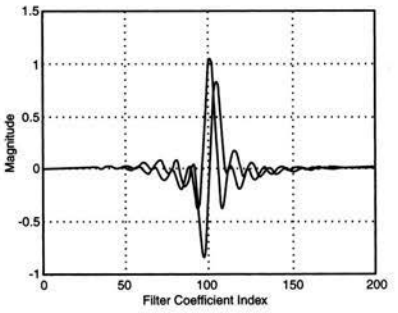
Figure 7.13 A Baseband Square Root Nyquist Filter



7.2.2 *Passband Square Root Nyquist Shaping Filters*

For using passband square root Nyquist shaping filters, as shown in Figure 7.14, the peak-to-average ratio for a 16 CAP/QAM signal after these filters is about 17 dB.

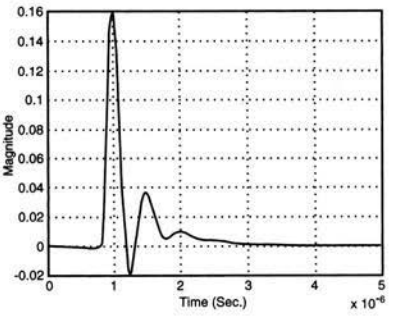
Figure 7.14 Passband Square Root Nyquist Filters



7.2.3 *Baseband Channel Impulse Response*

For a baseband signal using fourth order Butterworth transmit and receive filters with corner frequencies of 200 kHz over a 2 mile, 26-gauge twisted-pair loop, as shown in Figure 7.15, the peak-to-average ratio for a four-level signal after the equivalent channel is about 15.2 dB.

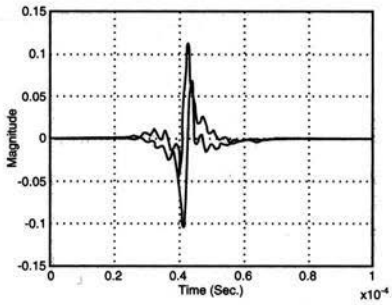
Figure 7.15 A Baseband Channel Impulse Response



7.2.4 *Passband Channel Impulse Response*

For a passband equivalent channel defined by a passband Nyquist filter with a baud rate of 125 kHz and a center frequency of 83.33 kHz over a 2 mile, 26-gauge twisted-pair loop, as shown in Figure 7.16, the peak-to-average ratio for a four-level signal after the equivalent channel is about 18 dB.

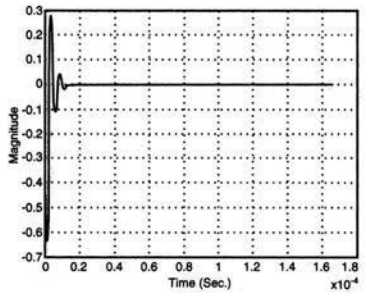
Figure 7.16 Peak-to-Average Ratio for a Passband Channel



7.2.5 *Baseband Echo Path*

For a baseband echo path also using fourth order Butterworth transmit and receive filters with corner frequencies of 200 kHz in conjunction with a 2 mile, 26-gauge twisted-pair loop, as shown in Figure 7.17, the peak-to-average ratio for a four-level signal after the echo path is about 16.2 dB. The Baseband echo path is defined for each path with a baseband signal.

Figure 7.17 Echo Path Impulse Response



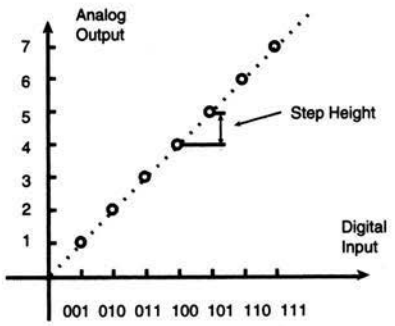
PARs after transmit filters are of concern for DACs while PARS after channel and echo path are of concern for ADCs.

7.3 *ADC and DAC Characteristics*

Data symbols are generated, received, and processed in a digital format while they are carried over a transmission channel in analog formats. Data symbols are converted to analog format in a transmitter with a Digital to Analog Converter (DAC). Data symbols are recovered in a receiver first through an Analog to Digital Converter (ADC). Figure 7.18

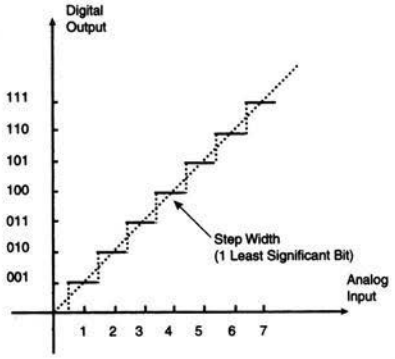
represents the ideal relationship between the digital input and analog output of a DAC. Discrete analog voltage levels are generated according to corresponding digital inputs.

Figure 7.18 Ideal Digital to Analog Conversion Relationship



Conversely, Figure 7.19 represents the ideal relationship between the analog input and digital output of an ADC. A continuous analog input signal is quantified into discrete digital values.

Figure 7.19 Ideal Analog to Digital Conversion Relationship



7.3.1 *Calculation of Quantization Noise*

Although quantization noise exists for a DAC device, the effect might not be obvious because the DAC takes digital input. On the other hand, the effect of quantization noise is always there for an ADC. The voltage difference between the analog input and corresponding digital output values acts as a quantization noise from an ADC, as shown in Figure 7.20.

Figure 7.20 Calculation of Quantization Noise

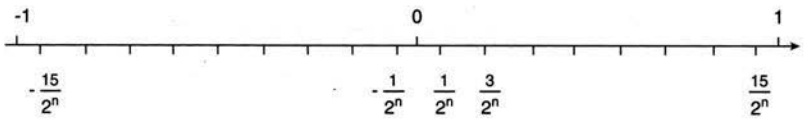


Figure 7.20 is a good reference to calculate the amount of quantization noise. An N bits ADC can represent a normalized voltage range of −1 to +1 with a step size of

$$\frac{1}{2^{N-1}}$$

An N bits ADC can have a quantization error whose magnitude range is

$$-\frac{1}{2^N} - \frac{1}{2^N}$$

The average quantization error power or quantization noise level is

$$e_q = \frac{1}{\frac{1}{2^N} - \left(-\frac{1}{2^N}\right)} \int_{-\frac{1}{2^N}}^{\frac{1}{2^N}} x^2 dx = \frac{2^{N-1}}{3} x^3 \Big|_{-\frac{1}{2^N}}^{\frac{1}{2^N}} = \frac{1}{3}\left[\frac{1}{2^N}\right]^2$$

Assuming the maximum value that an ADC or DAC can represent is 1 and the minimum is −1 (that is, the maximum magnitude is 0 dB), the quantization noise of an ADC is[1]

$$e_q = -10 \times \log_{10} 3 - 20 \times N \times \log_{10} 2 = -4.77 - 6.02N \text{ dB}$$

About 6 dB of quantization noise level reduction is associated with every bit of resolution increase. For $N = 12$, we have

$$e_q = -4.77 - 6.02N = -77.01 \text{ dB}$$

On the other hand, a signal with a peak-to-average voltage ratio of K can be represented with a signal level of

$$S_{PAR_K} = 20 \times \log_{10} \frac{1}{K}$$

For K=5.75, corresponding to a clipping rate of 10^{-8}, we have

$$S_{PAR_K} = 20 \times \log_{10} \frac{1}{5.8} = -15.27dB$$

Therefore, the maximum signal-to noise-ratio (SNR) represented by an N bits ADC with a PAR of 5.75 is then

$$SNR = S_{PAR_K} - e_q = -15.27 + 77.01 = 67.74dB$$

Table 7.1 lists the maximum representable SNR for other ADC resolutions and PAR values.

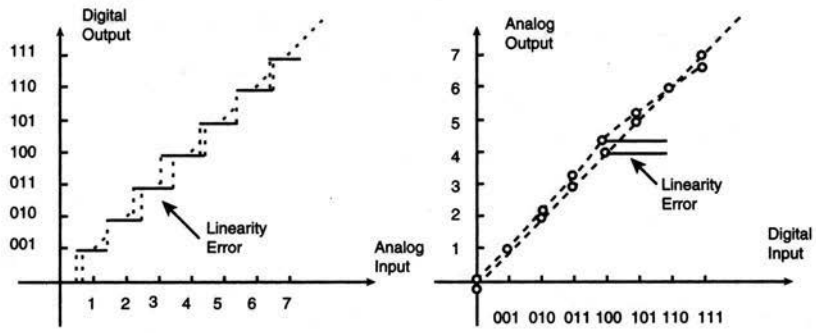
Table 7.1 Maximum SNR (dB)

	8 bits	9 bits	10 bits	11 bits	12 bits	13 bits	14 bits
PAR 1	52.93	58.95	64.97	70.99	77.01	83.03	89.05
PAR 2	46.91	52.93	58.95	64.97	70.99	77.01	83.03
PAR 3	43.39	49.41	55.43	61.45	67.47	73.49	79.51
PAR 4	40.89	46.91	52.93	58.95	64.97	70.99	77.01
PAR 5	38.95	44.97	50.99	57.01	63.03	69.05	75.07
PAR 6	37.37	43.39	49.41	55.43	61.45	67.47	73.49

7.3.2 *ADC and DAC Nonlinearity*

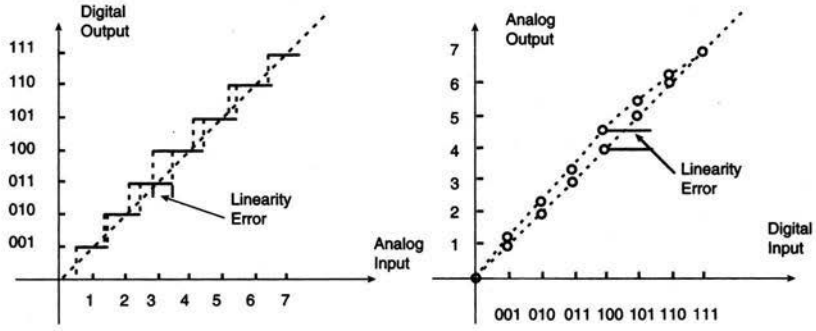
In practice, input and output values of a DAC or ADC do not always match. For an ADC, the range of analog input corresponding to a particular digital output might be bigger or smaller than desired or offset a little. For a DAC, the analog output corresponding to a particular digital input might be off-set a little. *Nonlinearity* is the term that refers to these input/output value deviations. For a DAC or ADC with many bits, the offset can be greater than 1 bit. The effect of the nonlinearity is the reduction of DAC or ADC effective resolution. Figure 7.21 shows the best straight line linearity error for which the overall linearity errors are minimized.

Figure 7.21 Best Straight Line Linearity Error



Conversely, Figure 7.22 shows the end-point matched linearity error for which end points of input and output are matched. The best-straight-line and end-point linearity errors are defined through different calibration methods.

Figure 7.22 End Point Linearity Error



The effect of nonlinearity can also be characterized as additional quantization noise enhancement. The nonideal ADC quantization noise at ith step (between two adjacent digital outputs) can be described as

$$e_{q_i} = \frac{1}{\frac{1}{2^N} + \Delta_i - \left(-\frac{1}{2^N} + \Delta_{i-1}\right)} \int_{-\frac{1}{2^N}+\Delta_{i-1}}^{\frac{1}{2^N}+\Delta_i} x^2 dx = \frac{1}{3\left(\frac{2}{2^N} + \Delta_i - \Delta_{i-1}\right)} x^3 \Big|_{-\frac{1}{2^N}+\Delta_{i-1}}^{\frac{1}{2^N}+\Delta_i}$$

$$= \frac{1}{3\left(\frac{2}{2^N} + \Delta_i - \Delta_{i-1}\right)} \left(\left(\frac{1}{2^N} + \Delta_i\right)^3 + \left(\frac{1}{2^N} - \Delta_{i-1}\right)^3\right)$$

in which Δ_i and Δ_{i-1} are amounts of deviations at the high end and low end of the analog input range. For the special case of

$$e_{q_i} = e_{q_n}$$

(that is, the ADC nonlinearity is represented by its nonlinearity at the ith step) and

$$\Delta_i = \Delta_{i-1} = \Delta$$

we have

$$e_{q_n} = \frac{2^{N-1}}{3}\left(2\left(\frac{1}{2^N}\right)^3 + 6\frac{1}{2^N}\Delta^2\right) = \frac{1}{3}\left(\frac{1}{2^N}\right)^2 + \Delta^2$$

The ratio of quantization noise with nonlinearity to that of ideal is

$$\frac{e_{q_n}}{e_q} = \frac{\frac{1}{3}\left(\frac{1}{2^N}\right)^2 + \Delta^2}{\frac{1}{3}\left(\frac{1}{2^N}\right)^2} = 1 + 3 \times 2^{2N}\Delta^2$$

These ratios of nonlinearity quantization noise enhancement are summarized in Table 7.2 for different values of Δ.

Table 7.2 Nonlinearity Noise Level (dB)

Δ	2^{-N-1}	$2^{-N-0.5}$	2^{-N}	$2^{-N+0.5}$	2^{-N+1}	$2^{-N+1.5}$	2^{-N+2}
e_{q_n}/e_q	11.14	8.45	6.02	3.98	2.43	1.38	0.75

A nonlinearity of 1/4 bit can cause a quantization noise enhancement of 2.43 dB while a nonlinearity of 1/2 bit can cause a quantization noise enhancement of 6.02 dB, which is equivalent to the loss of one effective bit. In practice, the worst case nonlinearity decides the available ADC or DAC resolution.

7.4 DAC and ADC Dynamic Range Requirements

The dynamic range of a DAC or an ADC defined by their precision should be comparable with that required by the line code, error rate, and the channel condition of a DSL system. The required DAC precision can be different for different digital transmit filters and line codes. The required ADC precision is further affected by the twisted-pair loop channel and the echo path.

7.4.1 DAC Resolution Requirements for Baseband Transmitters

For a baseband transmitter without digital filters, the required resolution for a DAC is the same as that for the baseband line signal. For example, a four-level baseband signal needs only a DAC of 2 bits, while an eight-level baseband signal needs only a DAC of 3 bits. Additional signal spectrum shaping is carried out by analog filters after the DAC.

For a baseband transmitter with digital shaping filters, the required resolution for a DAC is determined by the following factors:

- The number of line signal levels
- The desired signal-to-noise ratio or error rate
- The peak-to-average voltage ratio of digital shaping filters

The average signal power is expressed as

$$\frac{n^2-1}{3}$$

The value n is the number of signal levels. For using a voltage difference of 2 between adjacent signal levels, the probability of error is

$$P_e = \frac{2}{\sqrt{2\pi}\sigma}\int_1^{\infty} e^{-\frac{y^2}{2\sigma^2}} dy$$

The value σ^2 is the variance of the noise. This can also be expressed as

$$P_e = \frac{2}{\sqrt{2\pi}}\int_{\frac{1}{\sigma}}^{\infty} e^{-\frac{y^2}{2}} dy = Q\left(\frac{1}{\sigma}\right)$$

$Q(x)$ is defined for this error probability function. The inverse of the noise power is the inverse function of the error probability, as expressed in the following equation:

$$\frac{1}{\sigma^2} = \left(Q^{-1}(P_e)\right)^2$$

The required SNR is

$$\frac{n^2 - 1}{3} = \left(Q^{-1}(P_e)\right)^2$$

Table 7.3 shows the required SNRs for baseband signals with different numbers of signal levels and different error rates.

Table 7.3 Required SNRs (dB)

Error Rate	Number of Signal Levels				
	4	8	16	32	64
10^{-6}	20.7	26.9	33.0	39.0	45.1
10^{-7}	21.6	27.8	33.9	39.9	46.0
10^{-8}	22.2	28.4	34.5	40.5	46.6

The results in Table 7.3 indicate that doubling the number of signal levels (equivalent to adding one more bit) for a baseband system costs approximately 6 dB of SNR.

Table 7.4 shows the required DAC resolution for a different number of signal levels and different error rates for a Nyquist shaping filter with a peak-to-average voltage ratio of 18 dB.

Table 7.4 Required DAC Resolution

Error Rate	Number of Signal Levels				
	4	8	16	32	64
10^{-6}	6	7	8	9	10
10^{-7}	6	7	8	9	10
10^{-8}	6	7	8	9	10

One or two extra bits might be necessary to allow the inclusion of other noise sources while meeting the same SNR objective. Results in Table 7.4 are obtained by equating the sum of SNR and PAR to the negative dB of the quantization noise level, as follows:

$$SNR + PAR = -e_q = 4.77 + 6.02N$$

The required number of bits is expressed as

$$N = \frac{1}{6.02}(SNR + PAR - 4.77)$$

7.4.2 DAC Resolution Requirements for Passband Transmitters

For a passband transmitter with digital shaping filters, the required resolution for a DAC is determined by the following factors:

- The constellation size
- The desired signal-to-noise ratio or error rate
- The peak-to-average voltage ratio of digital shaping filters

The average signal power is expressed as

$$\frac{2\left(2^{2n}-1\right)}{3}$$

The value n is the constellation size index or number of bits per dimension. The probability of error is

$$P_e = \frac{2}{\sqrt{\pi}\sigma}\int_1^{\infty} e^{-\frac{y^2}{\sigma^2}} dy$$

The value σ^2 is the variance of the noise. This also can be expressed as

$$P_e = \frac{2}{\sqrt{2\pi}}\int_{\frac{\sqrt{2}}{\sigma}}^{\infty} e^{-\frac{y^2}{2}} dy = Q\left(\frac{\sqrt{2}}{\sigma}\right)$$

The inverse of the noise power is the inverse function of the error probability, as shown in the following expressions:

$$\frac{2}{\sigma^2} = Q^{-1}(P_e)$$

or

$$\frac{1}{\sigma^2} = \frac{Q^{-1}(P_e)}{2}$$

The required SNR for a passband signal with a constellation size of 2^{2n} is

$$\frac{2^{2n}-1}{3}\left(Q^{-1}(P_e)\right)^2$$

Table 7.5 shows the required SNRs for different constellation sizes and different error rates.

Table 7.6 shows the required DAC resolution for different constellation sizes and different error rates for a Nyquist shaping filter with a peak-to-average ratio of 17 dB.

Table 7.5 Required SNRs (dB)

Error Rate	Constellation size				
	4	16	64	256	1024
10^{-6}	13.7	20.7	26.9	33.0	39.0
10^{-7}	14.6	21.6	27.8	33.9	39.9
10^{-8}	15.2	22.2	28.4	34.5	40.5

Table 7.6 Required DAC Resolution

Error Rate	Number of Signal Levels				
	4	16	64	256	1024
10^{-6}	5	6	7	8	9
10^{-7}	5	6	7	8	9
10^{-8}	5	6	7	8	9

Again, one or two extra bits might be necessary for a better quantization noise margin.

7.4.3 *DAC Resolution Requirements for DMT Transmitters*

For a DMT transmitter with 256 carriers and a maximum constellation size of 1,024, the PAR is around 28 dB, the required SNR is about 40 dB, and the required DAC resolution is as follows:

$$N = \frac{1}{6.02}(SNR + PAR - 4.77) = (40 + 28 - 4.77)\Big/6.02 = 105 \approx 11 bits$$

We might need a few extra bits to minimize the effect of quantization noise compared with other transmission impairments.[2] Therefore, a DMT transmitter might need a DAC resolution of 11 to 14 bits if no clipping is allowed.

The required DAC resolution of a DMT system can be relaxed significantly if clipping is allowed.[3] The power of the clipping noise can be expressed as

$$P_{clip} = 2\int_{A_{clip}}^{\infty}\left(x - A_{clip}\right)^2 \frac{e^{-\frac{x^2}{2\sigma^2}}}{\sqrt{2\pi}\sigma}dx \approx \sqrt{\frac{8}{\pi}}\frac{\sigma^2}{\mu^3 e^{\frac{\mu^2}{2}}}$$

in which

$\mu = \frac{A_{clip}}{\sigma}$ is the clipping ratio and

$\frac{\sigma^2}{P_{clip}} \approx \sqrt{\frac{\pi}{8}}\mu^3 e^{\frac{\mu^2}{2}}$ is the signal-to-clipping-noise power ratio.

For $\mu = 5.35$ or 15 dB, corresponding to a clipping rate of 10^{-7}, we have

$$\frac{\sigma^2}{P_{clip}} \approx 82 \text{ dB}$$

These calculations show that a DMT transmitter can be designed with a PAR of only 15 dB without much performance degradation. This could result in a reduction of about 2 bits in the DAC resolution requirement. Therefore with clipping, the required DAC resolution for a DMT transmitter is between 9 to 12 bits.

7.4.4 *The Effect of ADC Quantization Noise*

If a transmission channel has only a flat loss, the receiver ADC needs at least the same resolution as that of transmitter DAC. To minimize the effect of receiver ADC quantization noise under a certain receiver front-end noise level, we need a quantization noise level that is lower than that of the receiver front-end noise. The overall receiver front-end signal-to-noise ratio after the ADC is expressed as

$$SNR = \frac{P_{signal}}{\sigma_n^2 + \sigma_{ADC}^2} = \frac{P_{signal}}{\sigma_n^2}\frac{1}{1+\frac{\sigma_{ADC}^2}{\sigma_n^2}} = SNR_n\frac{1}{1+\frac{\sigma_{ADC}^2}{\sigma_n^2}}$$

The values are as follows:

P_{signal} is the received signal power.

σ_n^2 is the receiver front-end noise power.

σ_{ADC}^2 is the ADC quantization noise power.

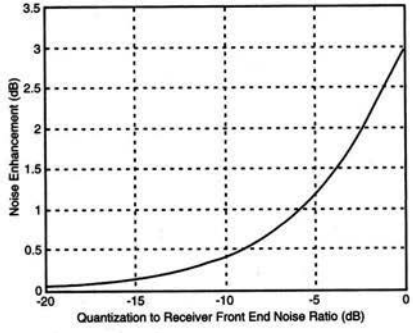
For the quantization noise limited case, σ_n^2 represents the DAC quantization noise power. We can let $\sigma_n^2 = \sigma_{ADC}^2$. For this assumption, σ_n^2 and σ_{ADC}^2 each need to be 3 dB lower compared to that calculated for ADC alone to meet the same *SNR* objective.

For the receiver front-end noise limited case, σ_n^2 represents the receiver front-end noise power. The noise enhancement introduced by the receiver ADC quantization is

$$1+\frac{\sigma_{ADC}^2}{\sigma_n^2}$$

Figure 7.23 shows the relationship between the noise enhancement and the quantization to the receiver front-end noise ratio. A ratio of one or 0 dB will increase the noise level by 3 dB, while a ratio of 0.25 or –6 dB will only produce a noise enhancement of 1 dB. This corresponds to one extra bit than the required number of bits calculated in Tables 7.4 and 7.6 and that calculated for the DMT transmitter.

Figure 7.23 Degree of Noise Enhancement



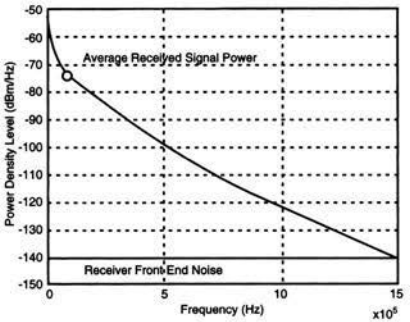
7.4.5 *ADC Precision Requirements Considering Channel Loss*

At the receiver front end, a twisted-pair loop channel can introduce a loss difference of as much as 40 dB within a signaling band; however, a portion of the channel with heavy signal losses can also tolerate a relatively high quantization noise level. In other words, the

signal-to-noise power density ratio at the high-frequency end, where heavy channel loss occurs, can be less than that required by a particular line code.

The use of an adaptive channel equalizer could automatically compensate the low signal-to-noise ratio at a certain frequency region. Figure 7.24 shows relationships between the received signal level, the average received signal level, and the receiver front-end noise level for a 2 mile, 26-gauge twisted-pair loop.

Figure 7.24 Received Signal and Noise Power Level



The required ADC resolution to recover all information delivered by this twisted-pair loop channel can be calculated as

$$(-75.2 + 140 + 20 - 4.77)/6.02 \approx 14 \text{ bits}$$

The values are as follows:

–75.2 dBm/Hz is the average received signal power density level.

–140 dBm/Hz is the receiver front-end noise power level.

The desired SNR is the average received signal power density minus the receiver front-end noise power density.

20 dB is for the received signal PAR.

If the received signal only uses a frequency spectrum of 200 kHz, such as the signal spectrum of HDSL, the average received signal level is –66.9 dBm/Hz, and the loss difference for a bandwidth of 200 kHz is about 30 dB. The required ADC resolution for this 200 kHz band with a four-level signal can be calculated as

$$(21.4 + 30 + 15 - 4.77)/6.02 \approx 11 \text{ bits}$$

The values are as follows:

21.4 dB is the required SNR for a four-level signal.

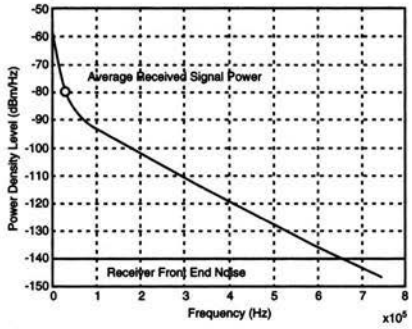
30 dB is the channel loss difference.

The desired SNR is the SNR for a four-level signal plus the channel loss difference.

15 dB is for the received signal PAR.

Figure 7.25 shows relationships between the received signal level, the average received signal level, and the receiver front-end noise level for a 3 mile, 26-gauge twisted-pair loop.

Figure 7.25 Received Signal and Noise Power Level



The required ADC resolution to recover all information delivered by this twisted-pair loop channel can be calculated as

$$(-79 + 140 + 20 - 4.77)/6.02 \approx 13 \text{ bits}$$

The values are as follows:

–79 dBm/Hz is the average received signal power density level.

–140 dBm/Hz is the receiver front-end noise power level.

The desired SNR is the average received signal power density minus the receiver front-end noise power density.

20 dB is for the received signal PAR.

If the received signal uses a frequency spectrum of only 40 kHz, such as the spectrum of the Basic Access Rate ISDN channel, the average received signal level is –66.5 dBm/Hz, and the loss difference for a bandwidth of 40 kHz is about 26 dB. The required ADC resolution for this 40 kHz band with a four-level signal can be calculated as

$$(21.4 + 26 + 15 - 4.77)/6.02 \approx 10 \text{ bits}$$

The values are as follows:

21.4 dB is the required SNR for a four-level signal.

26 dB is the channel loss difference.

The desired SNR is the SNR for the four-level signal plus the channel loss difference.

15 dB is for the received signal PAR.

7.4.6 *ADC Precision Requirements Considering Echo Path*

The echo level is usually much higher compared with the received signal level. The echo is attenuated by the hybrid circuit and bandpass filters in the case of a *Frequency Division Duplex* (FDD) system. For cases in which the transmit signal and received signal are further separated with the help of a digital echo canceller, a higher resolution ADC becomes necessary. For an assumed echo return loss of 15 dB, required ADC resolutions are calculated for the examples in section 7.4.5, "ADC Precision Requirements Considering Channel Loss."

The required ADC resolution to recover all information delivered by a 2 mile, 26-gauge twisted-pair loop channel can be calculated as

$$(-55 + 140 + 16 - 4.77)/6.02 \approx 16 \text{ bits}$$

The values are as follows:

–55 dBm/Hz is the average echo mixed with the received signal power density level.

–140 dBm/Hz is the receiver front-end noise power level.

The desired SNR is the average echo power density minus the average receiver front-end noise power density.

16 dB is for the echo mixed with the received signal PAR.

If the received signal uses a frequency spectrum of only 200 kHz, such as the signal spectrum of HDSL, the desired signal-to-noise ratio is increased by –55–(–66.9)=11.9 dB. The required ADC resolution for this 200 kHz band with a four-level signal can be calculated as

$$(21.4 + 11.9 + 30 + 16 - 4.77)/6.02 \approx 13 \text{ bits}$$

The values are as follows:

21.4 dB is the required SNR for a four-level signal.

11.9 dB accounts for the stronger echo level.

30 dB is the channel loss difference.

The desired SNR is the sum of the required SNR for a four-level signal, the stronger echo level, and the channel loss difference.

16 dB is for the received signal PAR.

The required ADC resolution to recover all information delivered by a 3 mile, 26-gauge twisted-pair loop channel can be calculated as

$$(-55+140+16-4.77)/6.02 \approx 16 \text{ bits}$$

The values are as follows:

–55 dBm/Hz is the average echo mixed with the received signal power density level.

–140 dBm/Hz is the receiver front-end noise power level.

The desired SNR is the average echo power density minus the average receiver front-end noise power density.

16 dB is for the echo mixed with the received signal PAR.

If the received signal use a frequency spectrum of only 40 kHz, such as the signal spectrum of the Basic Rate Access ISDN channel, the required signal-to-noise ratio is increased by –55–(–66.5)=115 dB. The required ADC resolution for this 40 kHz band with a four-level signal can be calculated as

$$(21.4+11.5+26+16-4.77)/6.02 \approx 12 \text{ bits}$$

The values are as follows:

21.4 dB is the required SNR for a four-level signal.

11.5 dB accounts for the stronger echo level.

26 dB is the channel loss difference.

The desired SNR is the sum of the required SNR for a four-level signal, the stronger echo level, and the channel loss difference.

16 dB is for the received signal PAR.

End Notes

1. W. Y. Chen, "The Distribution of Echo Signal and Required A/D Precision," *IEEE ISCAS '92.*

2. N. Al-Dhahir and J. M. Cioffi, "On the Uniform ADC Bit Precision and Clip Level Computation for a Gaussian Signal," *IEEE Trans. on Signal Processing,* vol. 44, no. 2 (February 1998): 434–438.

3. D. J. G. Mestdagh, P. Spruyt, and B. Biran, "Analysis of Clipping Effect in DMT-Based ADSL System," *Alcatel T1E1 Contribution,* T1E1.4/93-129 (May 10, 1993).

CHAPTER 8

Channel Equalization

The usable bandwidth of a twisted-pair telephone subscriber loop is much wider than the voice band telephony channel; however, the channel distortion is also more severe for using the full available bandwidth. Specifically, amplitude attenuation and phase delay could be very different at different frequency regions within the available bandwidth. A transmitting signal could become unrecognizable after going through a telephone subscriber loop because of the amplitude and phase distortion. The channel capacity estimation in the frequency domain only indicates the transmission potential of the telephone subscriber loop—but does not reveal any method of achieving that.

An information bit stream is usually converted into a sequence of data symbols. The transmission throughput is the product of the symbol rate and the number of bits carried by every data symbol. The faster the symbol rate, the higher the transmission throughput; however, the symbol rate is limited by the channel amplitude and phase distortion. Specifically, the channel distortion causes the data symbols to spread. Therefore, there are certain limitations to how close symbols can be lined up next to each other without the use of any channel distortion compensation technique.

The effect of channel distortion can be minimized using a channel equalizer, which can be used to control the spread of the data symbol after going through the channel. Dividing the available bandwidth into many smaller frequency regions where channel distortion becomes relatively insignificant also can minimize the effect of channel distortion. A channel equalizer also can be very useful even for the bandwidth divided DSL systems.

In theory, an equalizer should have a frequency response that is the inverse of the channel. In practice, a channel equalizer is normally implemented with a digital adaptive filter. An adaptive channel equalizer can be further categorized as linear or decision feedback, baud

rate or fractionally spaced, baseband or passband (depending on performance requirement), signal processing capability, and system architecture.

The development of the adaptive channel equalization technique has helped the evolution of the voice band modem technology. The adaptive channel equalization technique has also been successfully used for DSL systems to realize the transmission throughput potential available over the telephone subscriber loops. Equalizer coefficients and equalizer output signal-to-noise ratio (SNR) can characterize the implementation requirement and the effectiveness of an adaptive channel equalizer. Equalizer coefficients and output SNR can be obtained iteratively through the simulation of the adaptation process or directly through some matrix calculation in conjunction with channel and noise models.

This chapter addresses issues related to the determination of equalizer coefficients and equalizer output SNR, based on the matrix calculation method. Detailed results are derived for the following equalizer configurations:

- *Adaptive Linear Channel Equalizer.* Concepts of channel equalization and adaptive filtering are discussed. Baud rate and fractionally spaced linear equalizer coefficients and equalizer output SNRs are calculated. The issue of noise enhancement is also addressed.
- *Decision Feedback Channel Equalizer (DFE).* DFE equalizer coefficients and equalizer output SNRs are calculated for baud rate and fractionally spaced *feed forward filters* (FFF). The Tomlinson/Harashima precoding method is also introduced.
- *Passband Equalizer and Carrierless AM/PM (CAP).* Equalizer coefficients and output SNRs are calculated for the passband *Quadrature Amplitude Modulation* (QAM) system. A linear equalizer or the FFF of a DFE can be placed before or after the demodulation process. Linear equalizer and DFE structures for a CAP system are derived. Equalizer coefficients and equalizer output SNRs are also calculated for a CAP system.
- *Equalizer for Discrete MultiTone (DMT) Systems.* The concept of *intersymbol interference* for a DMT system is introduced. Equalizer coefficients and equalizer output SNRs are calculated for a DMT system based on the *Minimum Mean Square Error* (MMSE) criteria.

8.1 Adaptive Linear Channel Equalization

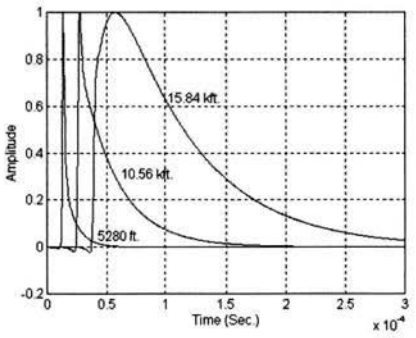
A channel equalizer can be used to minimize the effect of channel distortion; however, every twisted-pair loop has its own unique transmission characteristics due to the composition and the configuration of that particular loop. Furthermore, the transmission characteristics of a twisted-pair loop is slightly time varying and temperature dependent.

An adaptation process is used to identify the optimal channel equalizer coefficients and keep tracking possible variation of the channel characteristics. A linear equalizer is usually implemented with a digital *Finite Impulse Response* (FIR) filter. The output of a linear equalizer depends only on the received signal versus that of a DFE whose output depends on estimated data symbols.

Although there is enough signal-to-noise ratio to carry a signal over the twisted-pair loop channel, the channel distortion to the transmitted signal is very severe. At signaling rates of higher than a few hundred kHz, the received signal has a disbursing many times that of the signaling interval.

Figure 8.1 shows normalized impulse responses after 1, 2, and 3 miles of 26-gauge twisted-pair loops. Signaling intervals, or baud periods, are 12.5, 2.5, and 1 microseconds for signaling baud rates of 80 kHz, 400 kHz, and 1 mHz, respectively. Even for the 1 mile loop, the impulse response lasts more than 30 microseconds. The tail of the impulse response can interfere with the next baud signal if the baud period is shorter than that of the tail. This is called *channel intersymbol interference.*

Figure 8.1 Impulse Responses for Twisted-Pair Loops of Different Lengths



8.1.1 *Compensating for Channel Distortion*

In theory, the channel distortion can be compensated if you use a filter, with a frequency response that is the inverse of that of the twisted-pair loop channel, in front of the receiver. We let

$$H_F(f) = \frac{1}{H(f)}$$

$H_F(f)$ is the transfer function of the compensation filter.

$H(f)$ is the transfer function of the channel.

This channel compensation filter cannot be realized in analog format, however, because the *Fourier transform* of the inverse channel does not exit. For the simplified channel model of

$$H(d,f) = e^{-d\left(k_1\sqrt{f}+k_2 f\right)}e^{-jdk_3 f}$$

the transfer function for the compensation filter is expressed as

$$H_F(d,f) = e^{d\left(k_1\sqrt{f}+k_2 f\right)}e^{jdk_3 f}$$

The Fourier transform of this transfer function does not exist because $H_F(d,f) \to \infty$ when $f \to \infty$. On the other hand, the channel compensation can be realized in the sampled digital domain. The frequency response of the channel in the sampled digital domain is expressed as

$$H_s(f) = \frac{1}{T}\sum_{i=-\infty}^{\infty} H\left(f - \frac{i}{T}\right)$$

The frequency response of the compensation filter, also in the sampled digital domain, is expressed as

$$H_{s,F}(f) = \frac{1}{\frac{1}{T}\sum_{i=-\infty}^{\infty} H\left(f - \frac{i}{T}\right)}$$

The discrete frequency domain version of this compensation filter is expressed as

$$H_{s,F}(k) = H_{s,F}(k\Delta f) = \frac{1}{\frac{1}{T}\sum_{i=-\infty}^{\infty} H\left(k\Delta f - \frac{i}{T}\right)}$$

Filter coefficients of this digital compensation filter exist and can be obtained through the discrete Fourier transform using the following expression:

$$h_{s,F}(n) = h_{s,F}(n\Delta t) = \frac{1}{T}\sum_{k=0}^{n-1} H_{s,F}(k) e^{j2\pi kn\frac{\Delta t}{T}}$$

Filter coefficients of this digital compensation filter also can be obtained directly in the discrete time domain. It is preferable to have the combined output of the channel and compensation filter be zeros all the time except at one particular sampling instance, l:

$$\sum_i h(i)h_{s,F}(j-i) = 0, \quad j \neq l$$

$$\sum_i h(i)h_{s,F}(j-i) = 1, \quad j = l$$

Because data symbols are transmitted in sequence, every sampling instance can be made unique, corresponding to a particular data symbol. The received signal detected from this sequence of sampling instances can be made free of channel distortion. This condition can be expressed in a matrix format. An example of channel and filter lengths both being equal to 5 is expressed as

$$\begin{bmatrix} h(1) & 0 & 0 & 0 & 0 \\ h(2) & h(1) & 0 & 0 & 0 \\ h(3) & h(2) & h(1) & 0 & 0 \\ h(4) & h(3) & h(2) & h(1) & 0 \\ h(5) & h(4) & h(3) & h(2) & h(1) \\ 0 & h(5) & h(4) & h(3) & h(2) \\ 0 & 0 & h(5) & h(4) & h(3) \\ 0 & 0 & 0 & h(5) & h(4) \\ 0 & 0 & 0 & 0 & h(5) \end{bmatrix} \begin{bmatrix} h_{s,F}(1) \\ h_{s,F}(2) \\ h_{s,F}(3) \\ h_{s,F}(4) \\ h_{s,F}(5) \end{bmatrix} = \begin{bmatrix} 0 \\ 0 \\ 0 \\ 0 \\ 1 \\ 0 \\ 0 \\ 0 \\ 0 \end{bmatrix}$$

These compensation filter coefficient values can be obtained by solving the above set of overly specified linear equations. In general, the unit response does not need to be exactly in

the middle of the convolution span. The previous matrix relationship can be described in a simplified notation, as follows:

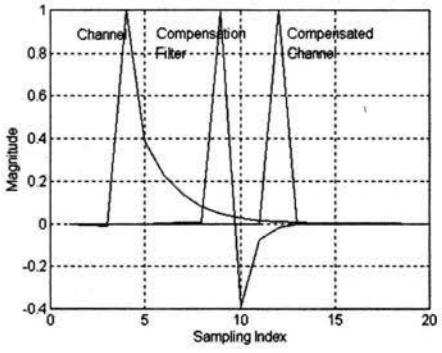
$$\overline{H}\overline{h}_{s,F} = \overline{p}$$

Because $\overline{H}$ is not a square matrix, the solution is expressed as

$$\overline{h}_{s,F} = \left(\overline{H}^T\overline{H}\right)^{-1}\overline{H}^T\overline{p}$$

Figures 8.2, 8.3, and 8.4 show normalized filter coefficients of compensation filters as well as original and compensated channel impulse responses for 1, 2, and 3 miles of 26-gauge twisted-pair loops, respectively. Because the channel impulse response is normalized, and compensation filter coefficients and compensated channel impulse response all have similar magnitudes, they are organized together in all three figures for the comparison of different shapes.

Figure 8.2 Channel and Compensation Filter for a 1 Mile, 26-Gauge Loop



This digital compensation filter is called a *linear channel equalizer* because the equalizer output is a linear combination of the received signal.[1] Equalizer coefficients obtained according to the previous matrix relationship results in what is called a *zero forcing channel equalizer*, which works well in a noiseless or low-noise environment.

Figure 8.3 Channel and Compensation Filter for a 2 Mile, 26-Gauge Loop

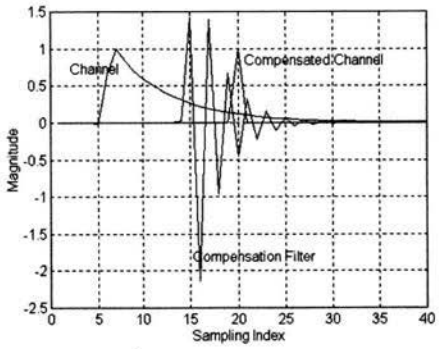
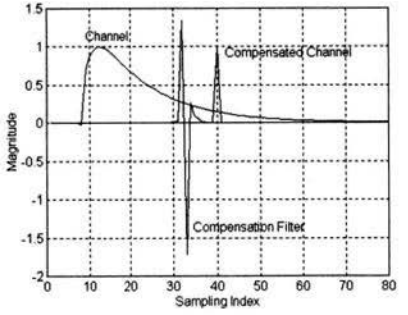


Figure 8.4 Channel and Compensation Filter for a 3 Mile, 26-Gauge Loop



8.1.2 *Obtaining Optimal Equalizer Coefficients*

For a twisted-pair channel with crosstalk and background noise, optimal equalizer coefficients are obtained through minimizing the mean square error between the desired unit response and the channel and equalizer combined output. The frequency domain derivation of this Minimum Mean Square Error equalizer is equivalent to the *Wiener Filter.*[2]

The received signal contains information of the current as well as past and future data symbols. The ideal equalizer output should only contain the current data symbol. The difference between the current data symbol and the output of the equalizer contains the error of the current data symbol estimation and residual channel distortion. Based on the assumption that the received signal and the error between the unit response and the equalizer output should not be correlated, we have

$$E\left\{\left[a(t)-\int_{-\infty}^{\infty}x(t-\alpha)q(\alpha)d\alpha\right]x(t-\tau)\right\}=0$$

The values are as follows:

$a(t)$ is the transmit signal.

$x(t)$ is the received signal.

$q(t)$ is the equalizer.

This expectation yields the relationship between the correlation of the transmitted signal and the received signal and the autocorrelation of the received signal:

$$R_{ax}(\tau)=\int_{-\infty}^{\infty}R_{xx}(\tau-\alpha)q(\alpha)d\alpha$$

The values are as follows:

$R_{ax}(t)$ is the correlation between the transmitted signal and the received signal.

$R_{xx}(t)$ is the autocorrelation of the received signal.

This can be equivalently expressed in frequency domain as

$$S_{ax}=(\omega)=S_{xx}(\omega)Q(\omega)$$

Therefore, the minimum mean square equalizer solution in frequency domain is

$$Q(\omega)=\frac{S_{ax}(\omega)}{S_{xx}(\omega)}$$

You can derive the discrete Minimum Mean Square Error equalizer solution directly in the discrete time domain. The instantaneous error between the desired data symbol and the equalizer output is expressed as

$$e_k=a_{k-d}-X_k^TQ_k$$

a_{k-d} is the desired data symbol after a channel delay of d signaling periods.

$X_k^T = [x_k \quad x_{k-1} \quad \ldots \quad x_{x-n+1}]$ is the received signal vector for an equalizer length of n.

$Q_k^T = [q_{1k} \quad q_{2k} \quad \ldots \quad q_{nk}]$ is the equalizer coefficient vector.

e_k is the error between the desired signal and the equalizer output.

We further expand the received signal as the convolution of the transmitted signal and the twisted-pair loop channel impulse response as

$$x_k = \sum_{i=1}^{l} a_{k-i+1} h(i) = [a_k \quad a_{k-1} \quad \ldots \quad a_{k-l+1}] \begin{bmatrix} h(1) \\ h(2) \\ \ldots \\ h(l) \end{bmatrix} + n_k = A_k{}^T \overline{h} + n_k$$

The channel impulse response, which has a duration of l and n_k, is the sampled receiver front-end noise.[3] The received signal vector can be expressed as

$$X_k^T = [a_k \quad a_{k-1} \quad \ldots \quad a_{k-l-n+2}] \begin{bmatrix} h(1) & 0 & 0 & 0 \\ h(2) & h(1) & 0 & 0 \\ h(3) & h(2) & 0 & 0 \\ \ldots & \ldots & \ldots & h(1) \\ h(l) & h(l-1) & 0 & h(2) \\ 0 & h(l) & 0 & h(3) \\ 0 & 0 & 0 & \ldots \\ 0 & 0 & 0 & h(l) \end{bmatrix} + [n_k \quad n_{k-1} \quad \ldots \quad n_{k-n+1}] = A_k^{nT} \overline{H} + N_k{}^T$$

$\overline{H}$ has a dimension of $l+n-1$ by n, and the data vector A_k^{nT} has a length of $l+n-1$. The expected value of the squared error, or mean squared error, for a particular equalizer Q is

$$E[e_k^2] = E[(a_{k-d} - X_k^T Q)^2]$$

The derivative of the mean squared error with respect to the equalizer coefficient vector, Q, is

$$\frac{\partial\left(E\left[e_k^2\right]\right)}{\partial Q} = -2E\left[\left(a_{k-d} - X_k^T Q\right)X_k^T\right]$$

By setting the derivative equal to zero, we obtain the optimal equalizer coefficient vector, Q_{opt}, for the minimum mean squared error as

$$Q_{opt}^T E\left[X_k X_k^T\right] = E\left[a_{k-d} X_k^T\right]$$

$$Q_{opt}^T = \left(E\left[X_k X_k^T\right]\right)^{-1} E\left[a_{k-d} X_k^T\right]$$

When the channel noise is set to zero, the Minimum Mean Square Error equalizer solution becomes the zero forcing equalizer solution:

$$Q_{opt} = \left(\overline{H}^T \overline{H}\right)^{-1} \overline{H}^T p$$

Figures 8.5, 8.6, and 8.7 show Minimum Mean Square Error equalizer coefficients for 1, 2, and 3 miles of 26-gauge twisted-pair loops, respectively, under different white background noise levels. The results in Figures 8.6 and 8.7 indicate that a balance exists between the degree of channel equalization and the amount of noise enhancement. Under a lower noise level, a better channel equalization can be realized.

Figure 8.5 Channel Equalizer for a 1 Mile, 26-Gauge Loop with Different Noise Levels

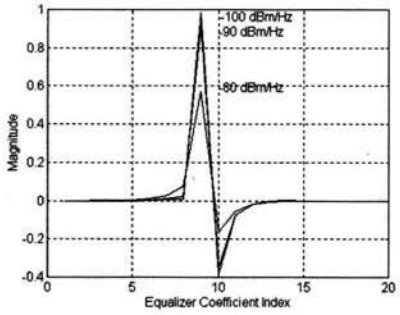


Figure 8.6 Channel Equalizer for a 2 Mile, 26-Gauge Loop with Different Noise Levels

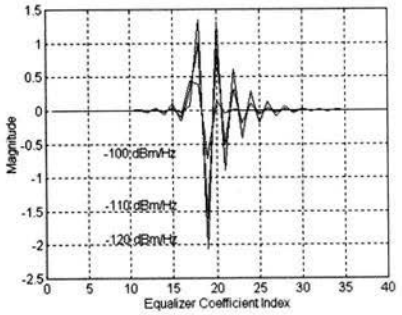
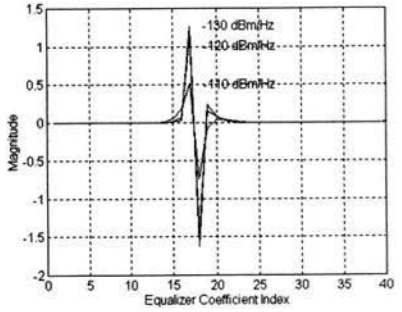


Figure 8.7 Channel Equalizer for a 3 Mile, 26-Gauge Loop with Different Noise Levels



In a hardware implementation, equalizer coefficient values are identified iteratively most often with the LMS algorithm[4]

$$Q_{k+1} = Q_k + \mu X_k \left(a_{k-d} - X_k^T Q_k \right)$$

for which the adjustment step size should satisfy the following condition:

$$\mu < \frac{1}{trE\left[X_k X_k^T\right]}$$

The value $trE\left[X_k X_k^T\right]$ refers to the sum of the diagonal elements of the matrix $E\left[X_k X_k^T\right]$.

If the received signal is properly normalized, that is, $E[x_k^2] = 1$ through receiver front-end amplification, the result will be

$$\mu < \frac{1}{n}$$

in which n is the length of the channel equalizer.

The expression

$$\xi_{\min} = E[a_{k-d}^2] - E[a_{k-d} X_k^T] Q_{op}$$

describes the Minimum Mean Square Error (MMSE) between the desired signal and the output of an optimal equalizer, which is determined by the receiver front-end noise level, the twisted-pair loop channel, and the length of the equalizer.

A 26-gauge, 10,560 foot loop with receiver front-end noise power density levels of –110 dBm/Hz, –120 dBm/Hz, and –130 dBm/Hz, for example, has MMSE levels of –18.3 dB, –27.9 dB, and –36.6 dB, respectively.

The actual mean square error between the desired signal and the output of an optimal equalizer is slightly higher than the MMSE by the amount of excessive MMSE due to the use of a finite adjustment step size. The amount of excessive MMSE is proportional to the adjustment step size and is described by the following expression:

$$excess\ \xi_{\min} \approx \mu \xi_{\min} trE[X_k X_k^T]$$

For a simple example of $E[x_k^2] = 1$ with an adjustment step size of $\mu = 1/80$, the amount of excessive MMSE is then

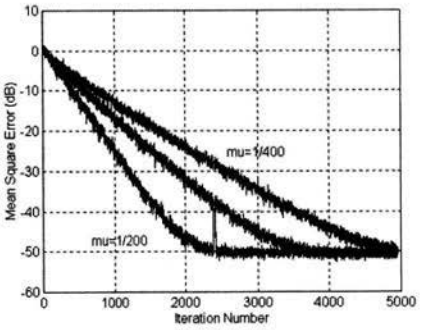
$$excess\ \xi_{\min} \approx 0.5 \xi_{\min}$$

The total mean square error between the desired signal and the output of an optimal equalizer is

$$\xi = excess\ \xi_{\min} + \xi_{\min} \approx 1.5 \xi_{\min}$$

This effect of a 50 percent addition is equivalent to raising the mean square error by the amount of 1.76 dB. Figure 8.8 shows convergence of the mean square error for adjustment step sizes of 1/200, 1/300, and 1/400 for a 1 mile, 26-gauge twisted-pair loop. The middle curve has an adjustment step size of 1/300. A slightly lower mean square error level can be observed for a step size of 1/300 compared with that for a step size of 1/200.

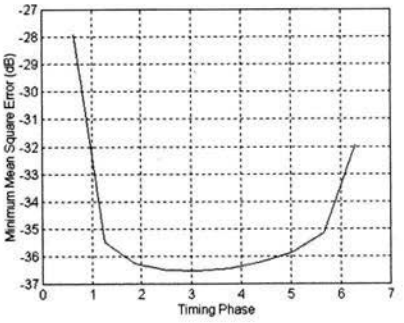
Figure 8.8 Convergence of an Adaptive Channel Equalizer



8.1.3 *Baud Rate Equalizer Performance*

The preceding derived equalizer operates at the signaling baud rate and, therefore, is also called the *baud rate equalizer.* It also can be called the *symbol rate* or the *symbol spaced equalizer.* The performance of a baud rate equalizer is very sensitive to the sampling timing phase because the sampled signal strength could be different relative to the background noise. Figure 8.9 shows the MMSE values for a 2 mile, 26-gauge twisted-pair loop with different sampling timing phases. These MMSE values can differ by as much as 9 dB at different timing phases. Ten sample points were taken for a phase rotation of 2π in Figure 8.9.

Figure 8.9 Equalizer Output Signal-to-Noise Ratio Versus Timing Phase



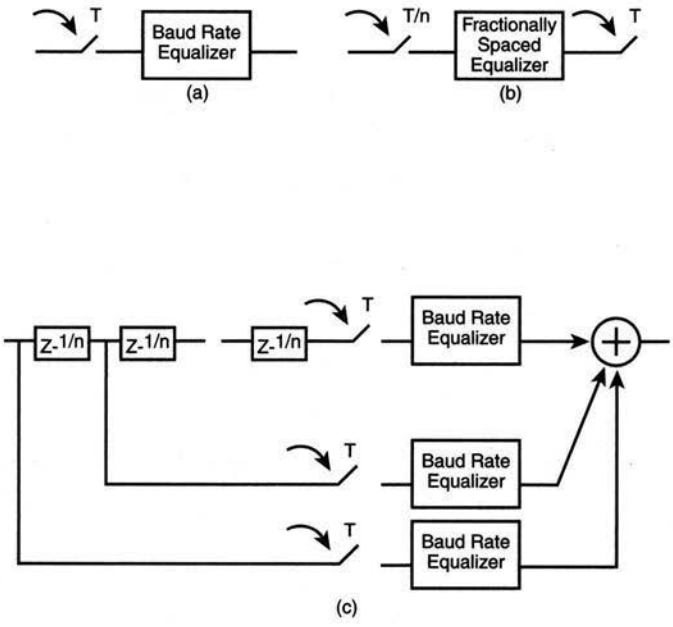
The effective bandwidth is half of the sampling rate or baud rate for this special baud rate equalizer case. Nyquist frequency is often used to describe the bandwidth defined by the half sampling frequency. The analog channel, including channel attenuation and receiver front-end noise, is folded along the Nyquist frequency due to the sampling process.

The interference caused by sampling images is often referred to as the *aliasing effect.* An analog filter with a Nyquist corner frequency is usually used to minimize the effect of aliasing. The performance of a baud rate equalizer also suffers from aliasing at the region near the half of the sampling frequency.

8.1.4 *Fractionally Spaced Equalizer Performance*

The alternative to the baud rate equalizer is the *fractionally spaced equalizer.*[5] A fractionally spaced equalizer has a data input rate a few times of the baud rate while maintaining the equalizer output rate at the baud rate. Figure 8.10 shows the structure of the fractionally spaced equalizer and its multiple baud rate equalizer equivalence. For example, a three times over sampled fractionally spaced equalizer can be considered as consisting of 3 baud rate equalizers, each of which has a third number of equalizer coefficients.

Figure 8.10 Multiple Equalizer Equivalence of a Fractionally Spaced Equalizer



The optimal fractionally spaced equalizer coefficients also can be derived from the discrete time domain. Given a two times over-sampled case, dividing the fractionally spaced equalizer into a phase 1 part and a phase 2 part, the instantaneous error between the desired signal and the output of a fractionally spaced equalizer is

$$e_k = a_{k-d} - X_k^{1T} Q_k^1 - X_k^{2T} Q_k^2$$

a_{k-d} is the desired data symbol after the channel delay of d signaling periods.

$X_k^{1T} = \begin{bmatrix} x_k & x_{k-2} & \cdots & x_{x-n} \end{bmatrix}$ and $X_k^{2T} = \begin{bmatrix} x_{k-1} & x_{k-3} & \cdots & x_{x-n+1} \end{bmatrix}$ are received signal vectors.

$Q_k^{1T} = \begin{bmatrix} q_{1k} & q_{3k} & \cdots & q_{(n-1)k} \end{bmatrix}$ is the equalizer coefficient vector for the phase 1 part of the fractionally spaced equalizer.

$Q_k^{2T} = \begin{bmatrix} q_{2k} & q_{4k} & \cdots & q_{nk} \end{bmatrix}$ is for the phase 2 part.

e_k is the error between the desired signal and the equalizer output.

Notice that both phase 1 and phase 2 equalizers have a length of $n/2$. We also have

$$x_k = \sum_{i=1}^{l/2} a_{k-i+1} h(1+2(i-1)) = \begin{bmatrix} a_k & a_{k-1} & \cdots & a_{k-l/2+1} \end{bmatrix} \begin{bmatrix} h(1) \\ h(3) \\ \cdots \\ h(l-1) \end{bmatrix} + n_k$$

for odd k and

$$x_k = \sum_{i=1}^{l/2} a_{k-i+1} h(2i) = \begin{bmatrix} a_k & a_{k-1} & \cdots & a_{k-l/2+1} \end{bmatrix} \begin{bmatrix} h(2) \\ h(4) \\ \cdots \\ h(l) \end{bmatrix} + n_k$$

for even k. We further have

$$X_k^{1T} = \begin{bmatrix} a_k & a_{k-1} & \cdots & a_{k-n/2-l/2+2} \end{bmatrix} \begin{bmatrix} h(1) & 0 & 0 & 0 \\ h(3) & h(1) & 0 & 0 \\ h(5) & h(3) & 0 & 0 \\ \cdots & \cdots & \cdots & h(1) \\ h(l-1) & h(l-3) & 0 & h(3) \\ 0 & h(l-1) & 0 & h(5) \\ 0 & 0 & 0 & \cdots \\ 0 & 0 & 0 & h(l-1) \end{bmatrix} + \begin{bmatrix} n_k & n_{k-2} & \cdots & n_{k-n/2} \end{bmatrix}$$

$$X_k^{2T} = \begin{bmatrix} a_k & a_{k-1} & \cdots & a_{k-n/2-l/2+2} \end{bmatrix} \begin{bmatrix} h(2) & 0 & 0 & 0 \\ h(4) & h(2) & 0 & 0 \\ h(6) & h(4) & 0 & 0 \\ \cdots & \cdots & \cdots & h(2) \\ h(l) & h(l-2) & 0 & h(4) \\ 0 & h(l) & 0 & h(6) \\ 0 & 0 & 0 & \cdots \\ 0 & 0 & 0 & h(l) \end{bmatrix} + \begin{bmatrix} n_{k-1} & n_{k-3} & \cdots & n_{k-n/2+1} \end{bmatrix}$$

With two baud spaced received signal vector defined as X_k^{1T} and X_k^{2T}, the expected value of the square error, or mean square error, for a particular equalizer vector, Q, is

$$E\left[e_k^2\right] = E\left[\left(a_{k-d} - X_k^{1T}Q^1 - X_k^{2T}Q^2\right)^2\right]$$

Q^1 and Q^2 represent the first and second sampling phase of the equalizer, Q, respectively. The derivative of the mean squared error with respect to the equalizer coefficient vectors Q^1 and Q^2 are

$$\frac{\partial\left(E\left[e_k^2\right]\right)}{\partial Q^1} = -2E\left[\left(a_{k-d} - X_k^{1T}Q^1 - X_k^{2T}Q^2\right)X_k^{1T}\right]$$

$$\frac{\partial\left(E\left[e_k^2\right]\right)}{\partial Q^2} = -2E\left[\left(a_{k-d} - X_k^{1T}Q^1 - X_k^{2T}Q^2\right)X_k^{2T}\right]$$

To obtain the optimal equalizer coefficient vector Q_{opt}, set the derivative equal to zero, as shown in the following expressions:

$$Q^{1T}E\left[X_k^1 X_k^{1T}\right] + Q^{2T}E\left[X_k^1 X_k^{2T}\right] = E\left[a_{k-d}X_k^{1T}\right]$$

$$Q^{1T}E\left[X_k^2 X_k^{1T}\right] + Q^{2T}E\left[X_k^2 X_k^{2T}\right] = E\left[a_{k-d}X_k^{2T}\right]$$

You also can use these expressions in an arranged matrix form as

$$\begin{bmatrix} E\left[X_k^1 X_k^{1T}\right] & E\left[X_k^1 X_k^{2T}\right] \\ E\left[X_k^2 X_k^{1T}\right] & E\left[X_k^2 X_k^{2T}\right] \end{bmatrix} \begin{bmatrix} Q^1 \\ Q^2 \end{bmatrix} = E\left[a_{k-d} \begin{bmatrix} X_k^1 \\ X_k^2 \end{bmatrix} \right]$$

The optimal equalizer solution is as follows:

$$\begin{bmatrix} Q_{opt}^1 \\ Q_{opt}^2 \end{bmatrix} = \left(\begin{bmatrix} E\left[X_k^1 X_k^{1T}\right] & E\left[X_k^1 X_k^{2T}\right] \\ E\left[X_k^2 X_k^{1T}\right] & E\left[X_k^2 X_k^{2T}\right] \end{bmatrix} \right)^{-1} E\left[a_{k-d} \begin{bmatrix} X_k^1 \\ X_k^2 \end{bmatrix} \right]$$

The matrix inverse exists as long as there is receiver front-end noise. Figures 8.11, 8.12, and 8.13 show normalized, fractionally spaced equalizer coefficients as well as baud rate equalizer coefficients, in little circles, as a comparison for 1, 2, and 3 miles of 26-gauge twisted-pair loops, respectively.

Figure 8.11 Fractionally Spaced Equalizers for a 1 Mile, 26-Gauge Loop

